AD_____

AWARD NUMBER: W81XWH-04-1-0085

TITLE: Functional Characterization of a Novel Pro-Apoptotic Transcription Regulatory Protein in Ovarian Cancer

PRINCIPAL INVESTIGATOR: Viji Shridhar, Ph.D.

CONTRACTING ORGANIZATION: Mayo Clinic
Rochester, MN 55905

REPORT DATE: December 2006

TYPE OF REPORT: Final

PREPARED FOR: U.S. Army Medical Research and Materiel Command
Fort Detrick, Maryland 21702-5012

REPORT DOCUMENTATION PAGE

Form Approved
OMB No. 0704-0188

1. REPORT DATE	2. REPORT TYPE	3. DATES COVERED
01-12-2006	Final	15 Dec 2003 – 14 Nov 2006

4. TITLE AND SUBTITLE

Functional Characterization of a Novel Pro-Apoptotic Transcription Regulatory Protein in Ovarian Cancer

5a. CONTRACT NUMBER

5b. GRANT NUMBER
W81XWH-04-1-0085

5c. PROGRAM ELEMENT NUMBER

6. AUTHOR(S)

Viji Shridhar, Ph.D.

E-Mail: shridhar.vijayalakshmi@mayo.edu

5d. PROJECT NUMBER

5e. TASK NUMBER

5f. WORK UNIT NUMBER

7. PERFORMING ORGANIZATION NAME(S) AND ADDRESS(ES)

Mayo Clinic
Rochester, MN 55905

8. PERFORMING ORGANIZATION REPORT NUMBER

9. SPONSORING / MONITORING AGENCY NAME(S) AND ADDRESS(ES)
U.S. Army Medical Research and Materiel Command
Fort Detrick, Maryland 21702-5012

10. SPONSOR/MONITOR'S ACRONYM(S)

11. SPONSOR/MONITOR'S REPORT NUMBER(S)

12. DISTRIBUTION / AVAILABILITY STATEMENT
Approved for Public Release; Distribution Unlimited

13. SUPPLEMENTARY NOTES
Original contains colored plates: ALL DTIC reproductions will be in black and white.

14. ABSTRACT

In an effort to identify genetic changes involved in ovarian cancer (OvCa) development, we performed differential display-PCR, cDNA microarray and suppression subtraction hybridization analyses (SHH) to identify early genetic alterations associated with OvCa. These studies resulted in identification of several genes differentially expressed in OvCa, including a novel gene encoding a transcription elongation-like protein with the ability to induce apoptosis and suppress cancer cell growth. We named the protein ProApoptotic Protein on chromosome X (PAPX). Pro-apoptotic protein on X (PAPX) is a novel nuclear protein with sequence homology to transcription elongation factor like 1 (TCEAL1) [1]. PAPX expression is down-regulated in majority of ovarian cancer cell lines and primary tumors [2]. Re-expression of PAPX induces cell death and attenuates cell growth. We therefore proposed to study the functional role of PAPX as a candidate tumor suppressor in ovarian cancer. We proposed to (1) determine effect of PAPX on tumor and cell growth in vivo and in vitro; (2) analyze genes regulated by PAPX by transcriptional profiling using microarray chips; and (3) identify proteins that interact with PAPX and elucidate the function of PAPX related to tumor suppression.

15. SUBJECT TERMS
Ovarian Cancer

16. SECURITY CLASSIFICATION OF:			17. LIMITATION OF ABSTRACT	18. NUMBER OF PAGES	19a. NAME OF RESPONSIBLE PERSON
a. REPORT	b. ABSTRACT	c. THIS PAGE			19b. TELEPHONE NUMBER *(include area code)*
U	U	U	UU	66	USAMRMC

TABLE OF CONTENTS

ABSTRACT
Pro-apoptotic protein on X (PAPX) is a novel nuclear protein with sequence homology to transcription elongation factor like 1 (TCEAL1) [1]. PAPX expression is down-regulated in majority of ovarian cancer cell lines and primary tumors [2]. Re-expression of PAPX induces cell death and attenuates cell growth. We therefore proposed to study the functional role of PAPX as a candidate tumor suppressor in ovarian cancer. We proposed to (1) determine effect of PAPX on tumor and cell growth *in vivo* and *in vitro*; (2) analyze genes regulated by PAPX by transcriptional profiling using microarray chips; and (3) identify proteins that interact with PAPX and elucidate the function of PAPX related to tumor suppression.

We reported on the epigenetic silencing of PAPX (Renamed TCEAL7 (Bex4) at the request of the reviewers) in ovarian cancer in the journal Oncogene in 2005 (Manuscript attached in the APPENDIX). The support from DOD is acknowledged in this manuscript. In our previous annual report, we provided the details of the experiments associated with Specific Aim#3 where we had utilized an antibody array to identify PAPX interacting proteins. The manuscript resulting from these experiments is under preparation. This manuscript is attached in the APPENDIX and the support from DOD is acknowledged in this article.

INTRODUCTION
We identified a novel pro-apoptotic nuclear protein with domain homology to $p75^{NTR}$-associated death executor (NADE) [3] and transcription elongation factor A-like 1 (TCEAL1) [1]. Amino acid alignment of PAPX and NADE reveals that PAPX contains a putative nuclear export signal, but no homology with the C terminal region of NADE that is shown to be involved in NGF-dependent regulation of NADE-induced apoptosis [4]. NADE is a nuclear pro-apoptotic protein involved in modulating apoptosis mediated by the low affinity neurotropin receptor [3]. Like NADE, PAPX is a pro-apoptotic nuclear protein, and forced expression of PAPX in ovarian cancer cell lines induces apoptosis. Although NADE is not implicated in carcinogenesis, expression of PAPX is lost or markedly reduced in ovarian cancer. The fact that PAPX is a pro-apoptotic protein and is lost in majority of ovarian tumor is highly significant because loss of expression of a pro-apoptotic protein could confer a survival advantage leading to the development of ovarian epithelial neoplasia.

1. Genomic structure of TCEAL7
Genomic structure of TCEAL7 revealed that it is made up of three exons with the ORF residing entirely within exon 3 (Figure 1). Exons 1, 2, and 3 are 109 bp, 118 bp and 949 bp long respectively. Introns 1 and 2 are 618 bp and 336 bp long respectively. The putative open reading frame codes for a 100 amino acid long polypeptide. The putative initiation codon occurs within a strong Kozak context [5, 6] and is preceded by an in-frame stop codon. The assembled gene mapped to Xq21.1-21.2 based on the Human Genome BLAST server database.

Figure 1. Genomic Structure of TCEAL7

2. Similarity alignment of TCEAL7 to other proteins
To identify potential functions of TCEAL7, a homology search using Blastp was performed [7]. Subsequent CLUSTALW sequence alignment analyses between TCEAL7 and two homologous proteins are shown in Figure 2. The highest identity was observed with the p75NTR-associated death executor (NADE) (37%) and with the transcription elongation factor A-like 1 (TCEAL1) (35%). TCEAL7 and NADE share high degree of homology except between residues 72-112 of NADE, a region essential for NGF-dependent regulation of NADE-induced apoptosis [3]. TCEAL7 and TCEAL1 share homologies in the N- and C-terminal regions, with a long stretch of similarity primarily in the helix-turn-helix motif found in many DNA binding proteins. TCEAL7 has both nuclear export signal (Fig 2B) and a putative nuclear localization signal underlined in Fig 2A.

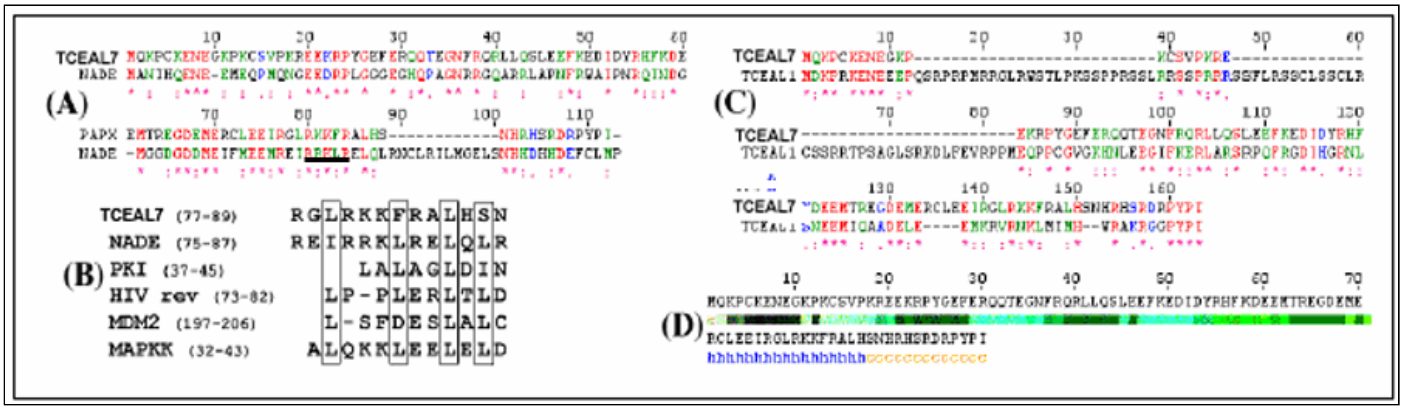

Figure 2. (A) Homology alignment of TCEAL7 and the p75NTR-associated death executor (NADE). The nuclear export signal of NADE is boxed. Identity (*), strongly similar (:), and weakly similar (.) alignments are shown at the bottom of each alignment. (B) TCEAL7 contains a conserved Rev-like NES motif. (C) Homology alignment of TCEAL7 and the transcription elongation factor A-like 1 (TCEAL1). C-terminal region containing helix-turn-helix motif found in many DNA binding proteins is underlined in TCEAL1. (D) Secondary structure prediction of TCEAL7 indicating the presence of helix-turn-helix motif.

3. Expression of TCEAL7 in ovarian carcinoma cell lines and primary tumors: To validate the results obtained by microarray and SSH analyses, TCEAL7 expression was tested in 7 ovarian cancer cell lines and in 24 primary ovarian tumors by semi-quantitative RT-PCR and northern blot analyses respectively (Figs. 3a and b). In addition, TCEAL7 expression was also determined in 50 ovarian tumors of different histologies using custom cDNA microarray (Fig. 3c). Complete loss or down-regulation of TCEAL7 is seen even in borderline tumors. The results are shown in **Figure 3** below.

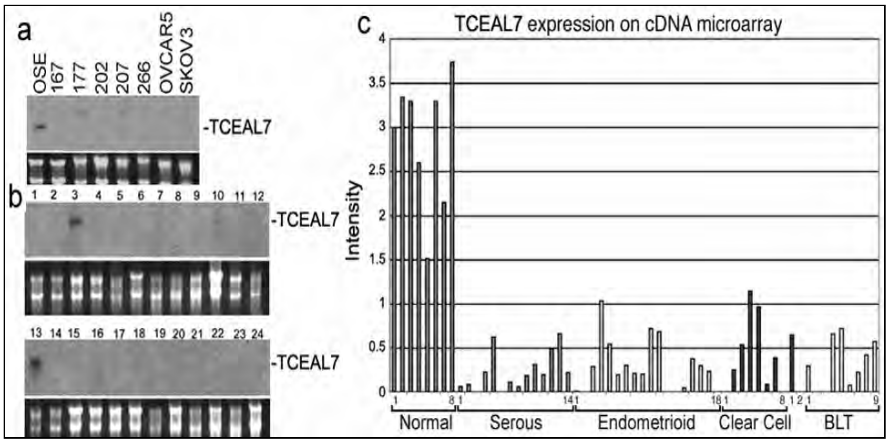

Figure 3. (a) Upper panel, Northern blot analysis of ovarian cell lines. Lower panel, ethidium bromide stained 18S and 28S showing equal loading. **(b)** Of 24 primary tumors, only three show expression of TCEAL7 by Northern blot analysis. **(c)** Analysis of TCEAL7 expression in 50 ovarian samples using custom cDNA microarray. BLT denotes borderline tumors.

4. Forced expression of TCEAL7 induces apoptosis:

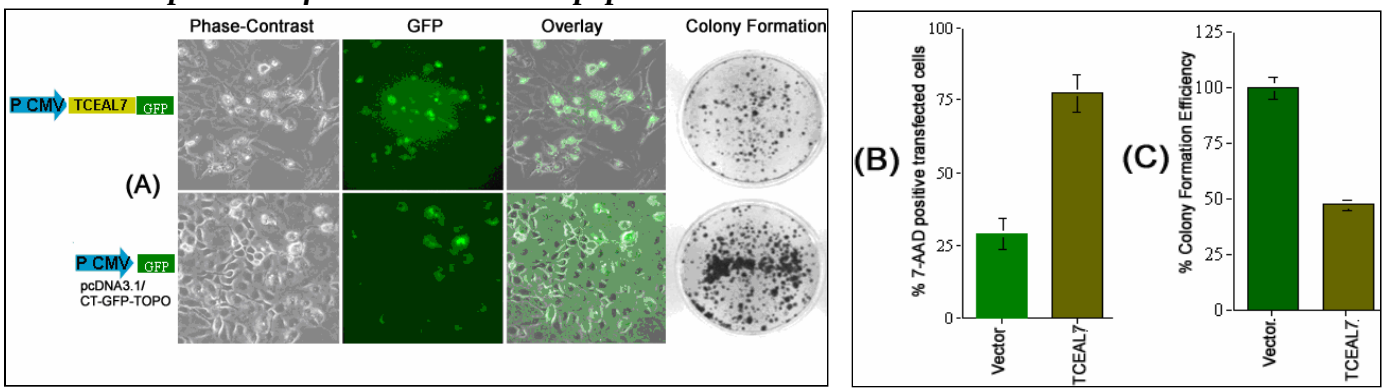

Figure 4: (A) Cells expressing TCEAL7-GFP fusion protein display apoptotic morphology visible under Phase-Contrast microscopy, while cells expressing vector GFP show normal morphology. **(B)** Markedly higher rate of apoptosis was observed in TCEAL7 expressing cells by flow-assisted 7-AADand Annexin V labeling. **(C)** TCEAL7 expressing cells form fewer colonies. Relative colony formation efficiency is about 55% less than vector control.

To determine the effect of TCEAL7 expression in ovarian cancer cells, TCEAL7 nonexpressing OV202 cells were transiently transfected with a TCEAL7-GFP fusion construct. Forced expression of TCEAL7 induces apoptosis and decreases the relative colony formation efficiency of ovarian cancer cells, as shown in Figure 4. Cells expressing TCEAL7 (GFP-labeled cells, 4A:upper panels) show morphology typical of cells undergoing apoptosis, whereas vector-transfected cells 4A: lower panels) display normal morphology. In colony formation assay, cells transfected with TCEAL7 form less number of colonies (4A: upper panel) compared to cells transfected with vector (4A: lower panel).

5. Mechanism of TCEAL7 inactivation

To investigate the mechanisms of TCEAL7 inactivation, several approaches were taken. First, 20 pairs of matched normal and primary ovarian tumors were different microsatellite markers within the TCEAL7 gene. LOH analysis revealed 25% (5/20) of tumors showed LOH in this region of the chromosome (data not shown). Second, mutational analysis of all three exons in 96 primary ovarian tumors showed no tumor specific changes (data not shown). In order to determine whether methylation controlled TCEAL7 expression, OV207 cells were treated with various concentrations of methyltransferase inhibitor, 5-aza-20-deoxycytidine (5-aza-dC) [8, 9]. Figure 5a shows a dose-dependent increase in TCEAL7 expression in OV207 following 5-aza-dC treatment. Consistent with this finding, genomic sequence analysis indicated 26 CpG sites around four SmaI sites in the promoter, exon 1, and intron 1 (Figure 5b). Primers flanking these SmaI sites were selected to amplify and sequence the bisulfite-modified DNA. Amplicon 1 contains SmaI site I at 738 bases upstream of exon 1 and includes two CpG sites. Amplicon 2 contains SmaI site II within exon 1 and
site III at 126 bases 30 of exon 1 and includes five other CpG sites. Amplicon 3 contains SmaI site IV in intron 1 at 286 bases 30 to site 3 and includes six additional CpG sites. Therefore, a total of 16 CpG sites were analyzed. Five CpG sites between amplicons 1 and 2 and between 3 and 4 were not included in the analysis. In order to distinguish unmodified from modified DNA, PCR was performed on bisulfite-modified DNA as previously described [10, 11]. Amplicons were gel purified and sequenced to determine the overall methylation status of 16 CpG sites. Methylated C's (indicated by asterisks in Figure 5b) are resistant to bisulfite modification and remain as C's, whereas unmethylated C's are converted to T's (Figure 5b). Since TCEAL7 maps to a region of X chromosome inactivation (Brown and Kay, 1999), we included somatic cell hybrids containing either active X [Y162.11C] (Xa) and inactive X [Y162.5E1T2] (Xi) as positive and negative controls in these analyses. Methylation analyses of bisulfite-modified DNAs from Xa and Xi cell lines showed differential methylation at sites II, III, and IV between two hybrid cell lines (Figure 5c, first & second row). However, CpG in SmaI site I was methylated in both the active and the inactive X. RT–PCR analysis of TCEAL7 expression in these hybridomas carrying either Xa or Xi chromosome showed loss of TCEAL7 expression in both lines (data not shown). These results suggest that methylation at SmaI site I might play a c critical role in controlling the expression of TCEAL7. Methylation of CpG in SmaI site I controls TCEAL7 expression in the somatic cell hybrid containing the active X.

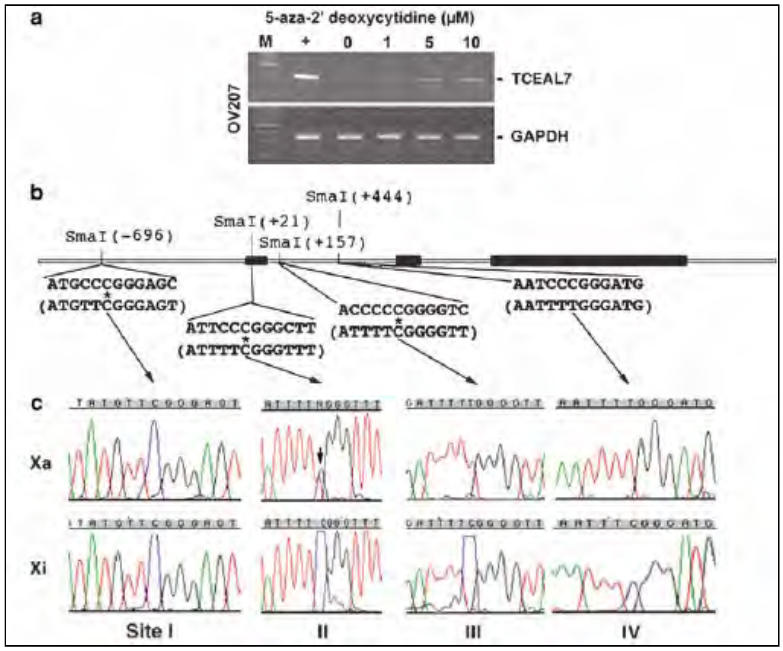

Figure 5: Methylation analysis of TCEAL7. **(a)** Induction of TCEAL7 expression in OV207 cell line by 5-aza-dC. PCR amplification of GAPDH is shown in the lower panel as a loading control. þ: positive control (OSEtsT). **(b)** Genomic structure and sequence of four
SmaI sites analysed. Methylated C's are indicated by asterisks. They are resistant to bisulfite modification, and therefore remain as Cs. Unmethylated C's are converted to T's. The bisulfite-modified sequences are indicated in parentheses. **(c)** Sequence chromatogram of four SmaI sites after bisulfite modification of genomic DNA purified from somatic cell hybrids containing Xa or Xi. Sequences highlighted in gray on top of chromatogram correspond to SmaI site sequences shown in panel b. The arrow indicates the presence of both methylated and unmethylated alleles at SmaI site II in Xa.

6. Methylation of CpG in SmaI site I controls TCEAL7 expression in the somatic cell hybrid containing the active X

In order to determine if methylation of CpG site I is inactivating TCEAL7 expression in Xa-containing cell line, cells were treated with various concentrations of 5- aza-dC. A dose-dependent increase in TCEAL7 expression in this cell line was observed following 5-aza-dC treatment (Figure 6a). Subsequent analysis of bisulfite modified DNA from 5-aza-dC-treated Xa cells revealed demethylation of site 1, concomitant with induction of TCEAL7 transcript (Figure 6b). These data suggest that site I methylation may control TCEAL7 expression in this cell line. In order to rule out the possibility of histone deacetylation as a mechanism of TCEAL7 transcriptional inactivation, Xa-containing cells were treated with various concentrations of the histone deacetylase inhibitor, trichostatin A. Trichostatin A did not affect the transcription of TCEAL7 in these cells (Figure 6c). To demonstrate that methylation of CpG in SmaI site I influences the promoter activities in vitro, amplicon 1 was subcloned into pGL3 reporter plasmid, and the CpG site I was mutated to ApG. Both plasmids were subjected to bisulfite modification, and modified plasmids were transfected into HeLa cells to determine the promoter activity of these two plasmids. As shown in Figure 6d, nonmutated plasmid showed diminished promoter activity compared to the mutated plasmid, suggesting that methylation of CpG site I in nonmutated plasmid suppressed promoter activity and that prevention of CpG site methylation by site-directed mutagenesis prevented this suppression of promoter activity.

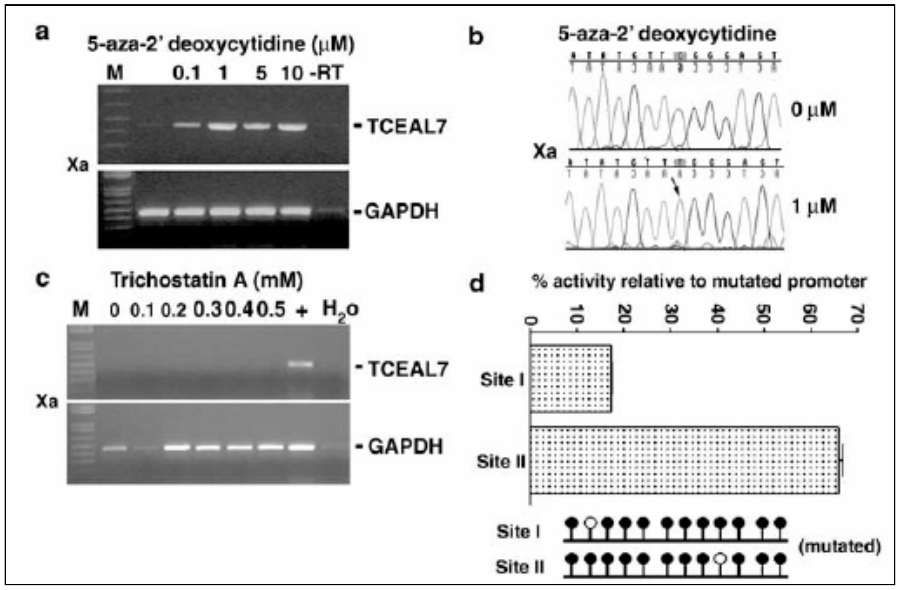

Figure 6: Methylation at SmaI site I controls TCEAL7 expression. **(a)** Agarose gel electrophoresis of RT–PCR showing dose dependent increase in the transcription of TCEAL7 following 72 h of exposure to increasing concentrations of 5-aza-dC in somatic cell hybrid Y162.11C with active X (Xa). GAPDH control is shown in the lower panel. No TCEAL7 product was detected in -RT control. **(b)** Sequence of bisulfite-modified DNA from Xa hybrid showing the methylation at site 1 before 5-aza-dC treatment. The arrow in the lower sequence indicates demethylation at this site after the treatment. **(c)** Increasing concentrations of TSA (0.1–0.5mM) treatments have no effect on TCEAL7 expression in Xa hybrid. þ: positive control (OSEtsT); H2O: water control; M: 100 bp ladder. **(d)** Methylation of CpG in SmaI site I suppresses promoter activity, whereas the mutation that prevents methylation of the site does not suppress promoter activity. WT: wild-type CpG; Mut: mutant ApG sequence in SmaI site I.

7. Methylation of CpG in SmaI site I reflects TCEAL7 inactivation in primary ovarian tumors

Since our data indicate using both in vitro promoter assay and methylation analysis that methylation at site I controls TCEAL7 transcription in the Xa cell line, we tested whether methylation at site I in primary tumors and cell lines is associated with loss of TCEAL7 expression. Methylation status of 16 CpG sites was determined by genomic sequencing of bisulfite-modified DNA. Representative chromatograms of bisulfite modified DNA corresponding to four SmaI sites in ovarian tumors are shown in Figure 7a. Semi-quantitative RT–PCR results for a subset of tumors are shown in Figure 7b. Consistent with the hypothesis that methylation of site I controls TCEAL7 expression, Biallelic methylation at site I in these samples reflects loss of TCEAL7 expression as evidenced by semi-quantitative RT–PCR analysis (Table 1, e.g. 4, 13, 206, 208, 402, 414, 34, 98, 121, 183, 235,

259, 339, and cancer cell lines). However, there were a few exceptions (Table 1, #45, 183, and 235). In these samples, TCEAL7 expression was lost although site I was hemimethylated, suggesting the involvement of other mechanisms in inactivation of TCEAL7. To determine if LOH could also be responsible for inactivation of TCEAL7, we analyzed both LOH and methylation in a subset of tumors. Majority of tumors with CpG site I methylation did not have LOH (Table 1, tumors highlighted in bold), suggesting that both mechanisms are not required to completely inactivate TCEAL7 expression. In addition, there was no correlation between the methylation status and age of patient. Together, these data are consistent with the hypothesis that TCEAL7 is monoallelically expressed and therefore requires a tumor-related epigenetic silencing to inactivate the active allele.

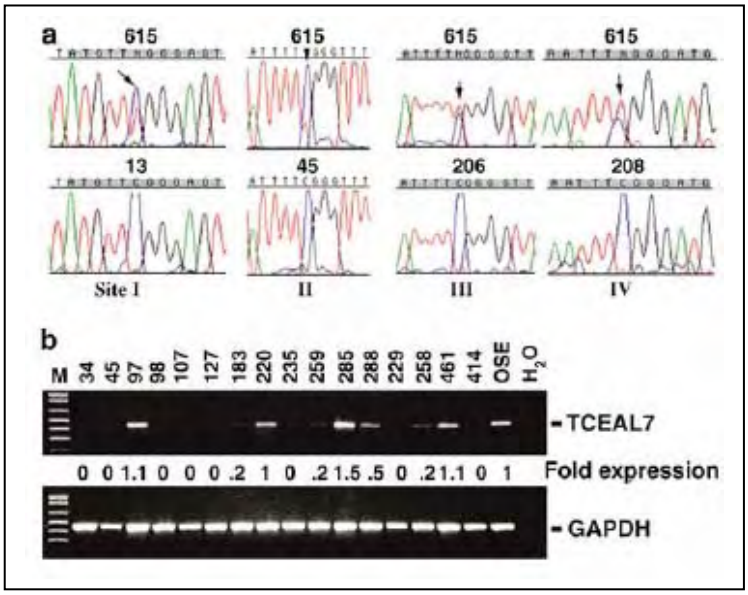

Figure 7: Genomic sequencing and expression analysis in primary ovarian tumor. **(a)** Representative chromatograms of bisulfite modified DNA from ovarian tumors. Sequences correspond to fourSmaI sites. Upper panels are taken from tumor #615. All four sites show hemimethylation (indicated by arrows). Examples of fully methylated CpGs in four SmaI sites are shown in the lower panel. **(b)** Expression of TCEAL7 in a small subset of tumors used in sequence analyses of bisulfite-modified DNA. Increase or decrease in fold expression compared to OSE is indicated between panels.

Table 1 Methylation status of sites I–IV in ovarian cell lines and primary tumors with corresponding TCEAL7 expression

	I	II	III	IV	RT–PCR	Age	LOH
OSEtsT	● □	● ● □	● □	□	++		
OSE54	● □	● ● □	● □	□	++		
OV167	● ●	● ● ●	● ●	●	–		
OV177	● ●	● ● ●	● ●	●	–		
OV202	● ●	● ● ●	● ●	●	–		
OV266	● ●	● ● ●	● □	●	–		
OVCAR5	● ●	● ● □	● □	●	–		
SKOV3	● ●	● ● ●	● □	●	–		
4	● ●	● ● □	● □	●	–	69	–LOH
13	● ●	● ● □	● ●	●	–	58	–LOH
34	● ●	● ● ●	● ●	●	–	44	
45	● □	● ● ●	● □	●	–	56	
97	● □	● ● ●	● □	●	++	55	+LOH
98	● ●	● ● ●	● □	●	–	57	–LOH
107	● ●	● ● ●	ND	●	–	48	–LOH
121	● ●	● ● ●	□	●	–	50	
183	● □	● ● ●	○	●	–	61	
206	● ●	● ● □	●	●	–	62	
208	● ●	● ● □	●	●	–	60	+LOH
220	● □	● ● ●	○	●	++	52	–LOH
235	● □	● ● ●	□	●	–	72	
259	● ●	● ● ●	□	●	–	54	
283	● ●	● ● ●	□	●	ND	64	
285	● ○	● ● ●	○	●	++++	70	–LOH
288	● □	● ● ●	○	●	+	80	
339	● ●	● ● ●	□	●	–	70	
358	● □	● ● ●	□	●	+	62	
402	● ●	● □	●	●	–	61	
414	● ●	● □	●	□	–	67	–LOH
461	● □	● ● ●	□	●	++	45	–LOH
615	● □	● □	□	□	ND	76	
656	● ND	● ND	●	●	ND	87	
657	● ND	● □	○	ND	ND	62	

Filled and unfilled circles represent methylated and unmethylated alleles, respectively. A circle with a line across represents hemimethylation. Expression X1.5-fold over OSE (++++), between 1.1 and 0.9-fold (++); p0.5 (+); no expression (–), not determined (ND); positive LOH (+LOH); negative LOH (_LOH). Samples used in RT–PCR (Figure 6b) and LOH analyses are highlighted in bold.

Based on the data presented above, we proposed to (1) determine effect of PAPX on tumor and cell growth *in vivo* and *in vitro*; (2) analyze genes regulated by PAPX by transcriptional profiling using microarray chips; and (3) identify proteins that interact with PAPX and elucidate the function of PAPX related to tumor suppression.

BODY

Aim #1: *Determine the effect of re-expression of PAPX on the colony formation efficiency, soft-agar growth, and tumorigenicity of ovarian cancer cells.*

Aim #1: *Determine the effect of re-expression of PAPX on the colony formation efficiency, soft-agar growth, and tumorigenicity of ovarian cancer cells.*

In our proposal we had the following experiments listed for this Specific Aim.

Task 1. To determine the effect of re-expression of PAPX on the malignant phenotypes of ovarian cancer cells:

a) Establish 4 PAPX- and 4 vector-transfected SKOV3 stable clones
b) Perform colony formation and soft agar growth assays in cell lines established in Task 1a
c) Perform assays to ascertain tumorigenic potential of stable cell lines established in Task 1a in nude mice

We elected to re-express PAPX in OV202, SKOV3, and A2780 to perform tumorigenic assays following re-expression. However, due to its pro-apoptotic property, we were not able to establish stable cell lines in these cells. *Therefore, we generated tetracycline-inducible SKOV3 cell line (as suggested by one of the reviewers).* Although the established tetracycline-inducible SKOV3 cell line proved to be tightly controlled by tetracycline compared to commercially available tetracycline-inducible cell lines, we were again unsuccessful in establishing a stable cell line due to minimal background level leakiness of expression. We are therefore opted to establish an alternative inducible system using Flp-In T-Rex from Invitrogen. **Using established cell line 293T Flp-In T-Rex, we were able to establish a stable cell line expressing inducible PAPX (**Figure 8).

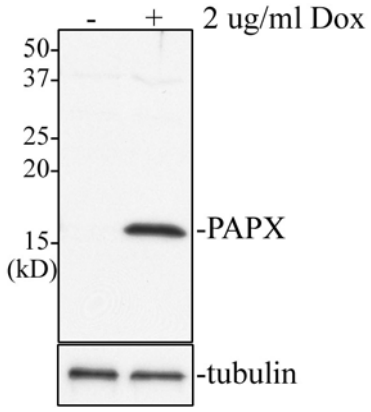

Figure 8. Inducible expression of PAPX in 293T Flp-In T-Rex system. Whole cell lysates were collected from cells treated with doxycycline for 24 h. Western blot analysis using affinity-purified PAPX antibody shows inducible expression of PAPX in doxycycline treated cells.

Our attempts to generate Flp-In T-Rex system in SKOV3 and A2780 are still ongoing.

An alternate more reliable approach to study the effect of a gene loss in tumorigenesis is to either generate a 1) stable knockdown of the gene *in vitro* in cell lines and 2) generate a knock out mouse model for *in vivo* studies.

<u>Results from Tasks 1a and b</u>

Due to the difficult nature of generating PAPX stable clones in SKOV3 cells and since none of the ovarian cancer cell lines (five Mayo established cell lines, SKOV3, OVCAR5, A2780, CP70, and C200) express PAPX, we were not able to perform RNAi-mediated knock-down to study the effect of PAPX down-regulation on tumorigenicity. Therefore we opted to generate shRNA downregulated stable clones in immortalized normal ovarian epithelial cells, OSE (tsT/hTERT) and test its tumorigenic potential *in vitro* and *in vivo*. Results from these experiments are described below and the *in vitro* data has been included as part of the manuscript currently under review in Cancer Cell. As stated in our previous report, ***PAPX has been renamed as TCEAL7 (transcription elongation factor A (SII)-like 7) in accordance with Genebank nomenclature.***

Previous studies by Westbrook *et al* indicates that primary epithelial cells immortalized with SV40 T-antigen and human catalytic subunit of telomerase (hTERT) provide an excellent model to test for genes associated with malignant transformation assessed by soft-agar growth [12]. Therefore, we tested the malignant transformation potential of TCEAL7 down-regulation in OSE(tsT)/hTert by soft-agar growth assay. To test whether down-regulation of TCEAL7 contributes to tumorigenesis of ovarian cancer, we selected an immortalized ovarian epithelial cell line (OSEtsT/hTERT) and down-regulated TCEAL7 expression by shRNA. The cells used for these studies are termed OSE(tsT) lines. Dr. Kalli has developed ovarian surface epithelial cell lines transduced with a temperature sensitive mutant of the SV40 large T antigen [13]. These cells proliferate continuously at 34°C but, upon destabilization of the T antigen, become quiescent at 39°C. These cells retain cytokeratin expression and senesce after 20-25 passages [14]. More recently, Dr. Kalli generated an apparently immortalized version of this cell line by transfecting the catalytic subunit of human telomerase hTert [OSE(tsT)/hTert]. These cells grow as efficiently at 37°C as at 34^{o}C, and have not currently undergone senescence (passage 65 and counting). They require surface attachment for growth and do not form colonies on soft agar (unpublished observation), indicating their lack of transformation. Because they are proliferating, they represent a long-term source of ovarian surface epithelial cells that can be transfected with various constructs and then selected for transgene expression. These cells are both geneticin and hygromycin B resistant.

9. Generation of shRNA downregulated TCEAL7 clones

For these studies, endogenous TCEAL7 expression in OSE(tsT)/hTert cells was downregulated by shRNAs. shRNAs targeted against two different regions of the TCEAL7 transcript were ligated into pRetroSuper [15]. The efficacy of shRNA mediated downregulation of TCEAL7 was evaluated by RT-PCR. Packaged retroviral stock were then used for transfecting OSE(tsT)/hTert cells. shRNA capable of suppressing >90% of expression were used. pRERO SUPER vector only construct was used a s a control. Several control and TCEAL7 siRNA clones were generated for each of the cell lines. Suppression of TCEAL expression was confirmed by RT-PCR. Transfection with shRNA targeted to TCEAL7 resulted in downregulation of TCEAL7 in two clonal lines of OSE(tsT/hTERT) (Fig 9A). No such downregulation was observed in clonal lines expressing non-silencing shRNA construct.

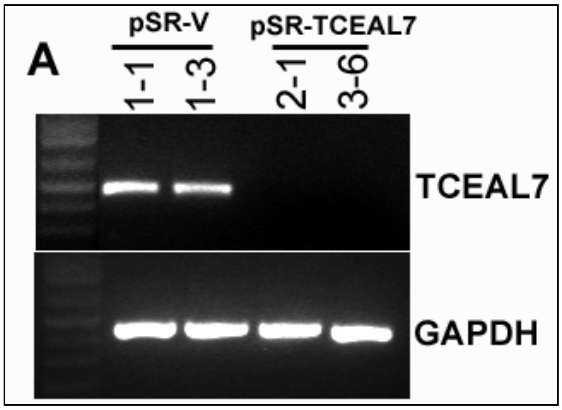

Fig 9A: Stable transfection of shRNA targeted to TCEAL7 transcript results in downregulation of TCEAL7. Agarose gel electrophoresis of RT-PCR products of TCEAL7 transcript levels in two stable pSR vector clones 1-1 and 1-3 (Lanes 2 and 3, top panel). Downregulation of TCEAL7 expression is seen in pSR- TCEAL7 shRNA clones 2-1 and 3-6 (Lanes 4 and 5, top panel). 1 Kb ladder is shown in lane 1. Lower panel shows control GAPDH levels in the clones tested.

Subsequent soft-agar growth assays of these cell lines indicate that down-regulation of TCEAL7 promotes significant soft-agar growth of OSE(tsT/hTERT) cells (Fig 6B-C).

10. Soft agar assay

Complete medium containing 0.8% low-melting point temperature agarose was poured into six well plates (2 ml per well) and allowed to solidify at 4°C to form a bottom layer. Control pSR and TCEAL7 shRNA downregulated OSE(ts/hTERT*)* cells (20,000 per well; vector 1-1 and 1-3 or TCEAL7 shRNA downregulated clones 2-1 and 3-6) were mixed in complete medium with 0.45% agarose and seeded as a top layer. The agarose was solidified at 4°C and then incubated at 34°C. Growth on soft agar was monitored for three weeks. Colonies were stained with 1 ml of PBS containing 0.5 mg/ml p-iodonitrotetrazolium violet, which is converted into colored product by live cells only. Micrographs were taken at 10x using a Spot II-RT digital camera (Nikon, Millburn, NJ), and colonies larger than 50 μm and 100 μm in diameter were counted.

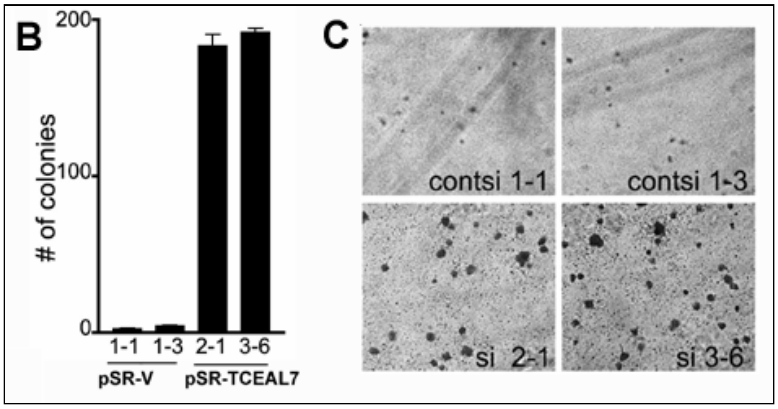

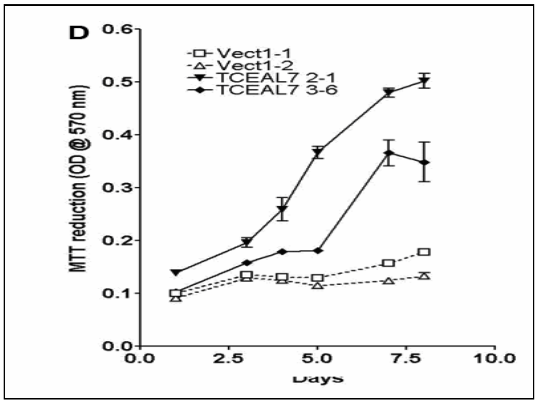

Fig 10B, Down-regulation of TCEAL7 promotes soft-agar growth of immortalized non-transformed OSE(tsT/hTERT). Control pSR and TCEAL7 shRNA downregulated OSE(ts/hTERT) cells (20,000 per well; vector 1-1 and 1-3 or TCEAL7 shRNA downregulated clones 2-1 and 3-6) were grown on soft agar for 3 weeks in triplicates. pSR- TCEAL7 shRNA clones 2-1 and 3-6 formed colonies on soft agar indicating anchorage independent growth, while the control pSR vector transduced clones did not. **C**, Representative photomicrographs of OSE(tsT/hTERT) cell lines grown on soft-agar. Colonies were stained with 1 ml of PBS containing 0.5 mg/ml p-iodonitrotetrazolium violet, which is converted into colored product by live cells only. Micrographs were taken at 10x using a Spot II-RT digital camera (Nikon, Millburn, NJ), and colonies larger than 50 µm and 100 µm in diameter were counted. **D,** MTT reduction assay indicates increased cell mass with down-regulation of TCEAL7 (lines represented by solid symbols).

11. Characterization of additional shRNA downregulated TCEAL7 clones.

Three additional shRNA TCEAL7 clones were generated and tested for soft agar growth and proliferative potential. All three clones 4-2, 4-4 and 12-2 showed higher proliferative rate and increased soft agar growth compared to vector transduced clones (figures 7A and B) indicating that the observed differences in transformation and proliferative potential was not just due to clonal variation.

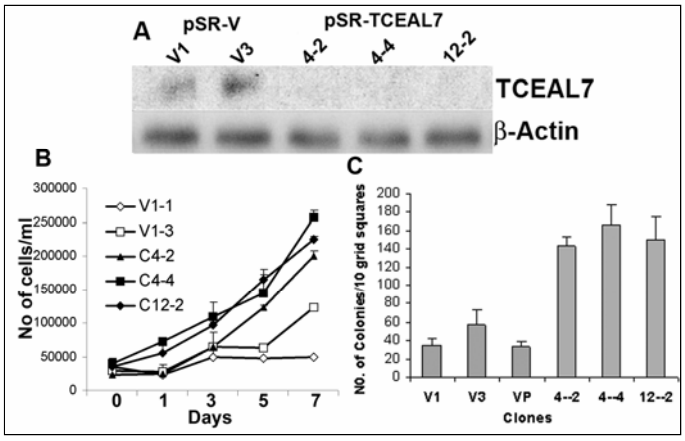

Figure 11: Down-regulation of TCEAL7 promotes proliferation and soft-agar growth. **A.** Western blot analysis of TCEAL7 expression in two vector-transduced and three shRNA-transduced (si4-2, 44-4 and 12-2) clones. Lower panel Beta actin loading controls. **B,** MTT reduction assay indicates increased cell mass with down-regulation of TCEAL7 (lines represented by solid symbols).**C,** Down-regulation of TCEAL7 increases soft-agar growth indicating transforming potential of TCEAL7 down-regulation. Bar graph of # colonies counted in the clones.

. Based on these data, we are currently testing vector clone 1, and a pooled vector clones, and shTCEAL7 clones 4-2 and 4-4 for their ability to form tumors in nude mice.

Task 1c: Perform assays to ascertain tumorigenic potential of stable cell lines established in Task 1a in nude mice. These experiments are still ongoing.

In preliminary in vitro experiments we have demonstrated the ability of immortalized non-tumorigenic ovarian surface epithelial (OSE(ts/ThTERT) cells with the downregulation of TCEAL7 to form colonies in soft agar compared to its vector counterpart (Figs 10 and 11). Several TCEAL7 downregulated and vector clones were generated for studies in vivo. These cells were not previously passaged in mice.

Aliquots containing 5 x 10^6 cells in 0.1 ml phosphate-buffered saline were mixed with 0.1 ml growth factor containing matrigel and injected subcutaneously into the right or left flanks of athymic nude mice. Each mouse was injected (sc) on both right and left flanks (one clone per flank) using TCEAL7 expressing clones named 4-2 and 4-4 and vector expressing clones V-1 and V-P. Use of both flanks allows reduced numbers of animals while increasing the sample number. Since these are ovarian cancer cells, we also injected these clonal lines

intraperitoneally to evaluate whether they will form ascites. Mice are being weighed twice weekly to monitor the loss or gain of weight consistent with disease progression. At the onset of ascites development, animals will be sacrificed according to approved guidelines (CO2 inhalation, MCE-15). The ascites will be collected for further evaluation to establish cell cultures and biochemical assays.

Animals in both sc and ip studies will be observed for up to 20 weeks for measurement of latency time or the failure to develop tumor nodules at the implantation site. At the time of sacrifice, tumors will be removed for histological assessment and storage in liquid nitrogen for subsequent studies to ensure that the TCEAL7 expression is still retained in these samples.

The following section describes the Experimental details of the ongoing mouse related studies.
Experiment 1: started under IACUC # A33603- subcutanous flank injections on 14 flanks from 14 separate mice per clone. Each mouse will receive 2 flank injections from 2 separate clones. The 4 clonal lines include V-1. V-P, 4-2, and 4-2.

Group 1: V-1 (OSE vector)-left flanks + clone 4-2 (OSE TCEAL7 down)-right flanks in 14 mice
Group 2: V-P (OSE vector)-right flanks + clone 4-4 (OSE TCEAL7 down)-left flanks in 14 mice
Experiment 1 total= 28 mice

Experiment 2 : i.p. injections of the 4 clonal lines V-1. V-P, 4-2, and 4-2 started under IACUC #A33603
V-1 (OSE vector) 13 mice
V-P (OSE vector) 13 mice
4-2 (OSE TCEAL7 down) 13 mice
4-4 (OSE TCEAL7 down) 13 mice
Experiment 2 total= 52 mice

The sample size per condition will allow 80% power to determine a 50% change in oncogenic potential that is statistically (and biologically) significant (alpha=0.05) (letter of collaboration, Dr. Ann Oberg). Mice will be monitored daily and growth of subcutaneous tumors measured twice weekly for 20 weeks with the tumor volume calculated according to the formula V = a2b/2, where a is the shortest and b the longest diameter. Data will be analyzed using repeated measurements ANOVA (analysis of variance) including a growth curve analysis. The sample size accounts for premature loss of mice before data can be obtained.

Repeating flank injections with increasing numbers of mice per clone may be required if the tumor growth of the TCEAL7 clones is a low percentage of 10-20% compared to the vectors. This low percentage tumor take rate may not be observed with the current experimental design. Similar studies in mice with immortalized normal cell lines have shown up to 50 mice per clone to obtain significant differences from the controls. In the case that Experiment 1 does not generate meaningful results, we will repeat the study with 40 mice per clone (Experiment 3).

Experiment 3: flank injections on 40 flanks from 40 separate mice per clone. Each mouse will receive 2 flank injections from 2 separate clones. The 4 OSE clonal lines include V-1, V-P, 4-2, and 4-4.

V-1 (OSE vector) on left flanks+ clone 4-2 (OSE TCEAL7 down) on right flanks in 40 mice V-P (OSE vector) on right flanks + clone 4-4 (OSE TCEAL7 down) on left flanks in 40 mice
Experiment 3 total # mice = 80
Experiments 1 + 2 + 3 = 160 mice
IACUC A33603 mice # used in the above proposed Experiments 1 & 2 = 53
Requested # mice = 160 - 53 = 107.

Specific Aim 2: To determine the transcriptional response induced by TCEAL7.
Due to the difficult nature of establishing stable cell lines in ovarian cancer as stated above, this project awaits the establishment of tetracycline-inducible ovarian cancer cell lines. Meanwhile, we used transient TCEAL7

expression and performed microarray analysis on these cells. Preliminary profiling analysis indicates upregulation of several apoptotic genes following PAPX transfection as reported earlier. Additional microarray analyses on U133Plus2 chips following TCEAL7 induction in 293T Flp-In T-rex system yielded relatively smaller # of differentially expressed genes with statistical significance. The experiments were run in duplicates.

Table 2: List of the top 20 out of 22215 probesets (sorted by p-value)

Rank	AffyID	CytoBand	GeneSymbol	Mean Diff (log2 scale)	Ratio of Means (raw scale)	t-statistic	p-value
1	211371_at LocusLink UnigeneID	15q22.31 /// 15q22.31	MAP2K5	-0.76102	0.59008	-10.49	0.008974
2	202875_s_at LocusLink UnigeneID	6p21.3	PBX2	-0.20342	0.86849	-5.034	0.03727
3	208719_s_at LocusLink UnigeneID	22q13.1	DDX17	-0.22579	0.85513	-5.021	0.03745
4	201140_s_at LocusLink UnigeneID	17q21.2	RAB5C	-0.17931	0.88313	-4.911	0.03905
5	205308_at LocusLink UnigeneID	8q21.11	CGI-62	-0.12223	0.91877	-4.829	0.0403
6	214250_at LocusLink UnigeneID	11q13	NUMA1	0.076561	1.0545	4.824	0.04038
7	204983_s_at LocusLink UnigeneID	Xq26.1	GPC4	-0.17038	0.88861	-4.556	0.04495
8	205967_at LocusLink UnigeneID	6p21.3	HIST1H4F	-0.17367	0.88658	-4.486	0.04627
9	206355_at LocusLink UnigeneID	18p11.22-p11.21	GNAL	-0.2241	0.85613	-4.482	0.04635
10	212037_at LocusLink UnigeneID	14q13.3	PNN	0.20182	1.1501	4.464	0.04669
11	205394_at LocusLink UnigeneID	11q24-q24	CHEK1	0.13398	1.0973	4.346	0.04908
12	211720_x_at LocusLink UnigeneID	12q24.2 /// 12q24.2	RPLP0	-0.16406	0.89251	-4.335	0.04932
13	211517_s_at LocusLink UnigeneID	3p26-p24	IL5RA	-0.13243	0.9123	-4.314	0.04976
14	216112_at UnigeneID	---	---	-0.14553	0.90405	-4.246	0.05125
15	205196_s_at LocusLink UnigeneID	7q22.1	AP1S1	-0.20717	0.86623	-4.206	0.05215
16	40489_at LocusLink	12p13.31	DRPLA	-0.23567	0.84929	-4.204	0.05219

Rank	AffyID	CytoBand	GeneSymbol	Mean Diff (log2 scale)	Ratio of Means (raw scale)	t-statistic	p-value
	UnigeneID						
17	201152_s_at LocusLink UnigeneID	3q25	MBNL1	0.13957	1.1016	4.178	0.05278
18	210549_s_at LocusLink UnigeneID	17q21.1	CCL23	-0.15237	0.89977	-4.172	0.05293
19	218647_s_at LocusLink UnigeneID	1p34.2	FLJ23476	0.18372	1.1358	4.037	0.05624
20	218010_x_at LocusLink UnigeneID	20q13.33	C20orf149	-0.17601	0.88515	-4.019	0.05668
21	220707_s_at LocusLink UnigeneID	22q13.1	FLJ23322	-0.22748	0.85412	-3.926	0.05918

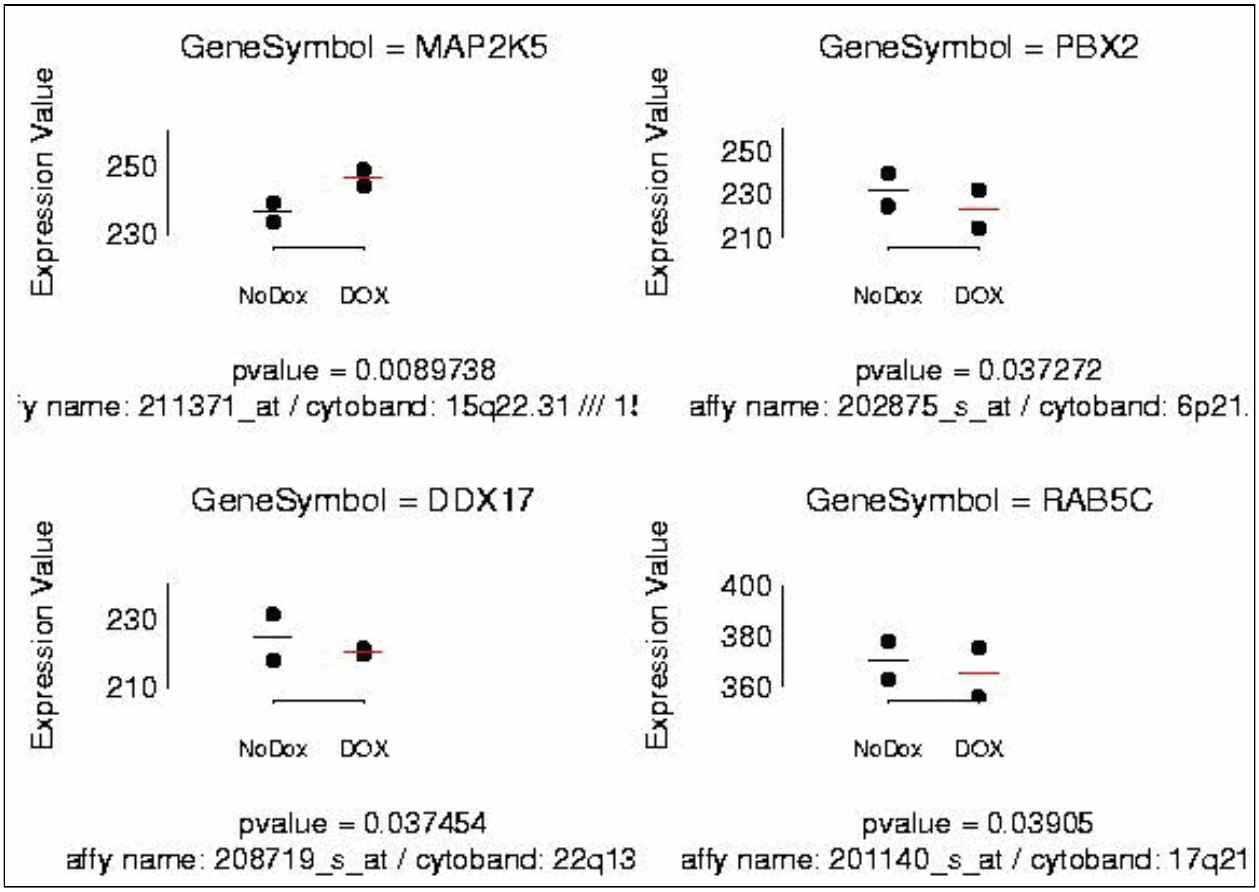

Fig 12: Representative Dot blots of differentially expressed genes on TCEAL7 induction in HEK293T cells. The gene symbols, expression values, p values and the chromosomal locations are indicated in each of the dot blots.

Aim #3: *Characterize cellular proteins interacting with TCEAL7.*

12: Identification of TCEAL7 interacting proteins

We utilized antibody array (Hypomatrix) containing antibodies against known proteins involved in apoptosis to screen for potential TCEAL7 interacting proteins. This analysis led to identification of three proteins (Bin1, DcR2, and FAST) to be potential interacting proteins (Figure 12).

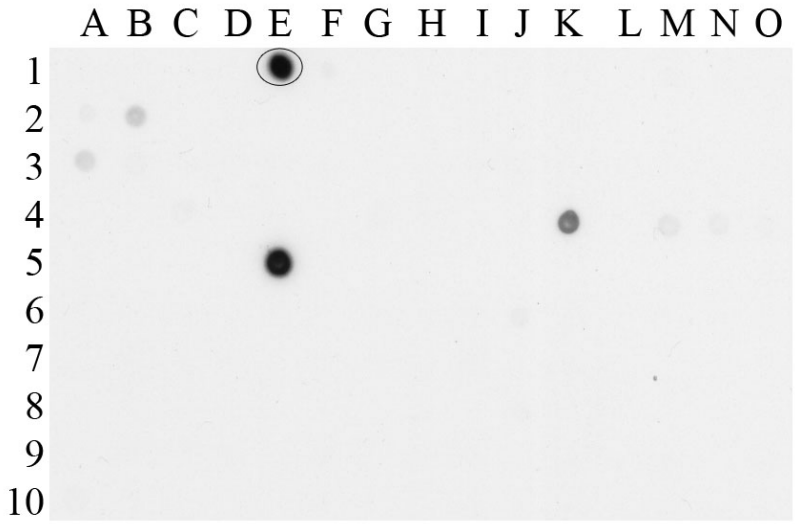

Figure 12. Protein-Protein interaction screening with the Antibody Array from Hypomatrix (CAT # HM4000). Bin1 is indicated by circle. The other two intense dots are DcR2 and FAST.

13. TCEAL7 associates with Bin1

Bin1 is a c-myc-interacting protein that regulates myc trans-activation [16-18]. Furthermore, Bin1 induces caspase-independent cell death [19]. Since TCEAL7 is also a nuclear protein, it is possible that TCEAL7 may modulate Bin1 interaction with myc. Moreover, TCEAL7 may cooperate with Bin1 in inducing cell death. Therefore, we selected Bin1 for further characterization. Immuno-precipitation results suggest that TCEAL7 interacts with Bin1 via BAR domain of Bin1 (Figure 13).

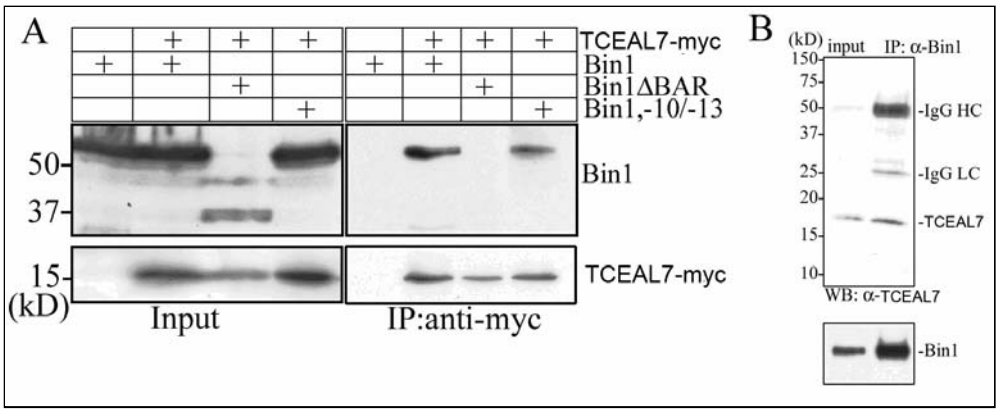

Figure 13. A: TCEAL7 co-immunoprecipitates full-length or Myc-binding domain-deleted Bin1 but not BAR domain-deleted Bin1, suggesting that TCEAL7 interacts with Bin1 through BAR domain of Bin1. **B**: Immunoprecipitation of Bin-1 also coimmunoprecipitates TCEAL7.

14: TCEAL7 co-operates with Bin1 to modulate Myc activity

To test whether TCEAL7cooperates with Bin1 in suppressing Myc activity, cells were transfected with TCEAL7 or Bin1 alone or together and myc activity was assessed by luciferase reporter gene containing ODC promoter (a natural promoter containing myc-binding site) or artificial E-box promoter (pEMS) [18]. The result shown in Figure 14A, suggest that TCEAL7suppresses myc activity as determined by pEMS. or an artificial promoter containing multimerized CACGTG E boxes that are bound by Myc (EMS promoter) (Figure 14B). In contrast, expression of TCEAL7 has no suppression effect on non-specific Bcl-2 or p21 promoter activity (Figure 14C). As shown in Figures 10A and 10B using either the ODC or the EMS promoter constructs, co-expression of Bin1 and TCEAL7 also suppresses Myc activity. However, no synergistic effect was observed with the co-expression of Bin1 and TCEAL7. Overexpression of the Bin1 (-10-13) isoform that lacks an intact c-Myc binding domain (MBD) partially attenuated TCEAL7 suppression on Myc activity. These results suggest a possibility that interaction between TCEAL7 and Bin1(-10/-13) titrates TCEAL7 away from Myc, thereby attenuating the ability of TCEAL7 to suppress the transactivation activity of Myc. On the other hand, co-

expression of TCEAL7 and the Bin1 mutant lacking an intact BAR domain (Bin1ΔB) produces maximal suppression of Myc. Taken together, these results suggest that TCEAL7 and Bin1 may act to suppress Myc transactivation activity.

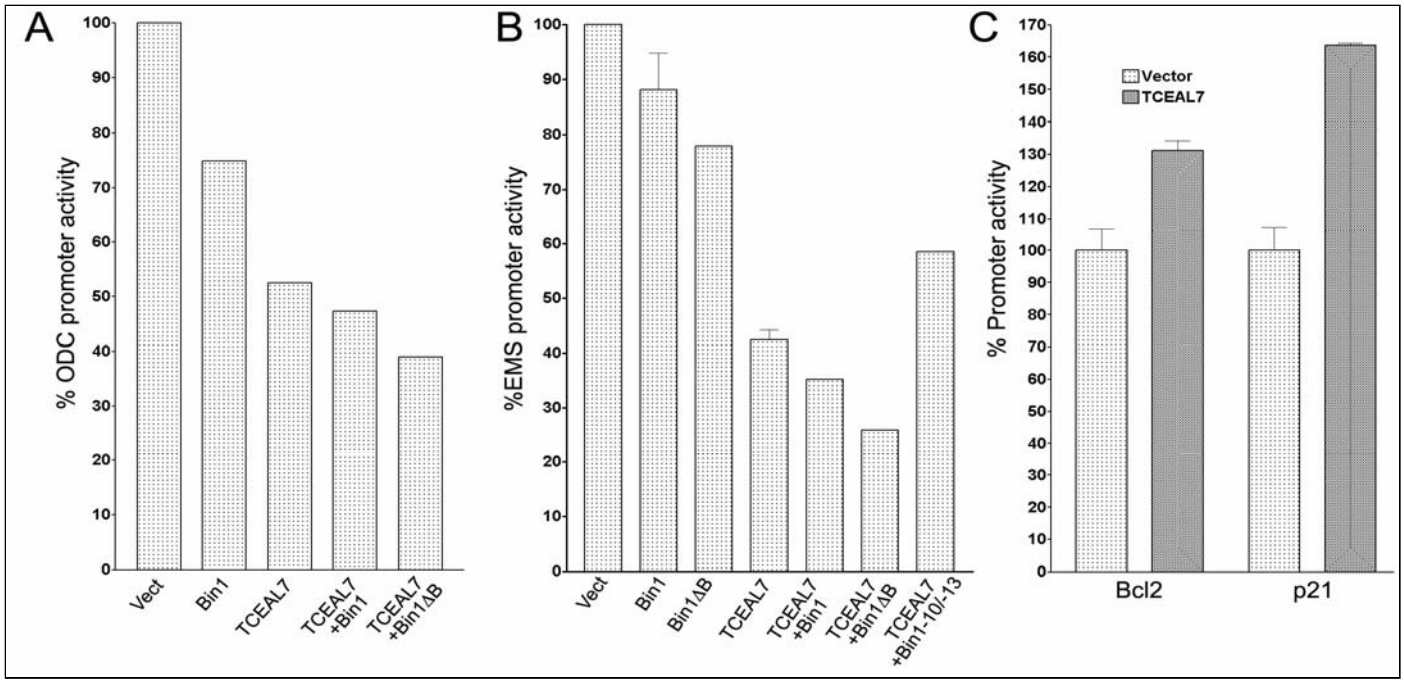

Figure 14. Suppression of c-Myc transcriptional activity by TCEAL7. **A**, TCEAL7 suppresses c-Myc transcriptional activity as determined by Ornithine decarboxylase (pODC) promoter luciferase activity. HeLa cells were seeded at 5 x10^5 per well in six well plates (in triplicates) one day prior to transfection. 0.5 μg Vector-GFP and 0.5 μg TCEAL7-GFP and/or various Bin 1 constructs were cotransfected with 0.5 μg pODC and 0.1 μg Renilla reporters, and luciferase activity was measured 24 hr post-transfection with Promega's Dual-Luciferase Reporter (DLR) assay system according to manufacturer's instructions. The relative light units (RLU) are expressed per μg protein after normalizing with Renilla luciferase. **B**, TCEAL7 suppresses c-Myc transcriptional activity as determined by E-box Myc Binding Site promoter luciferase activity. For c-Myc transcriptional activity luciferase assay, cells were transfected with Renilla luciferase plasmid, pEMS, and various constructs of Bin1 and TCEAL7. Twenty four hours after transfection, cells were lysed in passive lysis buffer and luciferase activity was measured with Promega's Dual-Luciferase Reporter system according to manufacturer's instructions. **C**, TCEAL7 enhances promoter activity of Bcl2 and p21. The luciferase activity was measured as above in the presence of either Bcl2 or p21 promoter reporters co-transfected with Renilla luciferase plasmid and TCEAL7 expression construct. The graphs depict luciferase activities relative to reporter (without TCEAL7) only controls. The data represents three trials performed in duplicates. All luciferase activities were normalized with Renilla luciferase activity to account for variability in transfection efficiency, and expressed as a percentage of the vector control.

15. TCEAL7 SUPPRESSES CYCLIN D1

To test whether TCEAL7 expression could affect the expression of Myc-target genes, we selected cyclin D1 since it is deregulated in various malignancies and plays a critical role in regulating cell cycle progression. Expression of TCEAL7 resulted in down-regulation of both promoter activity and steady-state protein levels of cyclin D1, as determined by luciferase reporter assay (Figure 15A) and immunoblot analysis, respectively (Figures 15B-C). Since TCEAL7 is not expressed in majority of cancer cell lines, we attempted to generate stable cell lines expressing TCEAL7 in cancer cells. However, due to growth inhibitory effect of TCEAL7 overexpression, we were not successful in generating stable cell lines. Therefore, we generated a cell line expressing inducible TCEAL7 in 293T-FlpIn(TRex) cells to further characterize the function of TCEAL7 (Figure 15D). We selected this cell line because it permits well-defined integration and regulated expression of TCEAL7. We then used this cell line to test whether TCEAL7 is recruited to cyclin D1 promoter by chromatin immunoprecipitation analysis using anti-TCEAL7 antibody. Chromatin immunoprecipitation (ChIP) and PCR was performed from extracts prepared from cells that were grown 24 hr under control or gene induction conditions. We observed enrichment of a fragment of the cyclin D1 promoter that contained the E box sequence recognized by c-Myc, but not other regions of the cyclin D1 promoter (Figure 6E). No enrichment of the E box-containing DNA fragment was detected in cells grown in the absence of TCEAL7 gene induction by doxycycline (Figure 15E). These results suggest that TCEAL7 is specifically recruited to the Myc-binding region on the

cyclin D1 promoter. Analysis of cyclin D1 expression in cell cycle-synchronized HeLa cells with nacodazole as described in the methodsshow that expression of TCEAL7 not only suppresses cyclin D1 expression but also delays its cell-cycle-regulated expression by at least six hours (Figure 15F). Accordingly, TCEAL7 expression also correlated with a reduction in the number of cells entering S phase as determined by BrdU labeling (Figures 15G and H). Taken together, these observations offered evidence that TCEAL7 targeted cyclin D1 expression through a mechanism that is consistent with modulation of Myc activity.

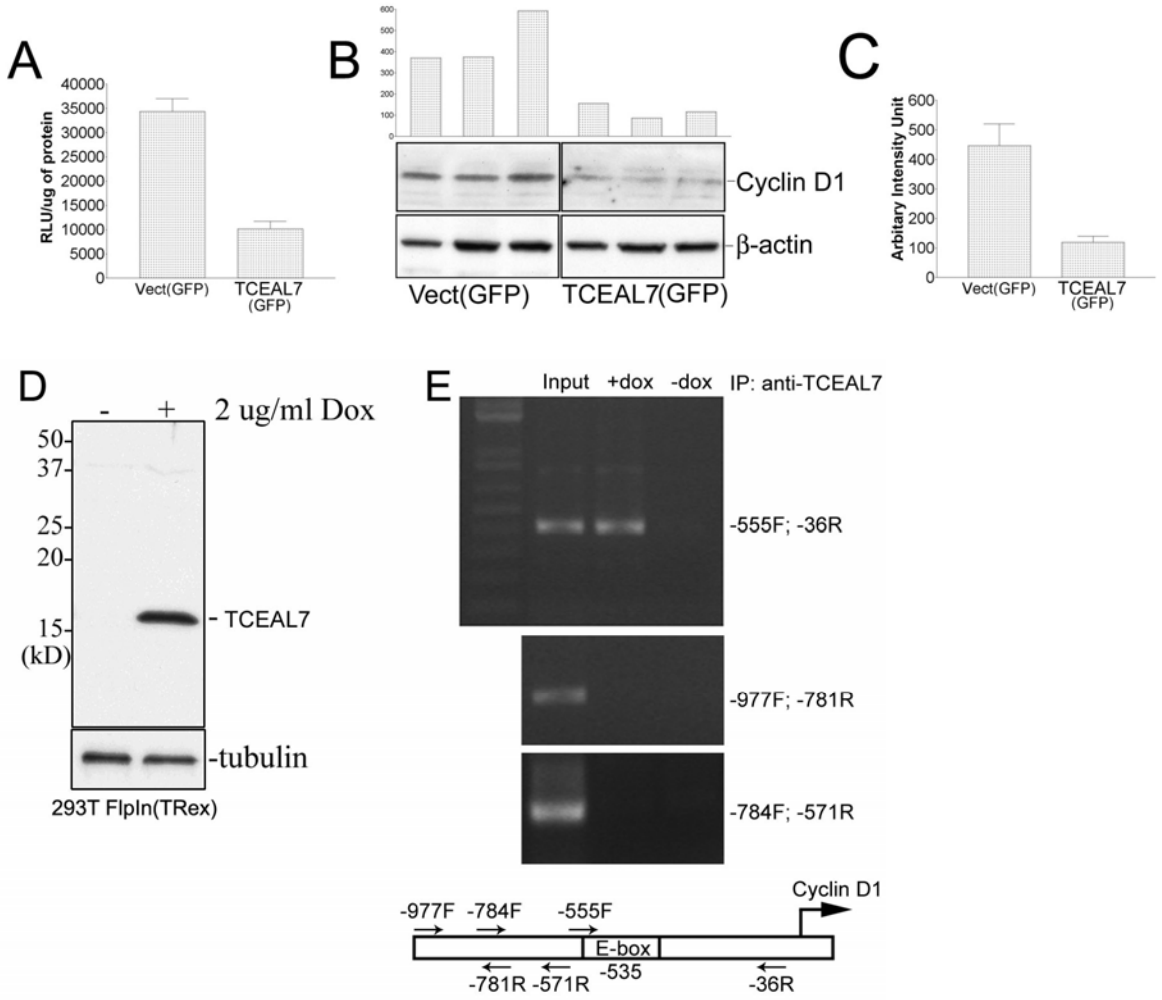

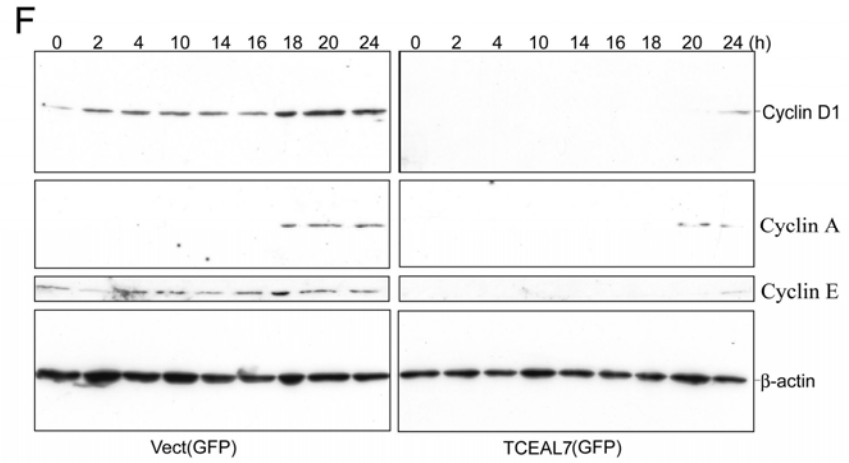

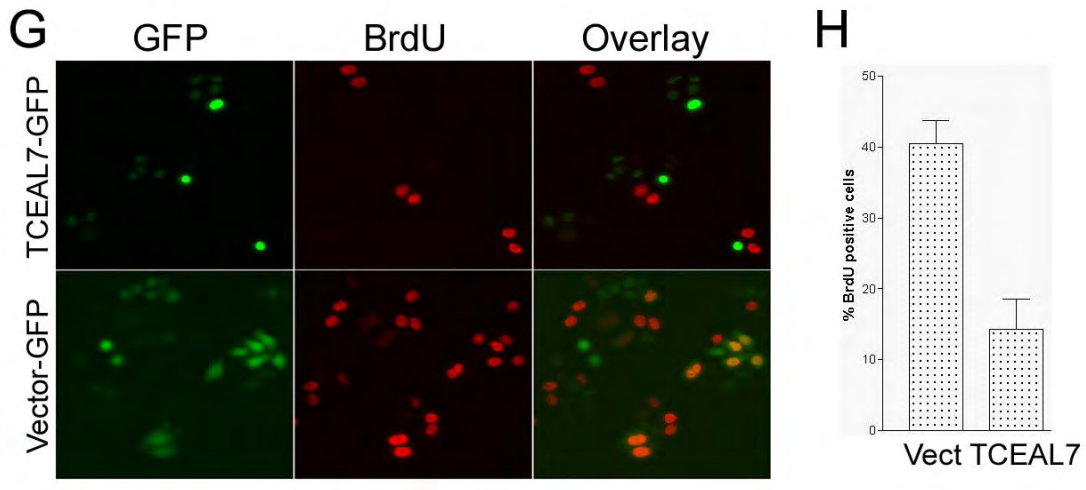

Figure 15:. TCEAL7 transcriptionally downregulates cyclin D1. **A**, TCEAL7 suppresses cyclin D1 promoter activity. HeLa cells were seeded at 5 x10^5 per well in six well plates (in triplicates) one day prior to transfection. 0.5 μg Vector-GFP and 0.5 μg TCEAL7- GFP constructs were cotransfected with 0.1 μg Renilla reporter and 0.5 μg of cyclin D1 promoter (D1-973LUC) driving luciferase reporter. Luciferase activity was measured 24 hr post-transfection with Promega's Dual-Luciferase Reporter (DLR) assay system according to manufacturer's instructions. The relative light units (RLU) are expressed per μg protein after normalizing with Renilla luciferase. **B**, TCEAL7 down-regulates cyclin D1 expression. Following 48 hrs of TCEAL7 transfection into HeLa cells, cell lysates were resolved on SDS-PAGE, and expression of cylcin D1 was determined with anti cyclin D1 antibody. Three lanes represent three independent transfections. **C**, Quantification of cyclin D1 expression by densitomeric analysis indicates down-regulation of cyclin D1 by TCEAL7. **D**, 24 hours doxycycline treatment of 293T FlpIn-TRex cells containing stable integration of TCEAL7 results in TCEAL7 expression (Lane 2). **E**, Doxycycline induced TCEAL7 expressing cells were subjected to ChIP analysis with anti TCEAL7 antibody and PCR amplified with specific cyclin D1 promoter primers as described in the Methods section. ChIP analysis indicates PCR amplification of cyclin D1 promoter containing E-box in sample pre-treated with doxycycline (with -36R and -555F primers). Lower panels show absence of cyclin D1 promoter PCR product outside the region of E-box in ChIP samples (-781R with -997F and -784F with -571R primer sets). Positions of primers and E-box are indicated in the schematic representation of cyclin D1 promoter relative to transcriptional start site. **F**, Suppression of cyclin D1 expression by TCEAL7 in cell-cycle synchronized HeLa cells. HeLa cells grown to 60-80% confluence in 10 cm dishes were treated with 2.5 μM nocodazole for 16 hours. Mitotic cells were collected, centrifuged, washed 2 times in PBS, and replated in regular growth medium. Cells lysates were collected at different time points and immunoblotting was performed using anti-cyclin D, E and A antibodies. Please note the basal levels of cyclin D1 in vector-transfected controls and upregulation of cylcin D1 in these cells 18 hrs after the cell-cycle release. In contrast, TCEAL7-tranfected cells showed induction of cyclin D1 only after 24 hrs following cell-cycle release. **G**, TCEAL7 expression results in reduction of BrdU-positive cells. BrdU labeling was performed as described in the methods section. Incorporated BrdU was detected by TRITC-conjugated anti-BrdU antibody (Becton Dickinson, Mountain View, CA). The *red* color, indicating BrdU staining, and TCEAL7-GFP positive cells were documented using a Spot camera. The total numbers GFP positive cells as well as BrdU-labeled cells were counted in 5–10 different fields of each well. **H**, Quantification of BrdU-positive cells in vector control and TCEAL7-tranfected cell populations.

16. MODEL: Based on the results from the present study, we propose the following model for suppression of Myc activity by TCEAL7 (Figure 16) (modified from Baudino and Cleveland 2001). In the model, Myc is in a transcriptionally competent state that is induced by Myc:Max interaction (1). When Max interacts with Mad, Myc is in a transcriptionally repressive state (2). Max switches between competence for transcriptional activation and repression based on its interaction with Myc or Mad (3). The association of bimodular or ternary complexes of Myc with TCEAL7, Bin1, or both proteins titers Myc away from Max, thereby licensing the availability of Max for interaction with Mad to repress Myc target genes which Myc expression persists (4). The Bin1 (-10-13) splice isoform lacking an intact MBD can weakly interact with TCEAL7 and thereby titer TCEAL7 away from Myc, thereby limiting the amount of Myc available to bind Max and to induce Myc target genes (5). By modulating Myc availability, TCEAL7 may indirectly limit formation of Mad/Max complexes that can regulate transcriptional targets such as cyclin D1 which directly control proliferation (6). In the model, down-regulation of TCEAL7 in cancer cells would effectively attenuate a negative regulatory pathway that can act to restrict Myc activity, thereby promoting Myc-induced malignant transformation.

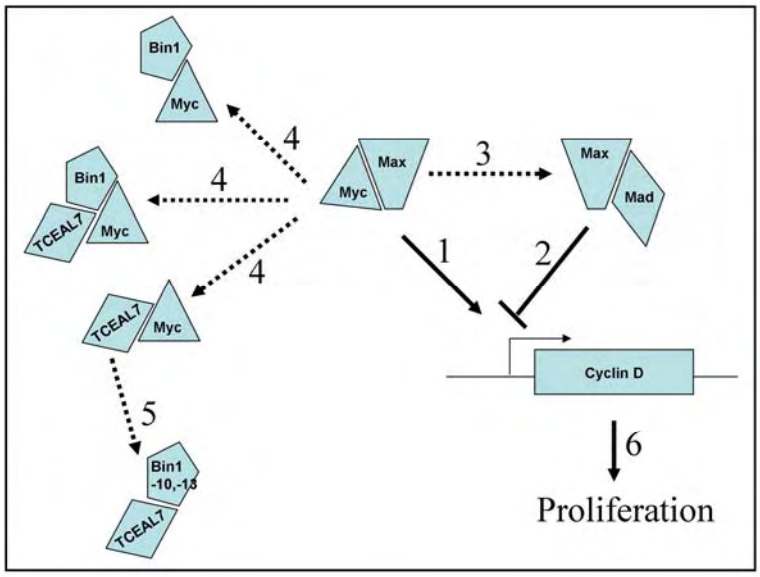

Fig 16: Proposed model for suppression of c-Myc by TCEAL7.
1, Myc induced transcriptional activation requires dimerization of Myc with Max.
2, Mad inhibits Myc activity by interacting with Max.
3, Max-Mad interaction titrates Max away from Myc, thus suppressing Myc activity.
4, Interaction of Bin1 and/or TCEAL7 with Myc may titrate Myc away from Max thus leading to inhibition of Myc activity.
5, Interaction of Bin1(-10/-13) and TCEAL7 may titrate TCEAL7 away from Myc, thus relieving its suppression on Myc.
6, Inhibition of Myc may result in suppression of cyclin D1 promoter activity and colony formation efficiency.

KEY RESEARCH ACCOMPLISHMENTS:

- Generation of antiTCEAL7- polyclonal antibody
- Identification of TCEAL7 as Bin1 binding protein
- Functional characterization of TCEAL7 and Bin1 interaction
- Identification of TCEAL7 as a regulator of Myc activity
- Validation of TCEAL7 expression in a large set of tumor samples
- Epigenetic silencing of TCEAL7 as a mechanism of inactivation of TCEAL7 expression.
- Establishment of tetracycline inducible 293T cell line expressing TCEAL7
- Transcriptional profiling of cells transiently expressing TCEAL7
- Identification of candidate targets of TCEAL7
- Characterization of TCEAL7 downregulated clones in terms of soft agar growth and proliferation.

REPORTABLE OUTCOMES:

ABSTRACTS

1. Julie Staub, Jeremy Chien, Rajeswari Avula, David I Smith, Scott H Kaufmann and **Viji Shridhar**. Epigenetic silencing of a novel tumor suppressor gene in ovarian cancer. Poster presentation AACR, 95th Annual meeting, Orlando, FL, 2004.

2. Jeremy Chien, Keishi Narita, Ravi Shridhar, Yunqian Pan , Julie Staub, Heyu Zhang, Jinping Lai, Lewis Roberts, Lynn C Hartmann, Scott H. Kaufmann, George C. Prendergast, and Viji Shridhar. Candidate tumor suppressor gene TCEAL7 associates with Bin1 and regulates Myc. Womens Cancer Program Oct 26, 2006, Mayo Clinic, Rochester, MN.

3. Ramandeep Rattan, Jeremy Chien, Keishi Narita, Julie Staub, Shailendra Giri and Viji Shridhar. A Putative Novel Tumor Suppressor Modulates NFκB activity. Oral presentation at the AACR, 98^{h} Annual meeting, Los Angeles, CA, 2007. Selected for Oral Presentation in a minisymposium.

MANUSCRIPTS

1. Chien J, Staub J, Avula R, Zhang H, Liu W, Hartmann LC, Kaufmann SH, Smith DI, **Shridhar V**. Epigenetic silencing of TCEAL7 (Bex4) in ovarian cancer. Oncogene 2005 Jul 28; 24(32):5089-100.

The support form DOD OCRP is acknowledged in the.

PATENTS APPLIED

A method of killing tumor cells by administering BEX4 polypeptide.

CELL LINES

- Generation of stable pSR vector only and TCEAL7 shRNA downregulated clones in OSEtsT/hTERT cells.

FUNDING APPLIED FOR BASED ON WORK

Department of Defense Ovarian Cancer Program, 2006- Idea Development Award.- Was not funded
National Cancer Institute, 2007- To be reviewed in July 2007

EMPLOYMENT OR RESEARCH OPPORTUNITIES APPLIED FOR AND/OR RECEIVED BASED ON EXPERIENCE/TRAINING SUPPORTED BY THIS AWARD.

- Based on the work supported by DOD, I hired Dr. Ramandeep Rattan, a postdoctoral research fellow, to determine the NF kappaB pathway modulated by TCEAL7.

- Dr. Rattan was successful in procuring a Postdoctoral Excellence Award from the Ovarian Cancer Research Foundation to pursue the detailed characterization of this pathway modulated by TCEAL7 in ovarian cancer.

CONCLUSIONS:

Identification of PAPX as a regulator of myc that is lost in several different carcinomas is highly significant as it may promote myc-induced malignant transformation by relieving repression on myc activity. These findings raise several important questions as well as previously indicated such as

1. What is the role of Bin1 –10,-13 isoform?
2. Can it promote myc activity by antagonizing TCEAL7 in TCEAL7expressing cells?
3. Is Bin1 –10,-13 upregulated in cancer?
4. Could TCEAL7 be targeted for therapy to counteract the effect of myc-induced transformation?

The fact that TCEAL7 expression is epigenetically silenced in ovarian cancer might be of clinical significance because unlike mutation where DNA information is irreversibly changed, epigenetic modification can be reversed by DNA methyl transferase inhibitors or histone modifying agents [20]. With the emerging role of the use of small molecule inhibitors that modify the enzyme activities of DNA methyl transferases and histone deacetylases in "epigenetic therapies" [21], TCEAL7 could serve as a potential target of such therapy. It is suggested that re-expression of silenced apoptotic genes by epigenetic therapy might re-sensitize drug resistant cancer cells to conventional chemotherapy [22]. In that sense, re-activation of TCEAL7 in chemoresistant ovarian cancer might be of clinical relevance. Finally, due to its widespread loss in ovarian cancer, TCEAL7 may potentially be used as an epigenetic marker for detection of ovarian cancers at earlier stages.

Recently, several cell culture and genetically engineered mouse models of ovarian human cell transformation in which co-expression of co-operating oncogenes and tumor suppressor genes have been described [23-26]. These models have been useful in defining minimum genetic alterations required for transformation in a genetically defined context. To date, most of these models have included genes already implicated in human tumorigenesis. With the emergence of the RNA interference technology as a means to silence gene expression, additional genes not previously implicated in human cell transformation have been identified [12, 27]. In this study using an immortalized normal ovarian epithelial cell, we have identified that silencing TCEAL7 confers these cells the property of soft agar growth, an *in vitro* hallmark of transformation. shRNA downregulated TCEAL7 clones formed colonies on soft agar while control vector transfected clones did not (Fig.2B). This provides a potentially new platform and identifies a new pathway that contributes to the transformed phenotype. Additional characterization of TCEAL7 downregulated clones showed increased proliferation and more importantly potentiated Myc induced transcription of the ODC promoter/reporter construct, implicating loss of TCEAL7 resulting in Myc driven transformation.

The answers to some of these questions may emerge following completion of our in vivo studies.

REFERENCES

1. Pillutla, R.C., et al., *Genomic structure and chromosomal localization of TCEAL1, a human gene encoding the nuclear phosphoprotein p21/SIIR.* Genomics, 1999. **56**(2): p. 217-20.
2. Shridhar, V., et al., *Identification of underexpressed genes in early- and late-stage primary ovarian tumors by suppression subtraction hybridization.* Cancer Res, 2002. **62**(1): p. 262-70.
3. Mukai, J., et al., *Structure-function analysis of NADE: identification of regions that mediate nerve growth factor-induced apoptosis.* J Biol Chem, 2002. **277**(16): p. 13973-82.
4. Mukai, J., et al., *NADE, a p75NTR-associated cell death executor, is involved in signal transduction mediated by the common neurotrophin receptor p75NTR.* J Biol Chem, 2000. **275**(23): p. 17566-70.
5. Kozak, M., *Interpreting cDNA sequences: some insights from studies on translation.* Mamm Genome, 1996. **7**(8): p. 563-74.
6. Kozak, M., *Initiation of translation in prokaryotes and eukaryotes.* Gene, 1999. **234**(2): p. 187-208.
7. Altschul, S.F., et al., *Gapped BLAST and PSI-BLAST: a new generation of protein database search programs.* Nucleic Acids Res, 1997. **25**(17): p. 3389-402.
8. Saitoh, F., et al., *Induction by 5-aza-2'-deoxycytidine, an inhibitor of DNA methylation, of Le(y) antigen, apoptosis and differentiation in human lung cancer cells.* Anticancer Res, 1995. **15**(5B): p. 2137-43.
9. Persengiev, S.P. and D.L. Kilpatrick, *The DNA methyltransferase inhibitor 5-azacytidine specifically alters the expression of helix-loop-helix proteins Id1, Id2 and Id3 during neuronal differentiation.* Neuroreport, 1997. **8**(9-10): p. 2091-5.
10. Herman, J.G., et al., *Methylation-specific PCR: a novel PCR assay for methylation status of CpG islands.* Proc Natl Acad Sci U S A, 1996. **93**(18): p. 9821-6.
11. Shridhar, V., et al., *Loss of expression of a new member of the DNAJ protein family confers resistance to chemotherapeutic agents used in the treatment of ovarian cancer.* Cancer Res, 2001. **61**(10): p. 4258-65.
12. Westbrook, T.F., et al., *A genetic screen for candidate tumor suppressors identifies REST.* Cell, 2005. **121**(6): p. 837-48.
13. Kalli, K.R., et al., *Functional insulin receptors on human epithelial ovarian carcinoma cells: implications for IGF-II mitogenic signaling.* Endocrinology, 2002. **143**(9): p. 3259-67.
14. Kalli, K.R., et al., *Pregnancy-associated plasma protein-A (PAPP-A) expression and insulin-like growth factor binding protein-4 protease activity in normal and malignant ovarian surface epithelial cells.* Int J Cancer, 2004. **110**(5): p. 633-40.
15. Brummelkamp, T.R., R. Bernards, and R. Agami, *A system for stable expression of short interfering RNAs in mammalian cells.* Science, 2002. **296**(5567): p. 550-3.
16. Sakamuro, D., et al., *BIN1 is a novel MYC-interacting protein with features of a tumour suppressor.* Nat Genet, 1996. **14**(1): p. 69-77.
17. Sakamuro, D. and G.C. Prendergast, *New Myc-interacting proteins: a second Myc network emerges.* Oncogene, 1999. **18**(19): p. 2942-54.
18. Elliott, K., et al., *Bin1 functionally interacts with Myc and inhibits cell proliferation via multiple mechanisms.* Oncogene, 1999. **18**(24): p. 3564-73.
19. Elliott, K., et al., *The c-Myc-interacting adaptor protein Bin1 activates a caspase-independent cell death program.* Oncogene, 2000. **19**(41): p. 4669-84.
20. Teodoridis, J.M., G. Strathdee, and R. Brown, *Epigenetic silencing mediated by CpG island methylation: potential as a therapeutic target and as a biomarker.* Drug Resist Updat, 2004. **7**(4-5): p. 267-78.
21. Esteller, M., *DNA methylation and cancer therapy: new developments and expectations.* Curr Opin Oncol, 2005. **17**(1): p. 55-60.
22. Balch, C., et al., *The epigenetics of ovarian cancer drug resistance and resensitization.* Am J Obstet Gynecol, 2004. **191**(5): p. 1552-72.
23. Connolly, D.C., et al., *Female mice chimeric for expression of the simian virus 40 TAg under control of the MISIIR promoter develop epithelial ovarian cancer.* Cancer Res, 2003. **63**(6): p. 1389-97.
24. Dinulescu, D.M., et al., *Role of K-ras and Pten in the development of mouse models of endometriosis and endometrioid ovarian cancer.* Nat Med, 2005. **11**(1): p. 63-70.
25. Flesken-Nikitin, A., et al., *Induction of carcinogenesis by concurrent inactivation of p53 and Rb1 in the mouse ovarian surface epithelium.* Cancer Res, 2003. **63**(13): p. 3459-63.
26. Orsulic, S., et al., *Induction of ovarian cancer by defined multiple genetic changes in a mouse model system.* Cancer Cell, 2002. **1**(1): p. 53-62.
27. Kolfschoten, I.G., et al., *A genetic screen identifies PITX1 as a suppressor of RAS activity and tumorigenicity.* Cell, 2005. **121**(6): p. 849-58.

EPIGENETIC SILENCING OF A NOVEL PROAPOPTOTIC TRANSCRIPTIONAL REGULATORY PROTEIN IN OVARIAN CANCER

JULIE STAUB[1], JEREMY CHIEN1, RAJESWARI AVULA[1], LYNN C HARTMANN[3], SCOTT H KAUFMANN[4], DAVID I SMITH[1] AND VIJI SHRIDHAR[1]*

Here we report on the cloning of a novel pro-apoptotic protein on chromosome X, first named PAPX due to its ability to induce apoptosis, and describe the functional consequences of its loss in ovarian cancer. PAPX codes for a 1.35 Kb transcript that was at least five-fold down-regulated in all tumors profiled (n=14) by cDNA microarray analysis and was also identified as an under-expressed gene in three of four SSH libraries constructed. Semi-quantitative RT-PCR analysis with primers flanking the open reading frame revealed a complete loss of expression in all seven ovarian cancer cell lines and a complete loss or markedly reduced levels of PAPX expression in 90% of primary ovarian tumors. 5-aza-2'-deoxycytidine treatment of the OV202 cell line induced PAPX expression in a dose-dependant manner implicating methylation in this induction. Methylation specific PCR in normal ovarian epithelial cells and in somatic cell hybrids with either the active or the inactive X as one of its human counterpart revealed that PAPX is subject to X chromosome inactivation. Loss of PAPX expression in 10 primary tumors and 7 cell lines correlated with methylation of the active expressed allele involving either site 3 within exon 1 or site 4 in intron 1. Both PAPX and pp21 homolog have domain homology with the transcription elongation factor A-like 1(TCEAL1). The pp21 homolog and the pro-apoptotic protein $p75^{NTR}$-associated death executor (NADE) are 39% and 37% identical respectively to PAPX. PAPX co-localizes with RNA Pol II in nuclear foci. Forced expression of PAPX in non-expressing ovarian cancer cells induces apoptosis, and reduces colony formation efficiency. These data implicates PAPX as a growth regulatory protein frequently inactivated in a majority of ovarian cancers and suggests it functions as a tumor suppressor. PAPX has been renamed Bex4 due to its homology to a family of brain expressed (bex) genes.

American Association for Cancer Research 95th annual meeting. March 27-31, 2004, Orlando, FL. Abstract #4184.

CANDIDATE TUMOR SUPPRESSOR GENE TCEAL7 ASSOCIATES WITH BIN1 AND REGULATES MYC

JEREMY CHIEN, KEISHI NARITA, RAVI SHRIDHAR , PAN YUNQINA, JULIE STAUB, HEYU ZHANG, JINPING LAI, LEWIS ROBERTS, LYNN C HARTMANN, SCOTT H. KAUFMANN, GEORGE C. PRENDERGAST, VIJI SHRIDHAR.

Transcription-elongation factor A-like 7 (TCEAL7) is a candidate tumor suppressor gene that is epigenetically silenced in ovarian cancer and other human cancers. TCEAL7 encodes a proapoptotic nuclear protein, the precise function of which is unknown. Here we report that TCEAL7 binds to a Myc-interacting isoform of the tumor suppressor protein Bin1 and that TCEAL7 inhibits Myc transactivation activity. TCEAL7-mediated down-regulation of Myc activity resulted in reduced cell proliferation and decreased expression of cyclin D1, an effect associated with recruitment of TCEAL7 to the E box-containing region of the cyclin D1 promoter that is bound by c-Myc. Finally, down-regulation of TCEAL7 in immortalized ovarian epithelial cells resulted in >4 fold increase in Myc activity, increased proliferation and anchorage-independent growth. We propose a model in which TCEAL7 modifies the transactivation activity of Myc through direct interactions with Myc and Bin1. Thus our findings extend the evidence of a tumor suppressor role for TCEAL7, and offer initial mechanistic insights into how this protein may modulate cell proliferation and transformation.

WOMENS' CANCER PROGRAM, MAYO CLINIC, Oct 27, 2006

A PUTATIVE NOVEL TUMOR SUPPRESSOR MODULATES NFκB ACTIVITY

RAMANDEEP RATTAN[1], JEREMY CHIEN[1], KEISHI NARITA[1], JULIE STAUB[1], SHAILENDRA GIRI[2] AND VIJI SHRIDHAR[1].

ABSTRACT

Ovarian cancer is the fourth most common cause of death from all cancers among women in the United States and the leading cause of death from gynecological malignancies. Using high throughput expression based screening strategies; we identified TCEAL7, a transcriptional elongation factor like protein as one of the downregulated gene in ovarian cancer. Expression of TCEAL7 is lost in >90% of primary ovarian tumors and in 100% of all the tested cell lines. Our initial studies showed forced expression of TCEAL7 induced apoptosis in ovarian cancer cells. Our more recent data indicate shRNA mediated down regulation of TCEAL7 in nonmalignant ovarian surface epithelial cells (OSEtsT/hTERT) leads to increased proliferation and conferred soft agar colony formation ability to these cells. Since alteration in the NFκB pathway is important in tumorigenesis and is common in almost every tumor, including ovarian, we investigated the relationship, if any, between TCEAL7 and NF B signaling. In TCEAL7 downregulated OSEtsT/hTERT stable clones, we observed that loss of TCEAL7 resulted in a higher basal activation state of NFκB, that was reversed by re-expression of TCEAL7. TCEAL7 also inhibited IL-8 induced NFκB DNA binding ability as observed by EMSA, although it did not alter the status of any cytoplasmic signaling participants (IKK-phosphorylation, IκB phosphorylation and degradation) of the NFκB pathway. Based on these findings, we hypothesize that TCEAL7 is a putative novel tumor suppressor gene in ovarian carcinoma and one of the mechanism by which it exerts its anti-tumor property is by the negative regulation of NFκB pathway, presumably at nuclear level, thus contributing to the transformation of ovarian cells and oncogenesis.

Oral Presentation in Mini Symposium-*American Association for Cancer Research* 98th annual meeting. April 2007, Los Angeles CA.

Based on the abstract, Dr. Ramandeep was awarded the prestigious scholar in training award at the AACR meeting in April 2007.

Oncogene (2005) 24, 5089–5100

www.nature.com/onc

Epigenetic silencing of TCEAL7 (Bex4) in ovarian cancer

Jeremy Chien[1], Julie Staub[1], Rajeswari Avula[1], Heyu Zhang[1], Wanguo Liu[1], Lynn C Hartmann[2], Scott H Kaufmann[3], David I Smith[1] and Viji Shridhar*[,1]

[1]*Division of Experimental Pathology, Department of Laboratory Medicine and Pathology, Mayo Clinic/Foundation, 200 First Street, SW Rochester, MN 55905, USA;* [2]*Division of Medical Oncology, Oncology Research, Department of Oncology, Mayo Clinic/Foundation, 200 First Street, SW Rochester, MN 55905, USA;* [3]*Department of Oncology Research, Mayo Clinic/Foundation, 200 First Street, SW Rochester, MN 55905, USA*

Epigenetic silencing by hypermethylation of CpGs represents a mechanism of inactivation of tumor suppressors. Here we report on the cloning of a novel candidate tumor suppressor gene *TCEAL7* inactivated by methylation in ovarian cancer. *TCEAL* codes for a 1.35 kb transcript that was previously reported to be downregulated in ovarian cancer by cDNA microarray and suppression subtraction cDNA (SSH) analyses. This report focuses on the elucidation of mechanisms associated with TCEAL7 downregulation. Expression of *TCEAL7* is downregulated in a majority of ovarian tumors and cancer cell lines but induced by 5-aza-2′-deoxycytidine treatment in a dose-dependant manner, implicating methylation as a mechanism of *TCEAL7* inactivation. Sequence analyses of bisufite-modified genomic DNA from somatic cell hybrids with either the active or the inactive human X chromosome reveal that *TCEAL7* is subjected to X chromosome inactivation. Loss of *TCEAL7* expression in primary tumors and cell lines correlates with methylation of a CpG site within the promoter. *In vitro* methylation of the CpG site suppresses promoter activity whereas selective demethylation of the *Sma*I site attenuates the suppression. Finally, re-expression of *TCEAL7* in cancer cell lines induces cell death and reduces colony formation efficiency. These data implicate TCEAL7 as a cell death regulatory protein that is frequently inactivated in ovarian cancers, and suggest that it may function as a tumor suppressor.
Oncogene (2005) **24,** 5089–5100. doi:10.1038/sj.onc.1208700; published online 2 May 2005

Keywords: ovarian cancer; methylation; tumor suppressor; apoptosis; proliferation

Introduction

In the United States, 27 000 women were diagnosed with ovarian cancer and approximately 14 000 were expected to succumb to the disease in 2004 (Jemal *et al*., 2004). Such high mortality rates are the direct result of a majority of patients presenting with advanced disease, and underscore the need for the development of better tools for the screening, diagnosis, and treatment of ovarian cancer. Increased understanding of genetic alterations associated with and the functional consequences of such alterations in cancer would provide the groundwork for development of early detection markers, novel therapeutic targets, and better management of ovarian cancer. Toward this goal, we performed cDNA microarray and suppression subtraction hybridization analyses to identify early genetic alterations associated with ovarian cancer. These studies resulted in the identification of several genes that are differentially expressed in ovarian cancer (Shridhar *et al*., 2001b, 2002). Based on our initial screen of several of these differentially expressed genes, we selected a novel proapoptotic protein for further analysis, and it is the focus of this study.

In the present manuscript, we describe the molecular cloning of a monoallelically expressed novel proapoptotic nuclear protein, TCEAL7, that shares amino-acid sequence homology with transcription elongation factor A-like 1 (TCEAL1/p21/SIIR/pp21) and pp21 homolog (WBP5/TCEAL6). TCEAL7 also shares sequence homology with $p75^{NTR}$-associated death executor (NADE). All four of these genes map to a region of X chromosome inactivation (Xq22.1-22.2). pp21 homolog and NADE map ~24 and ~42 kb telomeric to *TCEAL7*, respectively. The function of pp21 homolog is not yet characterized. However, its homolog, pp21, also on the X chromosome has been shown to suppress RSV LTR (Rous sarcoma virus long-terminal repeat) promoter activity and inhibit RSV LTR-mediated transformation in chicken embryo fibroblast (Yeh and Shatkin, 1994). The transcriptional repression of RSV LTR by pp21 requires an interaction with a *cis*-acting promoter element because pp21 does not bind DNA directly (Yeh and Shatkin, 1995). NADE is a proapoptotic protein involved in modulating apoptosis mediated by the low-affinity neurotropin receptor (Mukai *et al*., 2002). It contains a leucine-rich nuclear export signal (NES) in the carboxyl terminus, and its cytosolic localization is required for mediating p75NTR-induced apoptosis. It also contains a domain required for

*Correspondence: V Shridhar;
E-mail: shridhar.vijayalakshmi@mayo.edu
Received 9 February 2005; revised and accepted 8 March 2005; published online 2 May 2005

induction of apoptosis, a regulatory domain, a self-association domain, and a 14-3-3 interacting domain (Mukai *et al*., 2002).

We have made several original observations regarding the potential role of *TCEAL7* inactivation in ovarian tumorigenesis. First, we observed that the expression of *TCEAL7* is lost in >90% of primary ovarian tumors and cell lines. Second, we have shown that the loss of expression of *TCEAL7* in primary tumors and cell lines is due to methylation of the active expressed allele. Finally, forced expression of *TCEAL7* in deficient cell lines induces cell death and suppresses colony formation efficiency. These observations suggest that loss of expression of *TCEAL7* may promote the survival of cancer cells, leading to the development of ovarian cancer.

Results

Isolation and characterization of a novel cDNA

We identified an EST (AJ297363) within the Unigene cluster -Hs.21861 as a downregulated gene in three of four suppression subtraction libraries of primary ovarian tumors subtracted against normal ovarian epithelial cell brushings (OSEs) (Shridhar *et al*., 2002). cDNA microarray analysis of early- and late-stage ovarian tumors versus normal OSEs also revealed that this EST was at least fivefold downregulated in all 14 tumors analysed (Shridhar *et al*., 2001b).

Comparative sequence analysis of this fragment using the BLAST alignment revealed that the 306 bp fragment showed considerable sequence alignment with several ESTs. The homologous ESTs were assembled into a contig with the use of Sequencher 3 (Gene Codes Corp) software. The entire cDNA contig was sequenced twice with overlapping primers. The integrity of the full-length cDNA obtained by this electronic walking was confirmed by PCR analysis using PCR primers flanking each junction between EST clones. The assembled gene revealed that it is made up of three exons with the open reading frame (ORF) residing within exon 3 (Figure 1a). Exons 1, 2, and 3 are 109, 118, and 949 bp long, respectively. Introns 1 and 2 are 618 and 336 bp long, respectively, and follow the GT:AG rule. The ORF codes for a 100-amino-acid-long protein (Figure 1c) and contains a coiled-coil domain (Figure 1c, highlighted in black and Figure 1b), and the initiation codon is preceded by an in-frame stop codon within a strong Kozak context (Kozak, 1996) (Figure 1b).

Similarity alignment of TCEAL7 to other proteins

To identify potential domains of this novel gene, a Blastp search was performed (Altschul *et al*., 1997). The search revealed sequence similarity to brain-expressed (Bex) proteins, Bex1–3 (Figure 2a). The Bex proteins belong to a small family of genes comprised of *bex1* (Faria *et al*., 1998), *bex2* and *bex3* (Rapp *et al*., 1990; Mukai *et al*., 2000). We therefore named the newly identified gene, mapping between *bex2*, and *bex3* on X22.1–22.2, as bex4. All four *bex* genes are closely linked on the X chromosome and are predominantly expressed in the brain. However, recently, HUGO renamed *bex1* as *TCEAL8* and *bex4* as *TCEAL7*. For this reason, we will refer to *bex4* as *TCEAL7*. *TCEAL8* is ubiquitously expressed (Williams *et al*., 2002; Yang *et al*., 2002). Although tissue distribution of *bex3* is not well characterized, it is also known as p75 neurotropin receptor ($p75^{NTR}$)-associated death executor (NADE) and shown to interact with low-affinity receptor $p75^{NTR}$ in an NGF-dependent manner (Mukai *et al*., 2000, 2002). TCEAL7 and NADE show 50% sequence similarity within apoptosis-inducing domain and 77% sequence similarity with regulatory domain (Figure 2b).

Expression in ovarian carcinoma cell lines and primary tumors

To validate the results obtained by microarray and SSH analyses, *TCEAL7* expression was tested in seven ovarian cancer cell lines and in 26 primary ovarian tumors by semiquantitative RT–PCR. Short-term cultures of normal ovarian epithelial cells (OSE) and epithelial cell brushings (B) from patients without cancer served as positive controls. TCEAL7 expression is not detectable in any of the ovarian cancer cell lines (Figure 3a) and in majority of primary tumors, while short-term culture ovarian surface epithelial cells (OSE, sample #27) and immortalized OSE(tsT) (sample #28) express TCEAL7 (Figure 3b). Expression of TCEAL7 in short-term culture ovarian surface epithelial cells is further confirmed by Western blot using polyclonal antibodies against TCEAL7 (Figure 3c). Quantitative RT–PCR analysis using Light Cycler Assay indicates that TCEAL7 is significantly downregulated in ovarian tumors of different histologies (Figure 3d).

Mechanism of TCEAL7 inactivation

To investigate the mechanisms of *TCEAL7* inactivation, several approaches were taken. First, 20 pairs of matched normal and primary ovarian tumors were analysed for loss of heterozygosity (LOH) with two different microsatellite markers within the *TCEAL7* gene. LOH analysis revealed 25% (5/20) of tumors showed LOH in this region of the chromosome (data not shown). Second, mutational analysis of all three exons in 96 primary ovarian tumors showed no tumor-specific changes (data not shown). In order to determine whether methylation controlled *TCEAL7* expression, OV207 cells were treated with various concentrations of methyltransferase inhibitor, 5-aza-2′-deoxycytidine (5-aza-dC) (Saitoh *et al*., 1995; Persengiev and Kilpatrick, 1997). Figure 4a shows a dose-dependent increase in *TCEAL7* expression in OV207 following 5-aza-dC treatment. Consistent with this finding, genomic sequence analysis indicated 26 CpG sites around four *Sma*I sites in the promoter, exon 1, and intron 1 (Figure 4b). Primers flanking these *Sma*I sites were selected to amplify and sequence the bisulfite-modified

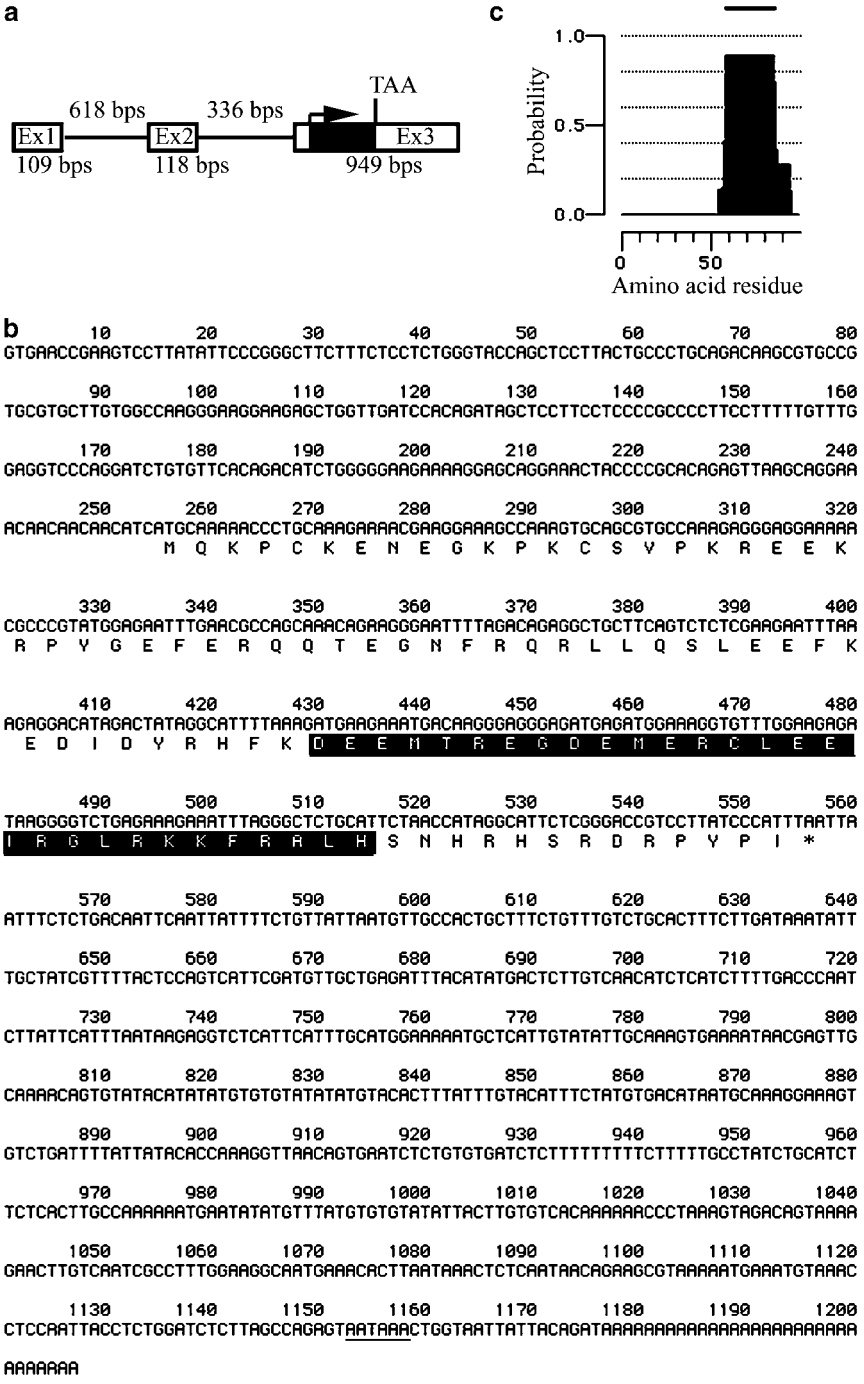

Figure 1 Genomic structure and cDNA sequence of TCEAL7. (**a**) Schematic representation of genomic structure of TCEAL7. The numbered boxes indicate exons. Exon and intron sizes are in base pairs (bp). The arrow within exon 3 is translational start site and stop codon is indicated by TAA. (**b**) cDNA sequence of TCEAL7 and predicted translation of amino acids. Coiled-coil domain is highlighted in black, and the polyadenylation sequence AATAAA is underlined. (**c**) Prediction of coiled-coil domain by MacStripe program

DNA. Amplicon 1 contains *Sma*I site I at 738 bases upstream of exon 1 and includes two CpG sites. Amplicon 2 contains *Sma*I site II within exon 1 and site III at 126 bases 3′ of exon 1 and includes five other CpG sites. Amplicon 3 contains *Sma*I site IV in intron 1 at 286 bases 3′ to site 3 and includes six additional CpG sites. Therefore, a total of 16 CpG sites were analysed. Five CpG sites between amplicons 1 and 2 and between 3 and 4 were not included in the analysis. In order to distinguish unmodified from modified DNA, PCR was performed on bisulfite-modified DNA as previously described (Herman *et al*., 1996; Shridhar *et al*., 2001a). Amplicons were gel purified and sequenced to determine the overall methylation status of 16 CpG sites.

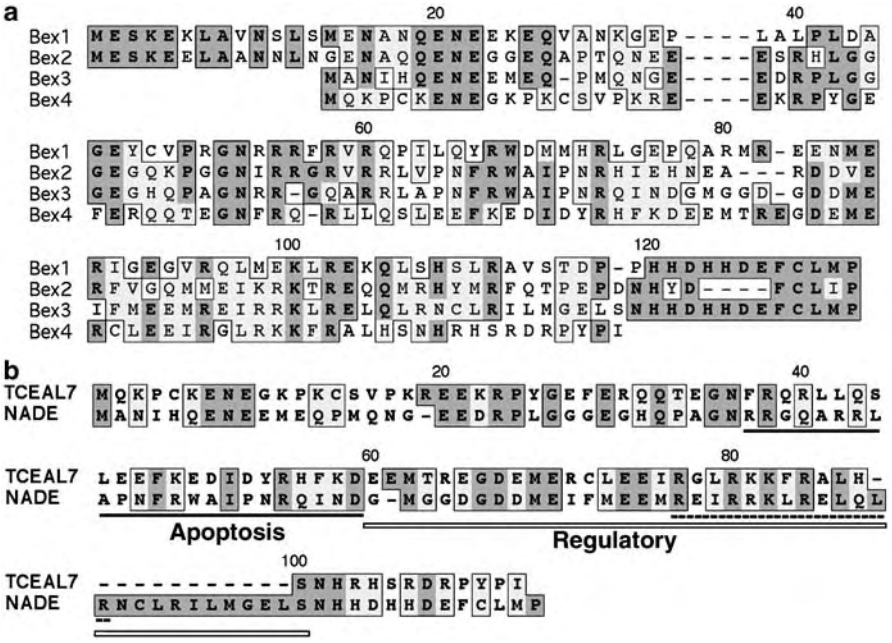

Figure 2 Sequence alignment with homologous proteins. (**a**) ClustalW alignment of TCEAL7 (Bex4) and other members of Bex protein family. Dark shading indicates identical residues in the Bex gene family. Light shading indicates homologous residues. Dashed lines represent gaps in the sequence alignment. (**b**) Sequence alignment between TCEAL7 and NADE (Bex3). Solid underline defines the apoptotic domain in NADE. Dashed line under the sequence represents NES. Clear underline indicates regulatory domain of NADE

Methylated C's (indicated by asterisks in Figure 4b) are resistant to bisulfite modification and remain as C's, whereas unmethylated C's are converted to T's (Figure 4b). Since *TCEAL7* maps to a region of X chromosome inactivation (Brown and Kay, 1999), we included somatic cell hybrids containing either active X [Y162.11C] (Xa) and inactive X [Y162.5E1T2] (Xi) as positive and negative controls in these analyses. Methylation analyses of bisulfite-modified DNAs from Xa and Xi cell lines showed differential methylation at sites II, III, and IV between two hybrid cell lines (Figure 4c, first & second row). However, CpG in *Sma*I site I was methylated in both the active and the inactive X. RT–PCR analysis of TCEAL7 expression in these hybridomas carrying either Xa or Xi chromosome showed loss of TCEAL7 expression in both lines (data not shown). These results suggest that methylation at *Sma*I site I might play a critical role in controlling the expression of TCEAL7.

Methylation of CpG in SmaI *site I controls TCEAL7 expression in the somatic cell hybrid containing the active X*

In order to determine if methylation of CpG site I is inactivating *TCEAL7* expression in Xa-containing cell line, cells were treated with various concentrations of 5-aza-dC. A dose-dependent increase in *TCEAL7* expression in this cell line was observed following 5-aza-dC treatment (Figure 5a). Subsequent analysis of bisulfite-modified DNA from 5-aza-dC-treated Xa cells revealed demethylation of site 1, concomitant with induction of *TCEAL7* transcript (Figure 5b). These data suggest that site I methylation may control *TCEAL7* expression in this cell line. In order to rule out the possibility of histone deacetylation as a mechanism of *TCEAL7* transcriptional inactivation, Xa-containing cells were treated with various concentrations of the histone deacetylase inhibitor, trichostatin A. Trichostatin A did not affect the transcription of *TCEAL7* in these cells (Figure 5c). To demonstrate that methylation of CpG in *Sma*I site I influences the promoter activities *in vitro*, amplicon 1 was subcloned into pGL3 reporter plasmid, and the CpG site I was mutated to ApG. Both plasmids were subjected to bisulfite modification, and modified plasmids were transfected into HeLa cells to determine the promoter activity of these two plasmids. As shown in Figure 5d, nonmutated plasmid showed diminished promoter activity compared to the mutated plasmid, suggesting that methylation of CpG site I in nonmutated plasmid suppressed promoter activity and that prevention of CpG site methylation by site-directed mutagenesis prevented this suppression of promoter activity.

Methylation of CpG in SmaI *site I reflects TCEAL7 inactivation in primary ovarian tumors*

Since our data indicate using both *in vitro* promoter assay and methylation analysis that methylation at site I controls *TCEAL7* transcription in the Xa cell line, we tested whether methylation at site I in primary tumors and cell lines is associated with loss of TCEAL7 expression. Methylation status of 16 CpG sites was determined by genomic sequencing of bisulfite-modified

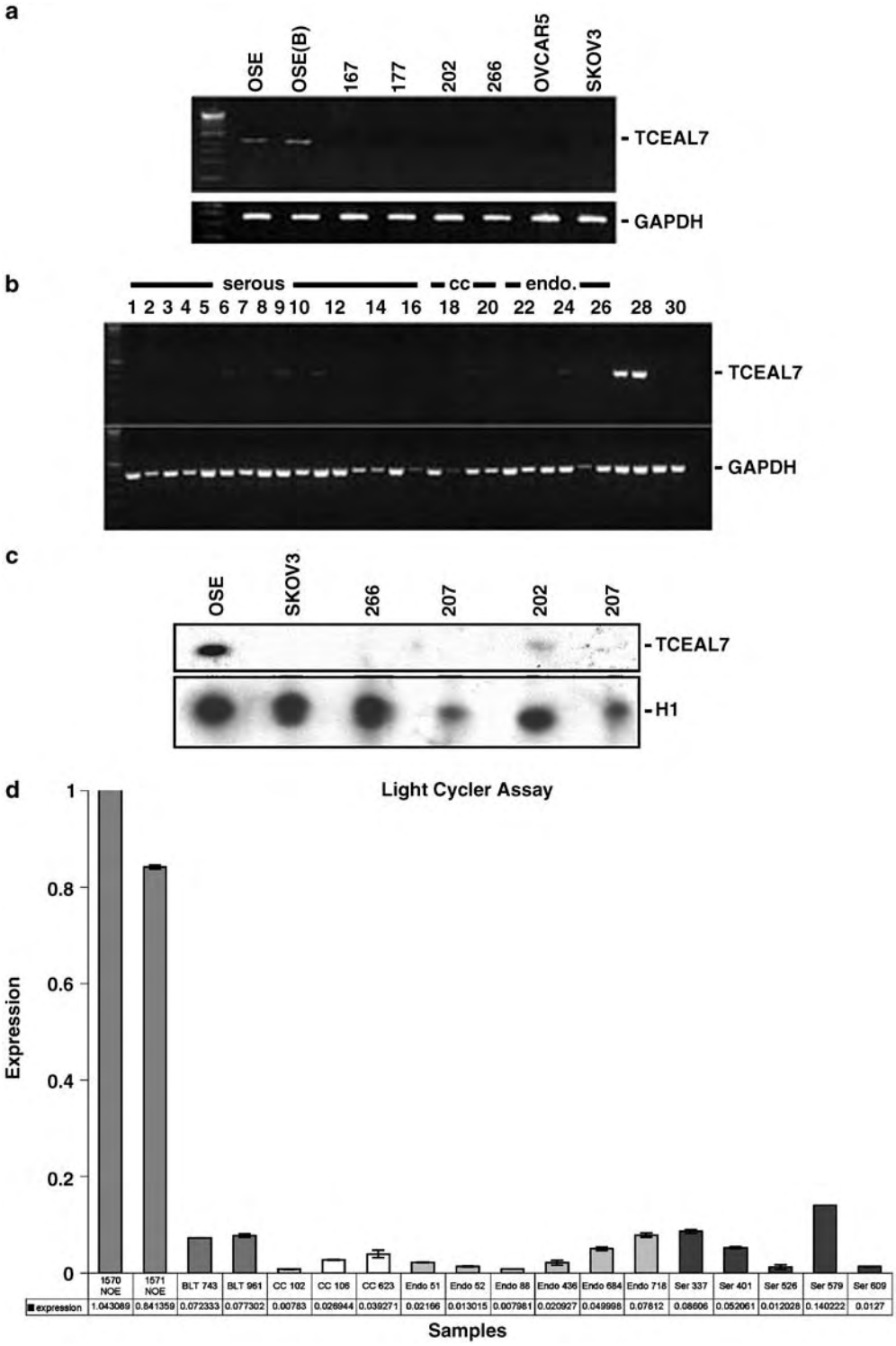

Figure 3 Expression analysis of TCEAL7 in ovarian cancer. (**a**) Agarose gel showing the RT–PCR products amplified with primers 99F and 523R in ovarian cell lines resolved on a 1.6% agarose gel. OSE: short-term cultured ovarian surface epithelial cells; OSE(B): ovarian surface epithelial cell brushing. (**b**) RT–PCR results of TCEAL7 expression in primary ovarian tumors. Samples are numbered and grouped according to tumor histology. Samples #27 and #28 are OSE and SV40 T-antigen immortalized OSE (OSE-tsT), respectively, and they were included as positive controls. Samples #29 and #30 are ovarian cell lines 167 and 177, and they were included as negative controls. The product of amplification with GAPDH primers F and R is shown in lower panels. (**c**) Western blot analysis indicates that TCEAL7 is expressed in normal OSE. Histone H1 immunoblot is shown in the lower panel as a loading control. (**d**) TCEAL7 is several-fold downregulated in primary ovarian tumors. Expression values obtained from triplicates and normalized to NOE expression are shown below the bars. NOE, BLT, Serous (ser), cc, and endo denote normal ovarian surface epithelium, borderline tumor, serous, clear cell, and endometrioid histologies, respectively

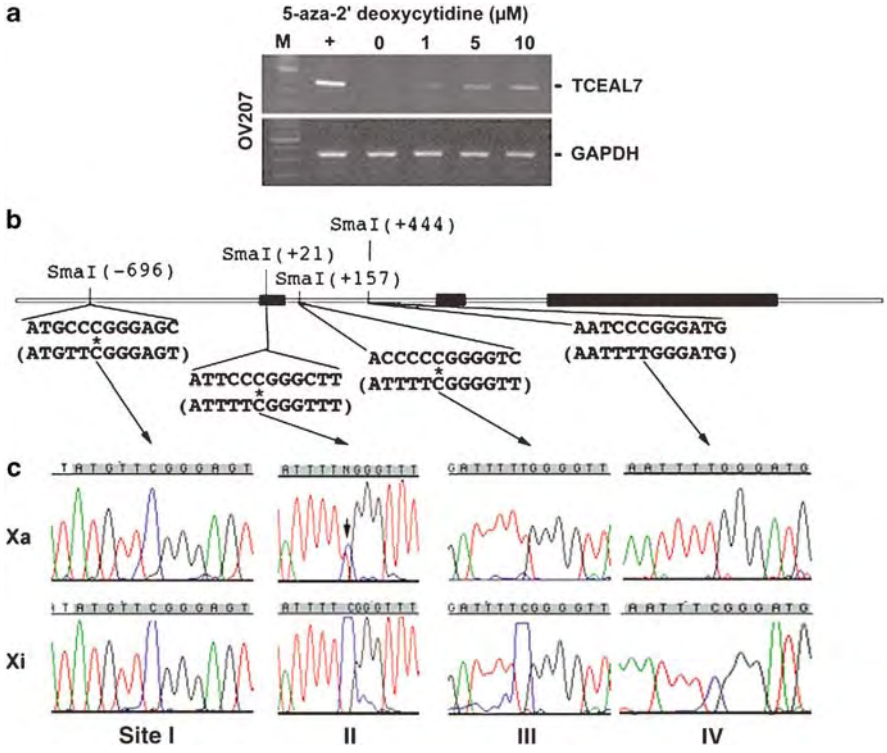

Figure 4 Methylation analysis of TCEAL7. (**a**) Induction of TCEAL7 expression in OV207 cell line by 5-aza-dC. PCR amplification of GAPDH is shown in the lower panel as a loading control. +: positive control (OSEtsT). (**b**) Genomic structure and sequence of four *Sma*I sites analysed. Methylated C's are indicated by asterisks. They are resistant to bisulfite modification, and therefore remain as Cs. Unmethylated C's are converted to T's. The bisulfite-modified sequences are indicated in parentheses. (**c**) Sequence chromatogram of four *Sma*I sites after bisulfite modification of genomic DNA purified from somatic cell hybrids containing Xa or Xi. Sequences highlighted in gray on top of chromatogram correspond to *Sma*I site sequences shown in panel b. The arrow indicates the presence of both methylated and unmethylated alleles at *Sma*I site II in Xa

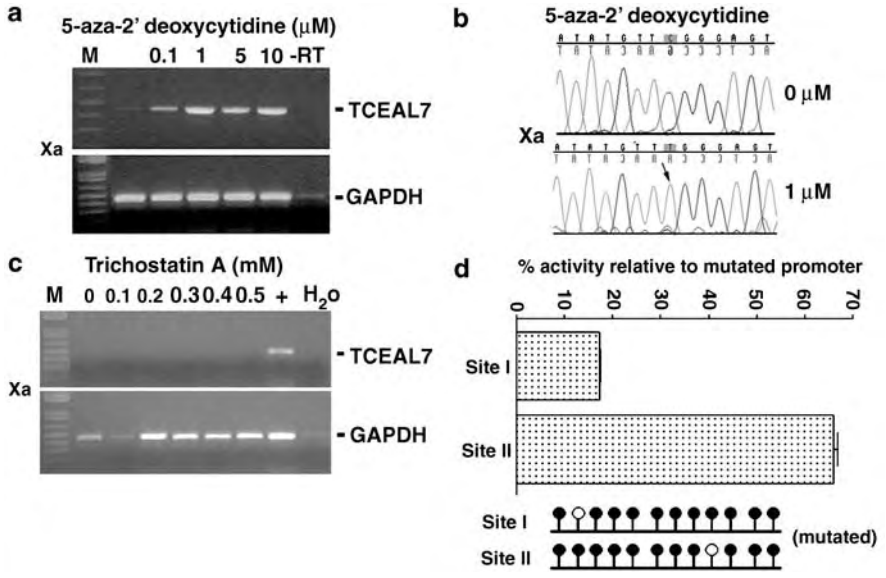

Figure 5 Methylation at *SmaI* site I controls TCEAL7 expression. (**a**) Agarose gel electrophoresis of RT–PCR showing dose-dependent increase in the transcription of TCEAL7 following 72 h of exposure to increasing concentrations of 5-aza-dC in somatic cell hybrid Y162.11C with active X (Xa). GAPDH control is shown in the lower panel. No TCEAL7 product was detected in −RT control. (**b**) Sequence of bisulfite-modified DNA from Xa hybrid showing the methylation at site 1 before 5-aza-dC treatment. The arrow in the lower sequence indicates demethylation at this site after the treatment. (**c**) Increasing concentrations of TSA (0.1–0.5 mM) treatments have no effect on TCEAL7 expression in Xa hybrid. +: positive control (OSEtsT); H_2O: water control; M: 100 bp ladder. (**d**) Methylation of CpG in *Sma*I site I suppresses promoter activity, whereas the mutation that prevents methylation of the site does not suppress promoter activity. WT: wild-type CpG; Mut: mutant ApG sequence in *Sma*I site I

DNA. Representative chromatograms of bisulfite-modified DNA corresponding to four *Sma*I sites in ovarian tumors are shown in Figure 6a. Semiquantitative RT–PCR results for a subset of tumors are shown in Figure 6b. Consistent with the hypothesis that methylation of site I controls TCEAL7 expression, biallelic methylation at site I in these samples reflects loss of TCEAL7 expression as evidenced by semiquantitative RT–PCR analysis (Table 1, e.g. 4, 13, 206, 208, 402, 414, 34, 98, 121, 183, 235, 259, 339, and cancer cell lines). However, there were a few exceptions (Table 1, #45, 183, and 235). In these samples, TCEAL7 expression was lost although site I was hemimethylated, suggesting the involvement of other mechanisms in inactivation of *TCEAL7*.

To determine if LOH could also be responsible for inactivation of TCEAL7, we analysed both LOH and methylation in a subset of tumors. Majority of tumors with CpG site I methylation did not have LOH (Table 1, tumors highlighted in bold), suggesting that both mechanisms are not required to completely inactivate TCEAL7 expression. In addition, there was no correlation between the methylation status and age of patient. Together, these data are consistent with the hypothesis that TCEAL7 is monoallelically expressed and therefore requires a tumor-related epigenetic silencing to inactivate the active allele.

Forced expression of TCEAL7 induces apoptosis

Since TCEAL7 shares domain homology with Bex3/NADE (Figure 2a), a known mediator of $p75^{NTR}$-induced apoptosis, the apoptotic potential of TCEAL7 was tested in ovarian cancer cells. At 48 h after transfection, morphological analysis of SKOV3 transiently transfected with TCEAL7-GFP fusion construct showed apoptotic morphology, such as cytoplasmic shrinkage and membrane blebbing (Figure 7a, upper panels), whereas vector-transfected cells (Figure 7a, lower panels) displayed normal morphology. To confirm that TCEAL7-transfected cells were undergoing apoptosis, nuclear morphologic analysis with Hoechst stain was performed on these cells. As shown in Figure 7a, expression of TCEAL7 produces pyknotic nuclei (indicated by arrows), while expression of GFP does not produce such phenotype. Quantitation of apoptotic cells indicated significantly higher percentage of apoptosis in TCEAL7-transfected cells compared to vector GFP-transfected cells (Figure 7b). Consistent with these results, forced expression of TCEAL7 suppressed clonogenic survival of OV202 ovarian cancer cells (Figure 7c).

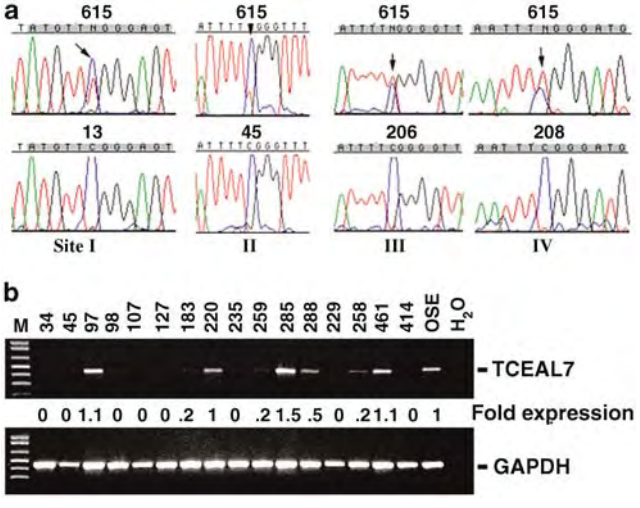

Figure 6 Genomic sequencing and expression analysis in primary ovarian tumor. (**a**) Representative chromatograms of bisulfite-modified DNA from ovarian tumors. Sequences correspond to four *Sma*I sites. Upper panels are taken from tumor #615. All four sites show hemimethylation (indicated by arrows). Examples of fully methylated CpGs in four *Sma*I sites are shown in the lower panel. (**b**) Expression of TCEAL7 in a small subset of tumors used in sequence analyses of bisulfite-modified DNA. Increase or decrease in fold expression compared to OSE is indicated between panels

Discussion

DNA methylation of cytosine residues in CpGs is associated with transcriptional silencing and plays an important role in X chromosome inactivation and gene imprinting during mammalian development (Li *et al*., 1992; Jaenisch and Bird, 2003) and in epigenetic silencing of tumor suppressors during carcinogenesis (Jones and Laird, 1999). Epigenetic silencing of tumor suppressors is well documented in cancer, and may represent a mechanism in Knudson's two-hit hypothesis. Epigenetic inactivation of tumor suppressors, such as the von Hippel–Lindau syndrome (VHL), breast cancer, type 1 (BRCA1), retinoblastoma (RB1), cyclin-dependent kinase inhibitor 2A and 2B (CDKN2A and 2B), mutL homolog 1 (MLH1), and adenomatous polyposis of the colon (APC), has been well documented in carcinogenesis (Jones and Laird, 1999; Baylin and Herman, 2000; Baylin and Bestor, 2002; Esteller *et al*., 2002; Jones and Baylin, 2002; Laird, 2003). Although homozygous or heterozygous deletions and mutations represent classical mechanisms of inactivation of tumor suppressors, epigenetic silencing by hypermethylation has also gained widespread acceptance as an additional mechanism of inactivation (Jones and Baylin, 2002). In fact, close to 50% of genes associated with familial forms of cancer are subjected to epigenetic silencing in various sporadic forms of cancer, in addition to a growing list of candidate tumor suppressor genes that are silenced by hypermethylation (Jones and Baylin, 2002). These reports highlight the significance of aberrant hypermethylation in carcinogenesis.

We believe that TCEAL7 is an excellent candidate tumor suppressor selectively inactivated in ovarian cancer. Expression of *pp21 homolog*, a related gene mapping 24 kb telomeric to *TCEAL7*, is not lost in ovarian cell lines tested. Expression of *bex3/NADE*, another related gene mapping 43 kb centromeric to *TCEAL7*, showed reduced expression in only two of

Table 1 Methylation status of sites I–IV in ovarian cell lines and primary tumors with corresponding TCEAL7 expression

	I			*II*				*III*	*IV*							*RT–PCR*	*Age*	*LOH*
OSEtsT	●	□	●	●	□	●	●	●	□	□	●	●	●	●	●	●	++		
OSE54	●	□	●	●	□	●	●	●	□	□	●	●	●	●	●	●	++		
OV167	●	●	●	●	●	●	●	●	●	●	●	●	●	●	●	●	–		
OV177	●	●	●	●	●	●	●	●	●	●	●	●	●	●	●	●	–		
OV202	●	●	●	●	●	●	●	●	●	●	●	●	●	●	●	●	–		
OV266	●	●	●	●	●	●	●	●	□	●	●	●	●	●	●	●	–		
OVCAR5	●	●	●	●	□	●	●	●	□	●	●	●	●	●	●	●	–		
SKOV3	●	●	●	●	●	●	●	●	□	●	●	●	●	●	●	●	–		
4	●	●	●	●	□	●	●	●	□	●	●	●	●	●	●	●	–	69	–LOH
13	●	●	●	●	□	●	●	●	●	●	●	●	●	●	●	●	–	58	–LOH
34	●	●	●	●	●	●	●	●	●	●	●	●	●	●	●	●	–	44	
45	●	□	●	●	●	●	●	●	□	●	●	●	●	●	●	●	–	56	
97	●	□	●	●	●	●	●	●	□	●	●	●	●	●	●	●	++	55	+LOH
98	●	●	●	●	●	●	●	●	□	●	●	●	●	●	●	●	–	57	–LOH
107	●	●	●	●	●	●	●	●	ND	●	●	●	●	●	●	●	–	48	–LOH
121	●	●	●	●	●	●	●	●	□	●	●	●	●	●	●	●	–	50	
183	●	□	●	●	●	●	●	●	○	●	●	●	●	●	●	●	–	61	
206	●	●	●	●	□	●	●	●	●	●	●	●	●	●	●	●	–	62	
208	●	●	●	●	□	●	●	●	●	●	●	●	●	●	●	●	–	60	+LOH
220	●	□	●	●	●	●	●	●	○	●	●	●	●	●	●	●	++	52	–LOH
235	●	□	●	●	●	●	●	●	□	●	●	●	●	●	●	●	–	72	
259	●	●	●	●	●	●	●	●	□	●	●	●	●	●	●	●	–	54	
283	●	●	●	●	●	●	●	●	□	●	●	●	●	●	●	●	ND	64	
285	●	○	●	●	●	●	●	●	○	●	●	●	●	●	●	●	++++	70	–LOH
288	●	□	●	●	●	●	●	●	○	●	●	●	●	●	●	●	+	80	
339	●	●	●	●	●	●	●	●	□	●	●	●	●	●	●	●	–	70	
358	●	□	●	●	●	●	●	●	□	●	●	●	●	●	●	●	+	62	
402	●	●	●	●	□	●	●	●	●	●	●	●	●	●	●	●	–	61	
414	●	●	●	●	□	●	●	●	●	□	●	●	●	●	●	●	–	67	–LOH
461	●	□	●	●	●	●	●	●	□	●	●	●	●	●	●	●	++	45	–LOH
615	●	□	●	●	□	●	●	●	□	□	●	●	●	●	●	●	ND	76	
656	●	ND	●	●	ND	●	●	●	●	●	●	●	●	●	●	●	ND	87	
657	●	ND	●	●	□	●	●	●	○	ND	●	●	●	●	●	●	ND	62	

Filled and unfilled circles represent methylated and unmethylated alleles, respectively. A circle with a line across represents hemimethylation. Expression $\geqslant$1.5-fold over OSE (+ + + +), between 1.1 and 0.9-fold (+ +); $\leqslant$0.5 (+); no expression (–), not determined (ND); positive LOH (+LOH); negative LOH (–LOH). Samples used in RT–PCR (Figure 6b) and LOH analyses are highlighted in bold

seven ovarian cancer cell lines. *TCEAL8*, located 256 kb telomeric to *TCEAL7*, is lost in only three of seven ovarian cancer cell lines (data not shown). Consequently, of the three highly identical genes in Xq22.1–22.2, only *TCEAL7* showed complete loss of expression in all the tested cell lines. Although these three genes mapping to the region could potentially be inactivation targets, we believe that *TCEAL7* is the most likely target gene since expression of *TCEAL7* is lost in >90% of primary ovarian tumors and 100% of the cell lines compared to other genes in this region.

Presumably, the presence of a tumor suppressor gene on the X chromosome would imply that males with only one X chromosome would be more prone to tumorigenesis than females with two X chromosomes. However, since *TCEAL7* is subjected to X chromosome inactivation and normally expressed from one allele, lack of second allele in male would not be significant.

The presence of a putative tumor suppressor gene on the X chromosome where one allele is inactivated as a result of X inactivation, a single hit in the active allele, would be sufficient to inactivate the gene. Under such a scenario, LOH, mutation, or methylation of the active allele could contribute to the loss of function of the tumor suppressor gene. Since we could not detect any mutation in 96 ovarian tumors we analysed by DHPLC, mutational inactivation may not be the predominant mechanism in the silencing of TCEAL7 in ovarian

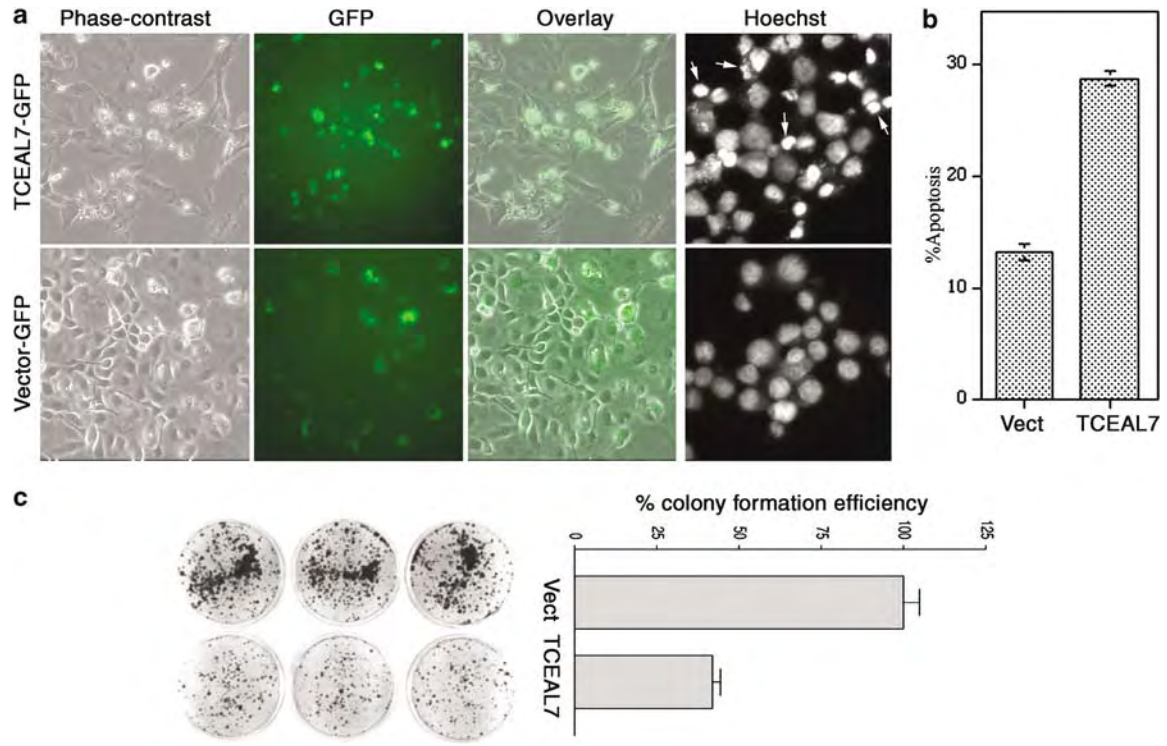

Figure 7 TCEAL7 induces cell death. (**a**) Forced expression of TCEAL7 resulted in apoptotic morphology in cells expression transfected with TCEAL7 (upper panels), whereas normal cell morphology was observed in control vector-transfected cells (lower panels). (**b**) Nuclear morphologic analysis shows pyknotic nuclei (indicated by arrows) in TCEAL7-transfected cells. (**c**) Quantitative analysis of apoptotic nuclei in these cells indicates a significant increase in apoptosis in cells transfected with TCEAL7

cancer. Analysis of LOH and TCEAL7 expression showed only one tumor with LOH with corresponding loss of TCEAL7 (Table 1, #208). In tumor #97, TCEAL7 expression was detected even though the tumor showed LOH, suggesting deletion of the inactive allele in this tumor. These data suggest that LOH may not be the main mechanism responsible for the inactivation of TCEAL7 in ovarian tumors. However, based on the fact that the *TCEAL7* expression is induced by demethylation on 5-aza-2′-deoxycytidine treatment, it seems most likely that methylation is the mechanism by which TCEAL7 is inactivated in a majority of primary ovarian tumors and cell lines. Consistent with this hypothesis, majority of cell lines and tumors with loss of *TCEAL7* expression showed hypermethylation of some specific CpG sites in the promoter region. These data suggest that epigenetic silencing as a major mechanism in TCEAL7 inactivation. Emerging evidence indicates that epigenetic silencing by methylation of tumor suppressor genes is a common mechanism leading to loss of function of the gene.

The fact that TCEAL7 expression is epigenetically silenced in ovarian cancer might be of clinical significance because unlike mutation where DNA information is irreversibly changed, epigenetic modification can be reversed by DNA methyl transferase inhibitors or histone-modifying agents (Teodoridis *et al*., 2004). With the emerging role of the use of small molecule inhibitors that modify the enzyme activities of DNA methyl transferases and histone deacetylases in 'epigenetic therapies' (Esteller, 2005), TCEAL7 could serve as a potential target of epigenetic therapy. It is suggested that re-expression of silenced apoptotic genes by epigenetic therapy might re-sensitize drug-resistant cancer cells to conventional chemotherapy (Balch *et al*., 2004). In that sense, re-activation of TCEAL7 in chemoresistant ovarian cancer might be of clinical relevance. Finally, due to its widespread loss in ovarian cancer, TCEAL7 may potentially be used as an epigenetic marker for detection of ovarian cancers at earlier stages.

Although recent data on the methylation status of several genes implicate a spreading of methylation and an overall increase in the frequency of methylated CpGs in the tumor cell lines and primary ovarian tumors, our data indicate that specific sites within the promoter as a target of methylation. Site-specific methylation in the BRCA1 regulatory region, specifically at the cyclic AMP response element, was observed in breast and ovarian tumors (Mancini *et al*., 1998). Site-specific methylation of Wilms tumor suppressor gene in rat mesotheliomas (Kleymenova *et al*., 1998), and in TIMP3 gene (Pennie *et al*., 1999) have been reported. More recently, specific methylation at −253 and −251 nt of the hMLH1 gene was observed in two of 60 primary gastric carcinomas, but not in the corresponding mucosa or in normal gastric samples (Deng *et al*., 2003). Consistent with these

reports, our analysis also indicates site-specific methylation may control TCEAL7 expression. This conclusion is further supported by our promoter analysis where site-specific mutation that prevents methylation at this site also prevented the epigenetic silencing of the promoter.

Although there is general consensus that transcriptional activities of X-linked genes are maintained in the somatic cell hybrids, there are exceptions to this rule (Brown and Robinson, 1997). Sequence analysis of genomic DNA from hybrids containing active X did not show any deletion or mutation of the primer annealing sites. While the reasons for this selective inactivation are not known, further analysis indicated that methylation of *TCEAL7* at CpG sites 1 and 2 was the mechanism of inactivation, as treatment with 5-aza-dC caused demethylation at this site and expression of *TCEAL7* in this cell line. Although demethylation of other genes involved in the transcription of *TCEAL7* could account for this induction, the fact that *in vitro* methylation of the promoter suppresses the promoter activity lends support to direct activation of the promoter on demethylation. Inactivation of *TCEAL7* during somatic cell hybrid generation appeared to be specific, since two flanking genes, namely *pp21 homolog* and *bex3/NADE*, were expressed by active X. Evidence for age-related methylation has been documented for tumor suppressor and tumor-related genes and in women with increasing age (Waki *et al*., 2003; Hatakeyama *et al*., 2004). We did not see a strong correlation to increasing age as a factor in biallelic methylation pattern seen at sites 1, 2, and 4 as evidenced by lack of biallelic methylation at site 3 in a majority of samples (17/24 primary tumor samples).

We find that re-expression of *TCEAL7* induces apoptosis, suggesting that the loss of TCEAL7 is not a random event in carcinogenesis, but a selected event that favors the survival of cancer cells. *TCEAL7* belongs to the family of brain-expressed proteins that includes the $p75^{NTR}$-associated death executor (NADE/Bex3). NADE/Bex3 has been shown to mediate apoptosis induced by $p75^{NTR}$ (Mukai *et al*., 2000). These data suggest that loss of function of the proapoptotic protein TCEAL7 in cancer cells may confer them survival advantage and may promote tumorigenesis. However, it should be noted that apoptosis associated with re-expression of TCEAL7 could be the result of over-expression, since TCEAL7 is monoallelically expressed in normal ovarian epithelial cells without detrimental effect to the cells. Functional analysis elucidating TCEAL7 interacting proteins will shed more light on the role of this nuclear protein plays in apoptosis regulation.

Materials and methods

Cell culture

Five of eight ovarian carcinoma cell lines (OV 167, OV 177, OV 202, OV 207, and OV 266) were low-passage primary lines established at the Mayo Clinic (Conover *et al*., 1998), while OVCAR-5 and SKOV-3 were from American Type Culture Collection (Manassas, VA, USA). All cells were grown according to the providers' recommendations.

Strategy for cloning the gene

BLAST search of the isolated sequence identified several homologous ESTs in the dbEST. The homologous ESTs were assembled into a contig with the use of Sequencher 3 (Gene Codes Corp, Ann Arbor, MI, USA) software. The integrity of the full-length cDNA obtained by this electronic walking was confirmed by PCR analysis using PCR primers flanking each junction between EST clones. The entire cDNA contig was sequenced twice with overlapping primers.

Immunoblotting

Western blot analysis was performed using whole-cell lysates from ovarian cell lines. Polyclonal antibodies against TCEAL7 were generated by injecting two rabbits with the recombinant full-length TCEAL7 protein purified from bacteria using pGEX expression system (Novagen, San Diego, CA, USA).

Light Cycler Assay

Using TCEAL7-F (5′-AAAAACCCTGCAAAGAAAAC GAA-3′) and TCEAL7-R (5′-CCATACGGGCGTTTTTC CT-3′) plus RPS9F (5′-TCGCAAAACTTATGTGACCC-3′) and RPS9R (5′-TCCAGCACCCCCAATC-3′) primers, duplex PCR amplification was carried out with Light-Cycler (Roche, Indianapolis, IN, USA) in the presence of SYBR-Green dye according to the following conditions: 1 min at 95°C for initial denaturation, followed by 40 cycles at 95°C (10 s), 58°C (15 s), and 72°C (20 s), followed by the measurement of fluorescence at the end of each cycle. After the 40th cycle, melting curve analyses were performed with Light-Cycler software by denaturing the sample at 95°C, rapidly cooling down to 65°C for 15 s, and measuring the fluorescence as the sample temperature was gradually raised to 95°C in steps of 0.1°C/s. Each run included a negative control and a known RPS9 control.

Assessment of methylation control

The somatic cell hybrid [Y162.11C] containing the active X (Xa) and OV 207 cell lines were treated with varying concentrations of 5-aza-2′-dc ranging from 1 to 5 μM the day after plating. After a 48 h exposure to 5-aza-2′-dc, the cells were harvested in Trizol (Gibco/Life Technologies, Rockville, MD, USA) for RNA extraction.

Genomic sequencing of bisulfite-modified DNA

The methylation status of *TCEAL7* was determined by genomic sequencing of bisulfite-modified DNA as described previously (Shridhar *et al*., 2001a). The PCR primers used for bisulfite-modified DNA are as follows: promoter region (site #1) MF1: 5′-TGT GAT TTA TAG TTG CGA TTT G-3′ and MR1: 5′-CCA ACC ACC TAT TTC TAC TAC T-3′; exon 1 and intron 1–1 (sites #2 and #3) MF2A/B: 5′-ATT AGG AGT TGA CGT GAA TCG-3′ and MR2A/B: 5′-CTA TTC CAA TCA TTA ATT CAC CC-3′; intron 1–2 (site #4) MF3: 5′-GTA TGT GTT GGT GTG TGG AGA AAG-3′ and MR3: 5′-AAA CCT AAA CCT TAC AAA ACC GCG-3′. The annealing temperatures for the three primer sets were 54°C for sites 1–3 and 65° C for site 4.

Semiquantitative RT–PCR

A 50–100 ng portion of reverse-transcribed cDNA was used in a multiplex reaction with TCEAL7-99F: 5′-GCA GGA AAC AAC AAC AAC AT-3′ and reverse primer TCEAL7-523R: 5′-AAG TGC AGA CAA ACA GAA AGC AGT GG-3′ and GAPDH forward (5′-ACC ACA GTC CAT GCC ATC AC-3′) and reverse primers (5′-TCC ACC ACC CTG TTG CTT GTA-3′). The primers for pp21 homolog and Bex3/NADE are as follows: pp21ORF F 5′-GAA GGA AGA GAG GTA GAC AG-3′, pp21ORF R 5′-GGG GTA AGG ATG GTT TCG AT-3′, Bex3/NADE F 5′-GTC TCT CTC CTT GCC TTT GT-3′, and Bex3/NADE R 5′-ATG GCA GGA GTC AAG GCA TA-3′. The PCR reaction mixes contained 50 mM KCl, 10 mM Tris-HCl (pH 8.3), 1.5 mM $MgCl_2$, 400 μM of each primer for TCEAL7 and 50 μM for the GAPDH primers, and 0.5 U of *Taq* polymerase (Qiagen, Valencia, CA, USA) in a 12.5 μl reaction volume. The conditions for amplification were 94°C for 3 min, and then 29 cycles of 94°C for 30 s, 58°C for 30 s, and 72°C for 30 s in a Perkin-Elmer-Cetus 9600 Gene-Amp PCR system. The products of the reaction were resolved on a 1.6% agarose gel. Band intensities were quantified using the Gel Doc 1000 photodocumentation system (Bio-Rad, Hercules, CA, USA) and its associated software and normalized with GAPDH controls.

Plasmid constructs

The coding region of TCEAL7 was amplified by PCR using primers (5′) GCA GGA AAC AAC AAC AAC ATC and (3′) TTA AAT GGG ATA AGG GAC GGT-3′ and cloned into pcDNA3/GFP-CT TOPO cloning vector from Invitrogen following the manufacturer's recommendations.

Promoter constructs

To investigate whether *Sma*I site I methylation suppresses TCEAL7 promoter activity, an 882 bp fragment containing 12 CpG sites including the *Sma*I sites I and II was cloned into *Xho*I and *Hind*III sites in pGL3 vector. Primers used for promoter construct were as follows: (a)-F/R, 5′-CCGC TCGAG GACTTACAGTTGCGATCTGG-3′/5-CCCAAGC TT CCTCCTTCCTGTCTGTATCC-3′. Constructs carrying single-site mutation of sites I and II were generated by mutating CCCGGG to CCAGGG so that it was no longer subjected to *in vitro* methylation.

Transient transfection and luciferase assays

HeLa cells were seeded at a density of 3×10^5/well in a six-well dish and grown to 60–70% confluence in complete growth media containing DMEM supplemented with 10% FBS. For each well, 2 μg of plasmid DNA and 0.01 μg of pRL-TK control vector (triplicate for each group) were cotransfected into cells with oligofectamine (Invitrogen, Carlsbad, CA, USA) according to the manufacturer's instructions. After incubation for 24 h, cells were harvested, and luciferase activities were measured by using a Dual-Luciferase Report Assay System (Promega, Madison, WI, USA) in an Analytical Luminometer Monolight 2010 (PharMingen, San Diego, CA, USA) according to the manufacturer's instructions. Relative luciferase activities were calculated as the ratio of firefly/Renilla luciferase.

In vitro *methylation*

In vitro methylation was carried out according to the methods described previously (Song *et al*., 2001). Briefly, TCEAL7 promoter constructs containing wild-type or mutated *Sma*I I site I were incubated overnight with three units of SssI (CpG) methylase (New England Biolabs, Beverly, MA, USA) in the presence (methylated) or absence (mock-methylated) of 1 mM *S*-adenosylmethionine, as recommended by the manufacturer. After purification with a QIAquick Gel Extraction Kit (Qiagen) and quantitation of DNA at A260 nm, equal amounts (2 μg) of methylated reporter constructs were transiently transfected into HeLa cell lines, and luciferase activities were measured as described above (Song *et al*., 2001). Individual reactions were monitored by digestion with *Sma*I restriction enzyme.

Densitometric analysis

Ethidium bromide-stained RT–PCR products of TCEAL7 and GAPDH were captured with GelDoc2000 system (Bio-Rad, Hercules, CA, USA), and densitometric analysis was performed using Quantity One software provided with Gel-Doc2000 system. TCEAL7 densitometric readings were normalized with that of corresponding GAPDH and expressed as fold increase or decrease compared to the TCEAL7 expression in OSE.

Assessment of cell viability

Cell viability was determined by examination of apoptotic morphology of nuclear staining with Hoechst 33258 as described previously.

Clonogenic assays

For clonogenic assays, flow-sorted vector GFP- and Bex4 GFP-containing cells (1000 cells/35 mm dish) were plated in triplicate, permitted to adhere overnight, and grown for 12–14 days to allow colonies to form. Cells were stained with Coomassie blue, digitally photographed, counted with Quantity One software (Bio-Rad), and expressed as % colony-forming efficiency.

Acknowledgements
We thank Dr Kimberly R Kalli (Mayo Clinic, Rochester) for the short-term cultures of OSE and Dr Mariano Rocchi (University of Bari, Italy) for the somatic cell hybrids used in this study. This work was supported by Department of Defense Grant W81XWH-04-1-0085 (to VS) and DAMD17-02-1-0473 (to VS, DIS, SHK, and LCH) and the Mayo Foundation (to VS).

References

Altschul SF, Madden TL, Schaffer AA, Zhang J, Zhang Z, Miller W and Lipman DJ. (1997). *Nucleic Acids Res.*, **25,** 3389–3402.

Balch C, Huang TH, Brown R and Nephew KP. (2004). *Am. J. Obstet. Gynecol.*, **191,** 1552–1572.

Baylin S and Bestor TH. (2002). *Cancer Cell*, **1,** 299–305.

Baylin SB and Herman JG. (2000). *Trends Genet.*, **16,** 168–174.

Brown AL and Kay GF. (1999). *Hum. Mol. Genet.*, **8,** 611–619.

Brown CJ and Robinson WP. (1997). *Am. J. Hum. Genet.*, **61,** 5–8.

Conover CA, Hartmann LC, Bradley S, Stalboerger P, Klee GG, Kalli KR and Jenkins RB. (1998). *Exp. Cell Res.*, **238,** 439–449.

Deng DJ, Zhou J, Zhu BD, Ji JF, Harper JC and Powell SM. (2003). *World J. Gastroenterol.*, **9,** 26–29.

Esteller M. (2005). *Curr. Opin. Oncol.*, **17,** 55–60.

Esteller M, Fraga MF, Paz MF, Campo E, Colomer D, Novo FJ, Calasanz MJ, Galm O, Guo M, Benitez J and Herman JG. (2002). *Science*, **297,** 1807–1808; discussion 1807–1808.

Faria TN, LaRosa GJ, Wilen E, Liao J and Gudas LJ. (1998). *Mol. Cell Endocrinol.*, **143,** 155–166.

Hatakeyama C, Anderson C, Beever C, Penaherrera M, Brown C and Robinson W. (2004). *Clin. Genet.*, **66,** 327–332.

Herman JG, Graff JR, Myohanen S, Nelkin BD and Baylin SB. (1996). *Proc. Natl. Acad. Sci. USA*, **93,** 9821–9826.

Jaenisch R and Bird A. (2003). *Nat. Genet.*, **33** (Suppl)**,** 245–254.

Jemal A, Tiwari RC, Murray T, Ghafoor A, Samuels A, Ward E, Feuer EJ and Thun MJ. (2004). *CA Cancer J. Clin.*, **54,** 8–29.

Jones PA and Baylin SB. (2002). *Nat. Rev. Genet.*, **3,** 415–428.

Jones PA and Laird PW. (1999). *Nat. Genet.*, **21,** 163–167.

Kleymenova EV, Yuan X, LaBate ME and Walker CL. (1998). *Oncogene*, **16,** 713–720.

Kozak M. (1996). *Mamm Genome*, **7,** 563–574.

Laird PW. (2003). *Nat. Rev. Cancer*, **3,** 253–266.

Li E, Bestor TH and Jaenisch R. (1992). *Cell*, **69,** 915–926.

Mancini DN, Rodenhiser DI, Ainsworth PJ, O'Malley FP, Singh SM, Xing W and Archer TK. (1998). *Oncogene*, **16,** 1161–1169.

Mukai J, Hachiya T, Shoji-Hoshino S, Kimura MT, Nadano D, Suvanto P, Hanaoka T, Li Y, Irie S, Greene LA and Sato TA. (2000). *J. Biol. Chem.*, **275,** 17566–17570.

Mukai J, Shoji S, Kimura MT, Okubo S, Sano H, Suvanto P, Li Y, Irie S and Sato TA. (2002). *J. Biol. Chem.*, **277,** 13973–13982.

Pennie WD, Hegamyer GA, Young MR and Colburn NH. (1999). *Cell Growth Differ.*, **10,** 279–286.

Persengiev SP and Kilpatrick DL. (1997). *Neuroreport*, **8,** 2091–2095.

Rapp G, Freudenstein J, Klaudiny J, Mucha J, Wempe F, Zimmer M and Scheit KH. (1990). *DNA Cell Biol.*, **9,** 479–485.

Saitoh F, Hiraishi K, Adachi M and Hozumi M. (1995). *Anticancer Res.*, **15,** 2137–2143.

Shridhar V, Bible KC, Staub J, Avula R, Lee YK, Kalli K, Huang H, Hartmann LC, Kaufmann SH and Smith DI. (2001a). *Cancer Res.*, **61,** 4258–4265.

Shridhar V, Lee J, Pandita A, Iturria S, Avula R, Staub J, Morrissey M, Calhoun E, Sen A, Kalli K, Keeney G, Roche P, Cliby W, Lu K, Schmandt R, Mills GB, Bast Jr RC, James CD, Couch FJ, Hartmann LC, Lillie J and Smith DI. (2001b). *Cancer Res.*, **61,** 5895–5904.

Shridhar V, Sen A, Chien J, Staub J, Avula R, Kovats S, Lee J, Lillie J and Smith DI. (2002). *Cancer Res.*, **62,** 262–270.

Song SH, Jong HS, Choi HH, Inoue H, Tanabe T, Kim NK and Bang YJ. (2001). *Cancer Res.*, **61,** 4628–4635.

Teodoridis JM, Strathdee G and Brown R. (2004). *Drug Resist. Update*, **7,** 267–278.

Waki T, Tamura G, Sato M and Motoyama T. (2003). *Oncogene*, **22,** 4128–4133.

Williams JW, Hawes SM, Patel B and Latham KE. (2002). *Mol. Reprod. Dev.*, **61,** 281–287.

Yang QS, Xia F, Gu SH, Yuan HL, Chen JZ, Yang QS, Ying K, Xia Y and Mao YM. (2002). *Biochem.Genet*, **40,** 1–12.

Yeh CH and Shatkin AJ. (1994). *Proc. Natl. Acad. Sci. USA*, **91,** 11002–11006.

Yeh CH and Shatkin AJ. (1995). *J. Biol. Chem.*, **270,** 15815–15820.

REVISED MANUSCRIPT UNDER PREPARATION

Candidate tumor suppressor gene TCEAL7 associates with Bin1 and regulates Myc

Jeremy Chien[1], Keishi Narita[1], Ravi Shridhar[2], Yunqian Pan [1], Julie Staub[1], Heyu Zhang[1], Jinping Lai[3], Lewis Roberts[3], Lynn C Hartmann[4], Scott H. Kaufmann[5], George C. Prendergast[6], and Viji Shridhar[1]

1. Department of Experimental Pathology, Mayo Clinic College of Medicine, Rochester, MN 55905
2. Department of Radiation Oncology, Wayne State University School of Medicine, Detroit, MI
3. Department of Gastroenterology and Hepatology, Mayo Clinic College of Medicine, Rochester, MN 55905
4. Department of Medical Oncology, Mayo Clinic College of Medicine, Rochester, MN 55905
5. Department of Oncology Research, Mayo Clinic College of Medicine, Rochester, MN 55905
6. Lankenau Institute for Medical Research, Wynnewood, PA 19096.

Running title: TCEAL7 regulates Myc

Keyword: TCEAL, Myc, Bin1, Ovarian Cancer

Correspondence: Please send request for materials and reprints to:
Viji Shridhar
Department of Experimental Pathology
Mayo Clinic College of Medicine
Rochester, MN 55905
shridhar.vijayalakshmi@mayo.edu

Summary

Transcription-elongation factor A-like 7 (TCEAL7) is a candidate tumor suppressor gene that is epigenetically silenced in ovarian cancer and other human cancers. TCEAL7 encodes a proapoptotic nuclear protein, the precise function of which is unknown. Here we report that TCEAL7 binds to a Myc-interacting isoform of the tumor suppressor protein Bin1 and that TCEAL7 inhibits Myc transactivation activity. TCEAL7-mediated down-regulation of Myc activity resulted in reduced cell proliferation and decreased expression of cyclin D1, an effect associated with recruitment of TCEAL7 to the E box-containing region of the cyclin D1 promoter that is bound by c-Myc. Finally, down-regulation of TCEAL7 in immortalized ovarian epithelial cells resulted in >4 fold increase in Myc activity, increased proliferation and anchorage-independent growth. We propose a model in which TCEAL7 modifies the transactivation activity of Myc through direct interactions with Myc and Bin1. Thus our findings extend the evidence of a tumor suppressor role for TCEAL7, and offer initial mechanistic insights into how this protein may modulate cell proliferation and transformation.

Significance

Expression of the proto-oncogene *myc* is frequently deregulated in cancer, and its transcriptional activity on specific target genes is required to promote cell growth and metabolism associated with cancer. Here, we show a novel mechanism by which Myc transcriptional activity is deregulated by loss of a negative regulatory protein TCEAL7. In this report, we show that TCEAL7 regulates Myc activity and selectively impairs Myc-induced proliferative pathway by inhibiting cyclin D1. In addition, we have also shown that shRNA-mediated down-regulation of TCEAL7 in immortalized ovarian epithelial cells leads to transformed phenotype. Our observations thus uncover a novel component of the negative regulatory pathway that act to restrict Myc activity and provide an initial mechanistic insight into how TCEAL7 may regulate Myc and modulate cell proliferation and malignant transformation. These results also provide an additional mechanism by which Myc activity could be deregulated in cancers, and suggest that deregulated Myc may play a greater role in oncogenesis of human tumors than previously appreciated.

Introduction

The c-Myc is a basic helix-loop-helix-zipper (bHLH-ZIP) transcription factor and belongs to *myc* family genes (Grandori et al., 2000). Expression of *myc* is frequently deregulated in tumors of diverse origins due to chromosomal translocations, rearrangements, amplifications, retroviral transductions, and viral insertions (Dalla-Favera et al., 1982; Grandori et al., 2000; Nesbit et al., 1999; Oster et al., 2002; Taub et al., 1982). Deregulated Myc expression affects proliferation, differentiation, and apoptosis of cancer cells and contributes to multi-step carcinogenesis (Baudino and Cleveland, 2001). When heterodimerized with another bHLH-ZIP transcription factor Max, Myc acquires the capacity to bind to the E-box DNA sequence and regulates the expression of a large number of target genes (Grandori and Eisenman, 1997). Recent studies indicate that as many as 10-15% of all genes in mice and flies may be influenced by Myc activity (Fernandez et al., 2003; Orian et al., 2003). Myc transcriptional activity is in turn regulated by other bHLH-ZIP transcription factors, such as MAD family members and Mnt, which associate with Max and titrate Max away from Myc (Grandori et al., 2000). Consistent with the model of Myc and Max as a heterodimeric binding partners, recent studies involving genome-wide screening of Myc and Max target genes show an overlap of target genes between Myc and Max (Fernandez et al., 2003; Orian et al., 2003). Myc activity is also modulated by the recruitment of chromatin remodeling and modifying complexes, such as SWI/SNF and TRAPP/GCN5, as well as other interacting proteins, such as YY1, AP2, MIZ1, SP1, BRCA1, and TFII-I which interact

with the C-terminal domain (CTD) of Myc, and p107, Bin1, MM-1 and AMY-1 which interact with the N-terminal domain (NTD) of Myc (Sakamuro and Prendergast, 1999).

Among the Myc NTD-interacting proteins, nuclear isoforms of Bin1 have been identified as modulators of transformation, apoptosis, tumorigenesis and transcriptional transactivation by Myc (DuHadaway et al., 2001; Elliott et al., 1999; Muller et al., 2004; Sakamuro et al., 1996). Bin1 proteins include two regions implicated in Myc binding, an SH3 domain located at the C-terminus and a Myc-binding domain located immediately upstream that mediate association with Myc boxes 1 and 2 in the N-terminal transactivation domain of Myc (Elliott et al., 1999; Pineda-Lucena et al., 2005; Sakamuro et al., 1996). Interestingly, Bin1 triggers apoptosis when restored in tumor cells where endogenous Bin1 is attenuated or mis-spliced, resulting in loss of nuclear functions, but not in cells which maintain endogenous Bin1 expression and nuclear functions (DuHadaway et al., 2001; Elliott et al., 2000; Galderisi et al., 1999; Ge et al., 1999; Ge et al., 2000; Tajiri et al., 2003). These data suggest that apoptotic property of Bin1 is coupled with deregulated Myc expression, and loss of Bin1 favors survival of tumor cells with deregulated Myc expression. Identification of additional factors that interact with Myc and Bin1 could further delineate the role of these Myc-interacting proteins in the context of deregulated Myc expression. Bin1 has an additional N-terminal region, termed the BAR (Bin/Amphiphysin/Rvs) domain, which is also important for its Myc modulatory activities, however, the mechanism underlying the nuclear action of this domain is unknown.

We have recently identified a novel transcription factor TCEAL7, belonging to a family of transcription elongation factor proteins, to be down-regulated in ovarian cancer in suppression subtraction hybridization and by transcriptional profiling analyses (Chien et al., 2005; Shridhar et al., 2001; Shridhar et al., 2002). Although the transcriptional regulatory roles of the TCEAL proteins are not known, their closely related protein TFIIS/TCEA is involved in transcription elongation and transcript fidelity (Jeon and Agarwal, 1996; Thomas et al., 1998). TFIIS/TCEA promotes 3' endoribonuclease activity of RNA polymerase II (pol II) and allows pol II to bypass transcript pause or "arrest" during elongation process (Thomas et al., 1998). On the other hand, TCEAL1/SIIR/p21 is a nuclear phosphoprotein implicated in repression of Rous sarcoma virus long terminal repeat (RSV LTR) transcription activity and suppression of transformation mediated by RSV LTR in a promoter context-dependent manner (Yeh and Shatkin, 1995). In this study, we show that TCEAL7 associates with Bin1, regulates Myc transcriptional activity, and inhibits growth by downregulating the Myc target gene cyclin D1.

Results

TCEAL7 is expressed in normal tissues but selectively down-regulated in cancer.

TCEAL7 was originally identified as an epigenetically silenced down-regulated gene in ovarian cancer by suppression subtraction hybridization and cDNA microarray analyses. To validate its down-regulation in cancer, TCEAL7 expression was determined by Northern analyses in multiple tissues, 7 ovarian cancer cell lines and 24 primary ovarian tumors. TCEAL7 is expressed as a 1.35 kb transcript in various normal tissues including ovary (Figure 1A and Supplementary Figure 1). In contrast, in ovarian cancer, TCEAL7 is down-regulated in all 7 tested cell lines (Figure 1B) and in 21 of 24 primary tumors (Figure 1C) but highly expressed in short-term cultures of ovarian surface epithelial cells (OSE). Microarray analysis of additional 51 ovarian tumors of differing histologies also indicates down-regulation of TCEAL7 transcripts in a majority of tumors (Figure 1D).

To determine whether TCEAL7 down-regulation is specific, expression of two other genes mapping close to TCEAL7 was tested in cancer cell lines by RT-PCR. pp21 homolog and

p75NTR-associated death executor (NADE) map 21 kb and 45 kb centromeric to TCEAL7 (Figure 1E). Results of RT-PCR analysis shown in Figure 1F indicate minimal loss of expression of pp21 homolog and NADE in cancer cell lines, demonstrating that down-regulation of TCEAL7 in cancer is specific. In summary, the majority of tumor cell lines of diverse origins show selective and complete loss of TCEAL7 expression.

TCEAL7 is also down-regulated in other cancers.

RT-PCR analysis also indicates that TCEAL7 is down-regulated in all cervical, liver, prostate, breast cancer cell lines tested, 5/8 brain cancer cell lines and 6/10 primary brain tumors (Figure 2). Furthermore, meta-analyses of gene expression in human cancers, which are available through the Oncomine database (http://oncomine.org), indicate that TCEAL7 down-regulation is associated with a more aggressive phenotype in various cancers (see Supplementary Figure 2). These results suggest that TCEAL7 is frequently down-regulated in various cancers and that its down-regulation is associated with advanced stages or aggressive phenotype.

TCEAL7 is a nuclear protein.

Multiple sequence alignment using CLUSTALW analysis indicates TCEAL7 shares amino acid sequence homology with other members of transcription elongation factor A-like (TCEAL) family, all mapping to X chromosome (see Supplementary Figure 3). To determine the localization of TCEAL7, GFP-fusion construct containing full-length TCEAL7 was transfected into HEK-293T cells. Fluorescence imaging indicates that TCEAL7 is exclusively localized to the nucleus (Figure 3A, upper panel). In contrast, free GFP is detected both in the nucleus and the cytosol (Figure 3A, lower panel). Similar results were also seen with HeLa and in ovarian cancer cell lines (data not shown). Immunofluorescence analysis of endogenous TCEAL7 with monoclonal antibodies in OSEtsT (ovarian surface epithelial cells immortalized with temperature sensitive large T antigen) also shows nuclear localization (Figure 3B). However, ectopic expression of myc-tagged TCEAL7 results in cytoplasmic and nuclear localization (Figure 3C). These results are consistent with the observation that TCEAL7 contains a putative nuclear export signal (Figure 3D). We therefore concluded that endogenous TCEAL7 localizes to the nucleus.

TCEAL7 associates with a nuclear isoform of the tumor suppressor protein Bin1.

Protein-protein BLAST analysis also indicates that TCEAL7 shares sequence similarity with $p75^{NTR}$-associated death executor NADE (bex3) (Chien et al. 2005). In addition, forced expression of TCEAL7 has been shown to trigger cell death (Chien et al. 2005). To test whether TCEAL7 is capable of associating with other pro- and anti-apoptotic proteins, protein lysates from OV202 cells transfected with FLAG-tagged TCEAL7 was incubated with Apoptosis Antibody Array™ containing 150 antibodies against apoptotic regulatory proteins. These analyses revealed interactions of TCEAL7 the adapter proteins Bin1, FAST kinase, and the TRAIL decoy receptor DcR2 (Figure 4A). Immunostaining of GFP-tagged TCEAL7 and endogenous Bin1 indicated that both proteins are co-localized in the nucleus (Figure 4B), consistent with their possible interaction. Therefore, we decided to further characterize the interaction between TCEAL7 and Bin1. Immunoprecipitation of endogenous TCEAL7 from nonmalignant ovarian surface epithelial cells, OSETs/T(hTERT) resulted in the enrichment of Bin1 (Figure 4C-Left panel). However, our repeated attempts to reveal this interaction by immunoprecipitation of Bin1 failed to show an interaction with TCEAL7 (Figure 4C, Right panel). This could probably be due to the antibody epitope masking the site of interaction between Bin 1 and TCEAL7 (See Discussion). To determine the interaction and domains responsible for such interaction, several HA- tagged full length and deletion-constructs were used in the immunoprecipitation assay (Figure 4D). Immunoprecipitation of exogenously expressed TCEAL7 in HeLa cells resulted in the enrichment of a full-length (FL) isoform of Bin1, but neither

the Bin1 (-10-13) splice isoform lacking an intact MBD nor a deletion mutant that lacks a large part of the BAR domain were enriched (Figure 4E right panel) as detected by antibody to the HA tag. Notably, c-Myc was also enriched in immunocomplex of TCEAL7 (Figure 4D), suggesting that TCEAL7, Bin1, and c-Myc may be capable of forming a ternary complex. Conversely, immunoprecipitation of Bin1 or c-Myc resulted in enrichment of TCEAL7 (Figure 4F). In contrast to Bin 1, we were able to detect endogenous TCEAL7-Myc interaction in OSEtsT(hTERT) cells (Figure 4G) in both directions. Taken together, these results suggest that TCEAL7, Bin1, and c-Myc can associate with each other.

TCEAL7 suppresses Myc transcriptional activity

Since Bin1 has been shown to regulate Myc transcriptional activity, we tested whether TCEAL7 could also regulate Myc activity. Expression of TCEAL7 suppresses Myc activity as determined by luciferase reporter containing either the ornithine decarboxylase (ODC) promoter (Figure 5A) or an artificial promoter containing multimerized CACGTG E boxes that are bound by Myc (EMS promoter) (Figure 5B). In contrast, expression of TCEAL7 has no suppression effect on non-specific Bcl-2 or p21 promoter activity (Figure 5C). As shown in Figures 5A and 5B using either the ODC or the EMS promoter constructs, co-expression of Bin1 and TCEAL7 also suppresses Myc activity. However, no synergistic effect was observed with the co-expression of Bin1 and TCEAL7. Overexpression of the Bin1 (-10-13) isoform that lacks an intact c-Myc binding domain (MBD) partially attenuated TCEAL7 suppression on Myc activity. These results suggest a possibility that interaction between TCEAL7 and Bin1(-10/-13) titrates TCEAL7 away from Myc, thereby attenuating the ability of TCEAL7 to suppress the transactivation activity of Myc. On the other hand, co-expression of TCEAL7 and the Bin1 mutant lacking an intact BAR domain (Bin1ΔB) produces maximal suppression of Myc. Taken together, these results suggest that TCEAL7 and Bin1 may act to suppress Myc transactivation activity.

TCEAL7 suppresses cyclin D1

To test whether TCEAL7 expression could affect the expression of Myc-target genes, we selected cyclin D1 since it is deregulated in various malignancies and plays a critical role in regulating cell cycle progression. Expression of TCEAL7 resulted in down-regulation of both promoter activity and steady-state protein levels of cyclin D1, as determined by luciferase reporter assay (Figure 6A) and immunoblot analysis, respectively (Figures 6B-C). Since TCEAL7 is not expressed in majority of cancer cell lines, we attempted to generate stable cell lines expressing TCEAL7 in cancer cells. However, due to growth inhibitory effect of TCEAL7 overexpression, we were not successful in generating stable cell lines. Therefore, we generated a cell line expressing inducible TCEAL7 in 293T-FlpIn(TRex) cells to further characterize the function of TCEAL7 (Figure 6D). We selected this cell line because it permits well-defined integration and regulated expression of TCEAL7. We then used this cell line to test whether TCEAL7 is recruited to cyclin D1 promoter by chromatin immunoprecipitation analysis using anti-TCEAL7 antibody. Chromatin immunoprecipitation (ChIP) and PCR was performed from extracts prepared from cells that were grown 24 hr under control or gene induction conditions. We observed enrichment of a fragment of the cyclin D1 promoter that contained the E box sequence recognized by c-Myc, but not other regions of the cyclin D1 promoter (Figure 6E). No enrichment of the E box-containing DNA fragment was detected in cells grown in the absence of TCEAL7 gene induction by doxycycline (Figure 6E). These results suggest that TCEAL7 is specifically recruited to the Myc-binding region on the cyclin D1 promoter. Analysis of cyclin D1 expression in cell cycle-synchronized HeLa cells with nacodazole as described in the methodsshow that expression of TCEAL7 not only suppresses cyclin D1 expression but also delays its cell-cycle-regulated expression by at least six hours (Figure 6F). Accordingly, TCEAL7 expression also correlated with a reduction in the number of cells entering S phase as

determined by BrdU labeling (Figures 6G and H). Taken together, these observations offered evidence that TCEAL7 targeted cyclin D1 expression through a mechanism that is consistent with modulation of Myc activity.

TCEAL7 suppresses colony formation efficiency of cancer cells

Consistent with its inhibition of Myc activity and subsequent suppression of cyclin D1 and cell cycle progression, forced expression of TCEAL7 reduces colony formation efficiency of HeLa cells (Figure 7). Both Bin1 and TCEAL7 individually are capable of suppressing colony formation. However, no additive effect in colony suppression was observed with co-expression of TCEAL7 and Bin1, suggesting that TCEAL7 and Bin1 may share the same pathway in suppression colony formation (Figure 7).

TCEAL7 down-regulation promotes soft-agar growth

To test whether down-regulation of TCEAL7 contributes to oncogenesis of ovarian cancer, we selected an immortalized ovarian epithelial cell line OSEtsT/hTERT and down-regulated TCEAL7 expression by shRNA. Previous studies by Westbrook *et al* indicates that primary epithelial cells immortalized with SV40 T-antigen and human catalytic subunit of telomerase (hTERT) provide an excellent model to test for genes associated with malignant transformation assessed by soft-agar growth (Westbrook et al., 2005). Therefore, we tested the malignant transformation potential of TCEAL7 down-regulation in OSEtsT/hTERT by soft-agar growth assay. Transfection with shRNA targeted to TCEAL7 resulted in down-regulation of TCEAL7 in two clonal lines of OSEtsT/hTERT (Figure 8A-B). No such down-regulation was observed in clonal lines expressing non-silencing shRNA construct. Subsequent soft-agar growth assays of these cell lines indicate that down-regulation of TCEAL7 promotes significant soft-agar growth of OSEtsT/hTERT cells (Figures 8B-C).

TCEAL7 down-regulation increases proliferation and promotes the basal Myc induced transcription of the ODC promoter/ reporter gene in OSEts/hTERT cells.

Using the MTS assay we determined the proliferation activity of two stable clones expressing pSR-vector (1-1 and 1-3) and two TCEAL7 down-regulated stable clones (2-1 and 3-6). As indicated in Figure 8D, pSR-TCEAL7 clones 2-1 and 3-6 proliferated at a higher rate compared to pSR-vector transduced clones. Since forced expression of TCEAL7 suppressed Myc induced transcription (Figures 5A and 5B), endogenous Myc activity was determined by luciferase reporter containing the ornithine decarboxylase (ODC) promoter in the two pSR-TCEAL7clones 2-1 and 3-6 compared to pSR-vector transduced clone 1-1. Down-regulation of TCEAL7 seems to promote the basal level of Myc activity by 4 to 5 fold in these immortalized ovarian epithelial cells (Figure 8E). In summary, our studies uncovered a novel pathway by which TCEAL7 imparts its growth inhibitory function and offer initial mechanistic insights into how this protein may modulate cell proliferation.

Discussion

c-Myc activity is upregulated in various malignancies and is critical for tumorigenesis (Baudino and Cleveland, 2001; Grandori et al., 2000; Nilsson and Cleveland, 2003; Sakamuro et al., 1996). Several mechanisms lead to the upregulation of c-Myc activity including amplification of the gene, upregulation of upstream growth factors or receptors, constitutive activation of downstream mediators, and down-regulation of negative regulators of Myc, such as Bin1 (Grandori et al., 2000; Sakamuro and Prendergast, 1999). In this study we offer evidence of a negative regulatory role for TCEAL7 in controlling Myc activity. This evidence is significant in light of the fact that TCEAL7 is substantially down-regulated in various cancer cell lines and

primary tumors, since our findings argue that TCEAL7 down-regulation may result in increased Myc activity.

Sequence homology between TCEAL7 and the p75NTR-associated death executor protein (Nade) and previous evidence that TCEAL7 can induce cell death (Chien et al., 2005) prompted us to examine how TCEAL7 influences cell survival and proliferation. Based on its ability to induce cell death, we tested whether TCEAL7 may potentially interact with other pro- and anti-apoptotic proteins. Analysis of candidate interacting proteins using the antibody array led to the identification of Bin1 as a TCEAL7 interacting protein. We have further shown that the interaction of TCEAL7 and Bin1 requires the BAR domain of Bin1, a region that was previously shown to be critical in inhibiting Myc transformation (Sakamuro et al., 1996). The most highly conserved 84 amino acid in the BAR domain of Bin1 is found to be essential for TCEAL7 interaction and is predicted to contain an α helical coil-coiled interaction domain (Lupas, 1996). Interestingly, TCEAL7 also contains a coil-coiled region (Chien et al., 2005) that could potentially interact with another coil-coiled containing protein such as Bin1. Therefore it is possible that the C-terminal coil-coiled domain of TCEAL7 may interact directly with the BAR domain of Bin1. We were able to detect these interactions with endogenously expressed proteins in OSE/tsT(hTERT) cells as well. Our inability to detect the endogenous interaction between Bin1 and TCEAL7 in the reverse direction could be partly due to the use of anti Bin1 antibody raised against the BAR domain- the region of interaction between TCEAL7 and Bin1.
Based on the observation that TCEAL7 interaction requires the integrity of the BAR domain of Bin1, which is required to inhibit Myc transformation, we investigated whether TCEAL7 affected Myc activity. Our analysis using either the ornithine decarboxylase (ODC) promoter or the artificial E-box promoter in a luciferase reporter assay system clearly indicated that TCEAL7 either alone or with Bin1 was capable of suppressing Myc activity. No synergistic effect on suppression of myc luciferase activity was observed with co-expression of TCEAL7 and Bin1, suggesting that TCEAL7 and Bin1 may be components of the same pathway. Interestingly, overexpression of Bin1 lacking the complete Myc binding domain (Bin1-10/-13) attenuated TCEAL7 suppression on Myc activity. These results suggest that Bin1, through its interaction with Myc and TCEAL7 via separate domains, may facilitate TCEAL7 in inhibiting Myc activity by helping deliver TCEAL7 to a Myc-containing complex. Further, we also found that an intact BAR domain and MBD is required for interaction and that TCEAL7, Bin1, and Myc could be co-immunoprecipitated with each other. These data suggest a model of ternary complex formation amongst TCEAL7, Bin1, and Myc. In one scenario, TCEAL7 may interact with Bin1 via the BAR domain and Bin1 may interact with both TCEAL7 and Myc via the MBD. The absence of an intact MBD, such as found in the Bin1 (-10/-13) splice isoform, would negate ternary complex formation by weakening the interaction with both TCEAL7 and Myc, thereby attenuating the inhibitory effect of TCEAL7 on Myc transactivation activity. It is also likely that Bin1 lacking intact MBD (-10/-13 isoform) through its interaction with TCEAL7 via BAR domain may partially titrate TCEAL7 away from the interaction with Myc, thus attenuating repression of TCEAL7 on Myc activity.

Secondary structure analysis of TCEAL7 indicates the presence of two helical domains with a short non-helical linker region between these domains (data not shown). Therefore, it is conceivable that TCEAL7 may contain a HLH domain which could mediate direct interaction with c-Myc. Consistent with this possibility, c-Myc could be co-immunprecipitated with TCEAL7. Our additional experiments using a Bin1 mutant lacking an intact BAR domain indicated that TCEAL7 could independently suppress Myc transcriptional activity, further supporting interaction between TCEAL7 and c-Myc. Nuclear role of TCEAL7 is further supported by the fact that endogenous TCEAL7 is localized to nucleus. However, it should be noted that ectopic expression of myc-tagged TCEAL7 also localizes to cytoplasm. This is in contrast to ectopic

expression of GFP-tagged TCEAL7, which exclusively localizes to the nucleus. This apparent difference in localization pattern could partly be explained by the presence of extra nuclear localization signal within GFP protein and by the presence of native putative nuclear export signal within TCEAL7.

Our data clearly indicate that a Myc target gene cyclin D1, which is frequently overexpressed in tumors of diverse origins, can be down-regulated by TCEAL7. Consistent with this, forced expression of TCEAL7 reduces colony formation efficiency of HeLa cells. The reduced colony forming abilities of both Bin1 and TCEAL7 were comparable, similar to what was observed with the suppression of Myc activity, with no additive or synergistic effect on co-transfection. These results suggest that both Bin1 and TCEAL7 function together in a single pathway in suppressing colony formation. In contrast to Bin1, expression of TCEAL7 is lost in a higher proportion of tumors and cell lines. Thus, while previous studies have clearly demonstrated that Bin1 can physically and functionally associate with Myc and inhibit malignant cell proliferation by both Myc-dependent and Myc-independent mechanisms, our results adds another dimension to this interaction.

It is interesting to note that although TCEAL7 suppresses Myc transactivation activity resulting in down-regulation of cylcin D1, it enhances Bcl2 and p21 promoter activities. These results are consistent with previous reports indicating that Myc activation suppresses Bcl2 and p21 expression (Eischen et al., 2001; Mitchell and El-Deiry, 1999; Seoane et al., 2002; Wu et al., 2003). These results highlight the functional significance of TCEAL7 as a Myc regulatory protein and provide further complexity in the functional regulation of Myc in proliferation and apoptosis.

Current models of Myc transcriptional activity require that Myc interact with Max. Myc activity is also indirectly influenced by other bHLH-Zip proteins, such as Mad and Mnt. These proteins associate with Max and competitively recruit Max away from Myc, thereby suppressing Myc activity. This model would suggest that Mad and Mnt could regulate the target genes shared by Myc and Max. However, based on the fact that Myc can interact with additional transcription factors and target genes independently of Max (Orian et al., 2003; Patel et al., 2004), regulation of Myc by Mad and Mnt may be limited to a subset of genes. These findings present a unique challenge to the identification of additional factors that associates with Myc and regulate Myc activity. Indeed, several transcription factors, such as YY1, Ap2, MIZ1, SP1, and BRCA1 have been shown to interact with Myc and modify Myc activity (Sakamuro and Prendergast, 1999). The conceptual value of these interactions may be to modulate the specificity of Myc for various target genes, for example, in different tissue types or at different periods during development or cell cycle transit.

Recently, several cell culture and genetically engineered mouse models of ovarian human cell transformation in which co-expression of co-operating oncogenes and tumor suppressor genes have been described (Connolly et al., 2003; Dinulescu et al., 2005; Flesken-Nikitin et al., 2003; Orsulic et al., 2002). These models have been useful in defining minimum genetic alterations required for transformation in a genetically defined context. To date, most of these models have included genes already implicated in human tumorigenesis. With the emergence of the RNA interference technology as a means to silence gene expression, additional genes not previously implicated in human cell transformation have been identified (Kolfschoten et al., 2005; Westbrook et al., 2005). In this study using an immortalized normal ovarian epithelial cell, we have identified that silencing TCEAL7 confers these cells the property of soft agar growth, an *in vitro* hallmark of transformation. shRNA down-regulated TCEAL7 clones formed colonies on soft agar while control vector transfected clones did not (Figure 8). This provides a

potentially new platform and identifies a new pathway that contributes to the transformed phenotype. Additional characterization of TCEAL7 down-regulated clones showed increased proliferation and more importantly potentiated Myc induced transcription of the ODC promoter/reporter construct, implicating loss of TCEAL7 resulting in Myc driven transformation. Taken together, these studies suggest that *TCEAL7* loss may promote transformation, cellular proliferation and survival of cancer cells. Given that the expression of TCEAL7 is down-regulated in more than 90% of primary ovarian tumors and cancer cell lines of different origins, it is possible that deregulated Myc as a result of TCEAL7 down-regulation may play a greater role in oncogenesis of human tumors than previously appreciated.

Based on the results from the present study, we propose the following model for suppression of Myc activity by TCEAL7 (Figure 9) (modified from Baudino and Cleveland 2001). In the model, Myc is in a transcriptionally competent state that is induced by Myc:Max interaction (1). When Max interacts with Mad, Myc is in a transcriptionally repressive state (2). Max switches between competence for transcriptional activation and repression based on its interaction with Myc or Mad (3). The association of bimodular or ternary complexes of Myc with TCEAL7, Bin1, or both proteins titers Myc away from Max, thereby licensing the availability of Max for interaction with Mad to repress Myc target genes which Myc expression persists (4). The Bin1 (-10-13) splice isoform lacking an intact MBD can weakly interact with TCEAL7 and thereby titer TCEAL7 away from Myc, thereby limiting the amount of Myc available to bind Max and to induce Myc target genes (5). By modulating Myc availability, TCEAL7 may indirectly limit formation of Mad/Max complexes that can regulate transcriptional targets such as cyclin D1 which directly control proliferation (6). In the model, down-regulation of TCEAL7 in cancer cells would effectively attenuate a negative regulatory pathway that can act to restrict Myc activity, thereby promoting Myc-induced malignant transformation.

Methods and Materials

Cell culture

Five of eight ovarian-carcinoma cell lines (OV 167, OV 177, OV 202, OV 207, and OV 266) were low passage primary lines established at the Mayo Clinic (14), while OVCAR-5 and SKOV-3 and as well as cervical (SiHa, CaSki, HT-3, HeLa, SW756, MS751, C-33-A, C-4- and ME-180), hepatocellular carcinomas (Hep3B, HepG2, HUH7, SNU182, SNU387, SNU423, SNU449, SNU475, SKHep1 and PLC5), prostate (BPH, Du 45, LnCAP and PC3), breast (HMEC, MCF-7, MCF-10A, MDA-MB-157, MDA-MB-361, MDA-MB-435, MDA-MB 468, UACC812 and UACC893), brain (total brain, D32, D37, M067, T989, U148, U251, U373) were from American Type Culture Collection (Manassas, VA). Normal Human Mammary Epithelial Cells (HMEC) is purchase from Clonetics Corp. (San Diego, CA). All cells were grown according to the providers' recommendations.

Northern Blot Analysis

The probe (PCR amplified ORF) was labeled using the random primer labeling system (Invitrogen, Carlsbad, CA) and purified using spin columns (100TE) from Clontech (Palo Alto, CA). Multiple Tissue Northern blot and Multiple Tissue Expression Array (Clontech) were hybridized at 68^{o} C with radioactive probes in a micro-hybridization incubator (Model 2000, Robbins Scientific, Sunnyvale, CA) for 1-3 hours in Express Hybridization solution and washed according to the manufacturer's guidelines**.**

Semi-quantitative RT-PCR

50-100 ng of reverse transcribed cDNA was used in a multiplex reaction with TCEAL7-99F: 5'- GCA GGA AAC AAC AAC AAC AT-3' and reverse primer TCEAL7-523R: 5'- AAG TGC AGA

CAA ACA GAA AGC AGT GG –3' and GAPDH forward (5' –ACC ACA GTC CAT GCC ATC AC-3') and reverse primers (5'- TCC ACC ACC CTG TTG CTT GTA-3'). The primers for pp21homolog and Bex3/NADE are as follows: pp21ORF F 5' GAA GGA AGA GAG GTA GAC AG 3', pp21ORF R 5' GGG GTA AGG ATG GTT TCG AT 3', Bex3/NADE F 5' GTC TCT CTC CTT GCC TTT GT 3', and Bex3/NADE R 5' ATG GCAG GAG TCA AGG CAT A 3'. The PCR reaction mixes contained 50 mM KCl, 10 mM Tris-HCl (pH 8.3), 1.5 mM $MgCl_2$, 400 μM concentration of each primer for TCEAL7and 50 μM for the GAPDH primers, and 0.5 units of Taq polymerase (Promega, Madison, WI) in a 12.5 μl reaction volume. The conditions for amplification were: 94°C for three min, then 29 cycles of 94°C for 30 sec, 58°C for 30 sec, and 72°C for 30 sec in a Perkin Elmer-Cetus 9600 Gene-Amp PCR system. The products of the reaction were resolved on a 1.6% agarose gel. Band intensities were quantified using the Gel Doc 1000 photo documentation system (Bio-Rad, Hercules, CA) and its associated software and normalized with GAPDH controls.

Plasmid Constructs

The coding region of TCEAL7 was amplified by polymerase chain reaction (PCR) using primers (5') GCA GGA AAC AAC AAC AAC ATC and (3') TTA AAT GGG ATA AGG GAC GGT-3' and cloned into pcDNA3/GFP-CT TOPO cloning vector from Invitrogen following the manufacturer's recommendation. Bin1 constructs (CMV99fe=FL, Bin1ΔBAR-C, Bin1-10/-13), pODC, and pEMS were generated as previously described (Elliott et al. 1999). Bcl2 (LB124) and p21 (1-Luc) promoter luciferase reporter plasmids were described previously (Wilson et al., 1996; Zeng et al., 1997).

cDNA Microarrays Analysis

The cDNA microarray data analysis was performed as previously described (Shridhar et al., 2001).

Immunofluorescence

Twenty-four hours after transfection of a TCEAL7-C terminal GFP fusion construct into OV202 cell line, the cells were fixed in 4% paraformaldehyde for 15 mins, washed, and incubated with TRITC conjugated phalloidin (Molecular Probe, Carlsbad, CA) for F-actin staining. For TCEAL7 and Bin1 colocalization, GFP-tagged TCEAL7 was transfected into HeLa cells. Cells were then fixed in 4% paraformaldehyde for 15 mins, washed, and incubated with 1:100 diluted mouse monocolonal antibodies against Bin1 for 1 hr (Elliott et al., 1999). After washing the cells, the cells were incubated with TRITC conjugated anti-mouse antibody for 1 hr. Immunoflurescence images are taken with SPOT Insight digital camera (Diagnostic Instruments, Sterling Heights, MI).

BrdU labelling

Twenty-four hours after transfection with vector-GFP or TCEAL7 GFP, cells were incubated in growth media containing 10 μM BrdU for 2 hours. At 2 hours, the cells were fixed in 4% paraformaldehyde for 10 min, permeabilized in 0.2% Triton X-100 for 5 min, and incubated with anti BrdU antibody from Becton Dickenson (1:10 in PBS, 5 mM $MgSO_4$ 100 U/ml DNAse) for 1 h. Incorporated BrdU was detected by TRITC-conjugated anti-BrdU antibody (Becton Dickinson, Mountain View, CA). The *red* color, indicating BrdU staining, and TCEAL7-GFP positive cells were documented using a Spot camera. The total numbers GFP positive cells as well as BrdU-labeled cells were counted in 5–10 different fields of each well. Two researchers independently made the measurements on all slides. The data were expressed as % BrdU positive cells.

Luciferase Reporter assay

The luciferase reporter gene under the control of the human cyclin D1 promoter (D1-973LUC) was provided by R Janknecht (Mayo Clinic, Rochester, MN). HeLa cells were seeded at 5 x10^5 per well in six well plates (in triplicates) one day prior to transfection. 0.5 μg Vector-GFP and 0.5 μg TCEAL7- GFP constructs were cotransfected with 0.5 μg D1-973LUC and 0.1 g Renilla reporters, and luciferase activity was measured 24 hr post-transfection with Promega's Dual-Luciferase Reporter (DLR) assay system according to manufacturer's instructions. The relative light units (RLU) are expressed per μg protein after normalizing with Renilla luciferase. For c-Myc transcriptional activity luciferase assay, cells were transfected with Renilla luciferase plasmid, pEMS or pODC, and various constructs of Bin1 and TCEAL7. Twenty four hours after transfection, cells were lysed in passive lysis buffer and luciferase activity was measured with Promega's Dual-Luciferase Reporter system according to manufacturer's instructions. All luciferase activities were normalized with Renilla luciferase activity to account for variability in transfection efficiency.

Cell-cycle synchronization

HeLa cells grown to 60-80% confluence in 10 cm dishes were treated with 2.5 μM nocodazole for 16 hours. The plates were tapped a few times to release the mitotic cells to the medium, and non-adherent cells were collected. Cells were centrifuged, wash 2 times in PBS, and replated in regular growth medium. Cells lysates were collected at different time points and immunoblotting was performed using anti-cyclin antibodies.

Antibody Array for screening TCEAL7 interacting proteins

Apoptosis AntibodyArray™ containing antibodies against 150 apoptotic regulating proteins from Hypomatrix (Worcester, MA) was used to screen TCEAL7 interacting proteins. Protein-protein interactions was determined by incubating AntibodyArray™ with the whole cell extracts from OV202 cells electroporated with 20 μg of Flag tagged TCEAL7 following the manufacturer's instructions. Briefly, the antibody array was incubated in blocking solution [5% milk in TBST (150 mM NaCl, 25 mM Tris, 0.05% Tween-20, pH 7.5)] for one hour with gentle shaking. Whole cell extracts from OV 202 cells transfected with flag tagged TCEAL7 was incubated with the antibody array for 2 hours at room temperature with gentle shaking. The array was washed with TBST, 3 x 15 minutes. TCEAL7 interacting proteins were detected with HRP-conjugated mouse monoclonal antibody against the Flag tag from Sigma after 2 hours of incubation followed by 3 x 15 minutes washes in TBST.

Immunoblotting

Equal amounts of protein (20 μg/lane) were separated by electrophoresis on an SDS gel containing a 4–12% acrylamide gradient and electrophoretically transferred to nitrocellulose. Blots were washed once with TBS, 0.2% Tween 20 (TBST) and blocked with TBST containing 5% non-fat dry milk for 1 h at 25°C. The blocking solution was replaced with a fresh solution containing a 1:500 dilution of rabbit anti-cyclin D1 (Cell Signaling Inc., Beverly, MA). After overnight incubation at 4°C, the blots were washed three times for 10 min each in TBS, 0.1% (w/v) Tween 20 and incubated with horseradish peroxidase-conjugated secondary antibody in 5% milk/TBST at 25°C for 1 h. After washing 3 times in TBST, the proteins were visualized using enhanced chemiluminescence (Amersham Biosciences, Piscataway, NJ). The blots were stripped and reprobed with antisera that recognize cyclin E and cyclin A or mouse monoclonal anti-β actin (Sigma, St. Louis, MO).

Immunoprecipitation

Cells transfected with different constructs of Bin1 and TCEAL7 were collected into lysis buffer A [50 mM Tris-HCl, pH 7.5; 150 mM NaCl; 1% Nonidet P40; 0.5% sodium deoxycholate; and 1x protease inhibitor cocktail (Roche Molecular Biochemicals, Indianapolis, IN)]. Lysates were passed through 28G needle 12 times and centrifuged at 12,000xg for 10 minutes. Supernatants were then incubated with different antibodies for overnight. Lysates were then incubated with 40 μl protein A-Sepharose for additional one hour. Precipitates were washed 4 times in lysis buffer A, 2 times in PBS, and extracted in 2x Laemmli buffer. Extracted proteins were resolved by SDS-PAGE and immunoblotted with specific antibodies.

Generation of TCAEL7 inducible system in 293T FlpIn TRex system

293T FlpIn TRex cells were purchased from Invtirogen and grown according to provider's protocol. These cells contain single flippase recombination target (FRT) sequence and stably integrated tetracyclin repressor. Upon transfection with plasmid containing TCEAL7 flanked by FRT sequence in pcDNA 5 FRT/TO together with pOG44 plasmid containing flippase will allow integration of TCEAL7 into the FRT site. Batch stable cell line was generated with the selection of 100 μg/ml hygromycin B. Proper integration of TCEAL7 into FRT site will disrupt LacZ reporter gene. Therefore, cells containing proper integration of TCEAL7 can be screened with β-gal assay. These cells will be negative for β-gal activity. Staining of batch stable clones indicated that >99% of the cells were β-gal negative.

ChIP

293T FlpIn TRex cells stably expressing doxycycline inducibleTCEAL7 were grown to 95% confluence in the presence or absence of 1 μg/ml doxycycline, and were cross-linked with 1% formaldehyde at room temperature for 10 min. The reaction was stopped by adding 1/10 volume of 1.25 M Glycine. Cells were then rinsed with ice-cold PBS twice and collected into lysis buffer A (1% SDS, 10mM EDTA, 50mM Tris, pH 8.1). Lysates were sonicated 12 times for 10 s each at the 55% output setting (Cole-Parmer Instruments, Model CP130) followed by centrifugation for 10 min at 10,000g. Supernatants were collected, and immunoprecipitation was performed overnight at 4°C with anti TCEAL7 antibody (1μg/100μl). After overnight incubation, 40 μl protein A-Sepharose and were added and the incubation was continued for another 1 hr. Precipitates were washed 4 times in lysis buffer A, twice in TE buffer and extracted in TE buffer containing 1% SDS by reverse cross-linking for overnight at 65°C. DNA fragments were purified with a QIAquick Spin Kit (Qiagen, Valencia, CA). For PCR, 10 ng of extracted DNA was used in 30 cycles of amplification at 95°C for 30s, 58°C for 30s, 72°C for 30s with cyclin D1 specific promoter primers. The following primers were used -36R-5'-CGT CCA GGT GAG AAC GTG AG-3' with -555F-5'- CAG GCA GGA CAT TGG CCC AT-3', -571R-5' CTC CTC CCA AAG CAC TGC TA-3' with -784F-5'-CAA TGC AGA TTC CCA GGC TC-3', and -781R-5'-TGG GGC AGA GCC TGG GAA TC-3' with -977F-5'-CAG CTG ACG GGC ACA CTG AC-3'. Primer pairs -36R and -555F span the Ebox of the cyclin D1 promoter.

Clonogenic assays

For clonogenic assays, 1 μg of vector, TCEAL7 and various constructs of Bin1 were transiently transfected into HeLa cells for 24 hours. Subsequently, 1000 cells/35 mm dish were plated in triplicates, permitted to adhere overnight, and grown for 12-14 days to allow colonies to form. Cells were stained with coomassie blue; digitally photographed, counted with BioRad GelDoc 2000 system and expressed as % colony forming efficiency.

Generation of shRNA down-regulated TCEAL7 clones in OSEtsT/hTERT

For these experiments, we used an immortalized version of the OSE(tsT) cell line transduced with a temperature sensitive mutant of the SV40 large T antigen (Kalli et al., 2002). These cells proliferate continuously at 34°C but, upon destabilization of the T antigen, become quiescent at 39°C. The OSE(tsT) cells were transduced with the catalytic subunit of human telomerase hTert [OSE(tsT)/hTert]. These cells grow as efficiently at 37°C as at 34°C, and have not currently undergone senescence (passage 65 and counting). They require surface attachment for growth. Because they are proliferating, they represent a long-term source of ovarian surface epithelial cells. For down-regulation of TCEAL7 expression, OSEtsT/hTERT were treated with retroviral supernatants to transduce pSUPER.retro constructs expressing short hairpin RNA (shRNA) targeting TCEAL7 mRNA (designated as pSR- TCEAL7). For control experiments, empty pSUPER.retro vector (designated as pSR alone) was used. The candidate siRNA sequences targeting TCEAL7 mRNA were generated using the Ambion server at www.ambion.com and screened based on criteria described previously (Berns et al., 2004) to select two sequences, targeting position 88-106 (T1) and 191-209 (T2) of TCEAL7 mRNA within the ORF. The oligonucleotide pairs used were the following: T1F (5'-GAT CC CC CGC CAG CAA ACA GAA GGG A TTC AAG AGA TCC CTT CTG TTT GCT GGCG TT TTT GGA AA-3'), T1R (5'- AGC TTA AAA ACG CCA GCA AAC AGA AGG GAT CTC TTG AAT CCC TTC TGT TTG CTG GCG GGG-3') T2F (5'- GAT CCC C GGG AGG GAG ATG AGA TGG AT TCA AGA GAT CCA TCT CAT CTC CCT CCC TTT TTA A), T2R (AGC TTA AAA AGG GAG GGA GAT GAG ATG GAT CTC TTG AAT CCA TCT CAT CTC CCT CCC GGG-3'). The underlined sequences in each forward primer indicate the 19-nucleotide stretches that form the hairpin. The oligonucleotide pairs were annealed and ligated into the BglII-HindIII sites of pSUPER.retro.puro vector following the manufacturer's protocol. The resulting two plasmid constructs were combined (designated as pSR-TCEAL7), packaged into infectious retrovirus in HEK293T cells expressing gag, pol and env proteins. For control experiments, empty pSUPER.retro vector (designated as pSR alone) was packaged into retrovirus. The conditioned medium containing pSUPER.retro viral particles was filtered through a 0.45-μm filter and stored at –80°C. For transfection, [OSE(tsT)/hTert] cells plated on the day before were incubated for 48 h with 1:1 mixture of the viral supernatants and fresh culture medium in the presence of 4 μg/ml polybrene. Several vector and shRNA transduced clones were selected in the presence of both geneticin and puromycin (for maintaining the SV40 T antigen and pSR vector) and hygromycin B (for the hTert construct). The efficacy of shRNA mediated down-regulation of TCEAL7 was evaluated by western blot using anti TCEAL7 antibody.

Soft agar assay

Complete medium containing 0.8% low-melting point temperature agarose was poured into six well plates (2 ml per well) and allowed to solidify at 4°C to form a bottom layer. Control pSR and TCEAL7 shRNA down-regulated OSE(ts/hTERT) cells (20,000 per well; vector 1-1 and 1-3 or TCEAL7 shRNA down-regulated clones 2-1 and 3-6) were mixed in complete medium with 0.45% agarose and seeded as a top layer. The agarose was solidified at 4°C and then incubated at 34°C. Growth on soft agar was monitored for three weeks. Colonies were stained with 1 ml of PBS containing 0.5 mg/ml p-iodonitrotetrazolium violet, which is converted into colored product by live cells only. Micrographs were taken at 10x using a Spot II-RT digital camera (Nikon, Millburn, NJ), and colonies larger than 50 μm and 100 μm in diameter were counted.

Proliferation assay

pSR-vector and pSR-TCEAL7 clones were plated at 2,000 cells/well in 96-well plates in triplicates in RPMI medium with 10% FCS (75μl/well). 24 hrs later and every day for 8 days,

MTS solution (5 mg/ml) was added to each well (20 µl per well). Following a 1-h incubation at 37^{o}C, the media was removed and 100 µl of DMSO was added to each well and the plates were read in a microtiter plate reader at 570nm. The experiment was repeated twice. Data were analyzed with GraphPad Prism software (San Diego, CA, USA).

Statistical analysis

All values are expressed as the mean ± SEM. Differences between two groups were compared using an unpaired two-tailed *t* test. When comparing multiple groups, one-way ANOVA followed by Newman-Keuls test was used. Results were considered significance when $P < 0.05$ at α=0.05.

Acknowledgements

This work was supported by Department of Defense grant W81XWH-04-1-0085, Edith and Bernie Waterman Foundation and the Mayo Foundation (both to V.S).

References

Baudino, T. A., and Cleveland, J. L. (2001). The Max network gone mad. Mol Cell Biol *21*, 691-702.

Berns, K., Hijmans, E. M., Mullenders, J., Brummelkamp, T. R., Velds, A., Heimerikx, M., Kerkhoven, R. M., Madiredjo, M., Nijkamp, W., Weigelt, B.*, et al.* (2004). A large-scale RNAi screen in human cells identifies new components of the p53 pathway. Nature *428*, 431-437.

Chien, J., Staub, J., Avula, R., Zhang, H., Liu, W., Hartmann, L. C., Kaufmann, S. H., Smith, D. I., and Shridhar, V. (2005). Epigenetic silencing of TCEAL7 (Bex4) in ovarian cancer. Oncogene *24*, 5089-5100.

Connolly, D. C., Bao, R., Nikitin, A. Y., Stephens, K. C., Poole, T. W., Hua, X., Harris, S. S., Vanderhyden, B. C., and Hamilton, T. C. (2003). Female mice chimeric for expression of the simian virus 40 TAg under control of the MISIIR promoter develop epithelial ovarian cancer. Cancer Res *63*, 1389-1397.

Dalla-Favera, R., Bregni, M., Erikson, J., Patterson, D., Gallo, R. C., and Croce, C. M. (1982). Human c-myc onc gene is located on the region of chromosome 8 that is translocated in Burkitt lymphoma cells. Proc Natl Acad Sci U S A *79*, 7824-7827.

Dinulescu, D. M., Ince, T. A., Quade, B. J., Shafer, S. A., Crowley, D., and Jacks, T. (2005). Role of K-ras and Pten in the development of mouse models of endometriosis and endometrioid ovarian cancer. Nat Med *11*, 63-70.

DuHadaway, J. B., Sakamuro, D., Ewert, D. L., and Prendergast, G. C. (2001). Bin1 mediates apoptosis by c-Myc in transformed primary cells. Cancer Res *61*, 3151-3156.

Eischen, C. M., Packham, G., Nip, J., Fee, B. E., Hiebert, S. W., Zambetti, G. P., and Cleveland, J. L. (2001). Bcl-2 is an apoptotic target suppressed by both c-Myc and E2F-1. Oncogene *20*, 6983-6993.

Elliott, K., Ge, K., Du, W., and Prendergast, G. C. (2000). The c-Myc-interacting adaptor protein Bin1 activates a caspase-independent cell death program. Oncogene *19*, 4669-4684.

Elliott, K., Sakamuro, D., Basu, A., Du, W., Wunner, W., Staller, P., Gaubatz, S., Zhang, H., Prochownik, E., Eilers, M., and Prendergast, G. C. (1999). Bin1 functionally interacts with Myc and inhibits cell proliferation via multiple mechanisms. Oncogene *18*, 3564-3573.

Fernandez, P. C., Frank, S. R., Wang, L., Schroeder, M., Liu, S., Greene, J., Cocito, A., and Amati, B. (2003). Genomic targets of the human c-Myc protein. Genes Dev *17*, 1115-1129.

Flesken-Nikitin, A., Choi, K. C., Eng, J. P., Shmidt, E. N., and Nikitin, A. Y. (2003). Induction of carcinogenesis by concurrent inactivation of p53 and Rb1 in the mouse ovarian surface epithelium. Cancer Res *63*, 3459-3463.

Galderisi, U., Di Bernardo, G., Cipollaro, M., Peluso, G., Cascino, A., Cotrufo, R., and Melone, M. A. (1999). Differentiation and apoptosis of neuroblastoma cells: role of N-myc gene product. J Cell Biochem *73*, 97-105.

Ge, K., DuHadaway, J., Du, W., Herlyn, M., Rodeck, U., and Prendergast, G. C. (1999). Mechanism for elimination of a tumor suppressor: aberrant splicing of a brain-specific exon causes loss of function of Bin1 in melanoma. Proc Natl Acad Sci U S A *96*, 9689-9694.

Ge, K., Duhadaway, J., Sakamuro, D., Wechsler-Reya, R., Reynolds, C., and Prendergast, G. C. (2000). Losses of the tumor suppressor BIN1 in breast carcinoma are frequent and reflect deficits in programmed cell death capacity. Int J Cancer *85*, 376-383.

Grandori, C., Cowley, S. M., James, L. P., and Eisenman, R. N. (2000). The Myc/Max/Mad network and the transcriptional control of cell behavior. Annu Rev Cell Dev Biol *16*, 653-699.

Grandori, C., and Eisenman, R. N. (1997). Myc target genes. Trends Biochem Sci *22*, 177-181.

Jeon, C., and Agarwal, K. (1996). Fidelity of RNA polymerase II transcription controlled by elongation factor TFIIS. Proc Natl Acad Sci U S A *93*, 13677-13682.

Kalli, K. R., Falowo, O. I., Bale, L. K., Zschunke, M. A., Roche, P. C., and Conover, C. A. (2002). Functional insulin receptors on human epithelial ovarian carcinoma cells: implications for IGF-II mitogenic signaling. Endocrinology *143*, 3259-3267.

Kolfschoten, I. G., van Leeuwen, B., Berns, K., Mullenders, J., Beijersbergen, R. L., Bernards, R., Voorhoeve, P. M., and Agami, R. (2005). A genetic screen identifies PITX1 as a suppressor of RAS activity and tumorigenicity. Cell *121*, 849-858.

Lupas, A. (1996). Prediction and analysis of coiled-coil structures. Methods Enzymol *266*, 513-525.

Mitchell, K. O., and El-Deiry, W. S. (1999). Overexpression of c-Myc inhibits p21WAF1/CIP1 expression and induces S-phase entry in 12-O-tetradecanoylphorbol-13-acetate (TPA)-sensitive human cancer cells. Cell Growth Differ *10*, 223-230.

Muller, A. J., DuHadaway, J. B., Donover, P. S., Sutanto-Ward, E., and Prendergast, G. C. (2004). Targeted deletion of the suppressor gene bin1/amphiphysin2 accentuates the neoplastic character of transformed mouse fibroblasts. Cancer Biol Ther *3*, 1236-1242.

Nesbit, C. E., Tersak, J. M., and Prochownik, E. V. (1999). MYC oncogenes and human neoplastic disease. Oncogene *18*, 3004-3016.

Nilsson, J. A., and Cleveland, J. L. (2003). Myc pathways provoking cell suicide and cancer. Oncogene *22*, 9007-9021.

Orian, A., van Steensel, B., Delrow, J., Bussemaker, H. J., Li, L., Sawado, T., Williams, E., Loo, L. W., Cowley, S. M., Yost, C.*, et al.* (2003). Genomic binding by the Drosophila Myc, Max, Mad/Mnt transcription factor network. Genes Dev *17*, 1101-1114.

Orsulic, S., Li, Y., Soslow, R. A., Vitale-Cross, L. A., Gutkind, J. S., and Varmus, H. E. (2002). Induction of ovarian cancer by defined multiple genetic changes in a mouse model system. Cancer Cell *1*, 53-62.

Oster, S. K., Ho, C. S., Soucie, E. L., and Penn, L. Z. (2002). The myc oncogene: MarvelouslY Complex. Adv Cancer Res *84*, 81-154.

Patel, J. H., Loboda, A. P., Showe, M. K., Showe, L. C., and McMahon, S. B. (2004). Analysis of genomic targets reveals complex functions of MYC. Nat Rev Cancer *4*, 562-568.

Pineda-Lucena, A., Ho, C. S., Mao, D. Y., Sheng, Y., Laister, R. C., Muhandiram, R., Lu, Y., Seet, B. T., Katz, S., Szyperski, T.*, et al.* (2005). A structure-based model of the c-Myc/Bin1 protein interaction shows alternative splicing of Bin1 and c-Myc phosphorylation are key binding determinants. J Mol Biol *351*, 182-194.

Ramaswamy, S., Ross, K. N., Lander, E. S., and Golub, T. R. (2003). A molecular signature of metastasis in primary solid tumors. Nat Genet *33*, 49-54.

Ramaswamy, S., Tamayo, P., Rifkin, R., Mukherjee, S., Yeang, C. H., Angelo, M., Ladd, C., Reich, M., Latulippe, E., Mesirov, J. P.*, et al.* (2001). Multiclass cancer diagnosis using tumor gene expression signatures. Proc Natl Acad Sci U S A *98*, 15149-15154.

Sakamuro, D., Elliott, K. J., Wechsler-Reya, R., and Prendergast, G. C. (1996). BIN1 is a novel MYC-interacting protein with features of a tumour suppressor. Nat Genet *14*, 69-77.

Sakamuro, D., and Prendergast, G. C. (1999). New Myc-interacting proteins: a second Myc network emerges. Oncogene *18*, 2942-2954.

Seoane, J., Le, H. V., and Massague, J. (2002). Myc suppression of the p21(Cip1) Cdk inhibitor influences the outcome of the p53 response to DNA damage. Nature *419*, 729-734.

Shridhar, V., Lee, J., Pandita, A., Iturria, S., Avula, R., Staub, J., Morrissey, M., Calhoun, E., Sen, A., Kalli, K.*, et al.* (2001). Genetic analysis of early- versus late-stage ovarian tumors. Cancer Res *61*, 5895-5904.

Shridhar, V., Sen, A., Chien, J., Staub, J., Avula, R., Kovats, S., Lee, J., Lillie, J., and Smith, D. I. (2002). Identification of underexpressed genes in early- and late-stage primary ovarian tumors by suppression subtraction hybridization. Cancer Res *62*, 262-270.

Tajiri, T., Liu, X., Thompson, P. M., Tanaka, S., Suita, S., Zhao, H., Maris, J. M., Prendergast, G. C., and Hogarty, M. D. (2003). Expression of a MYCN-interacting isoform of the tumor suppressor BIN1 is reduced in neuroblastomas with unfavorable biological features. Clin Cancer Res *9*, 3345-3355.

Taub, R., Kirsch, I., Morton, C., Lenoir, G., Swan, D., Tronick, S., Aaronson, S., and Leder, P. (1982). Translocation of the c-myc gene into the immunoglobulin heavy chain locus in human Burkitt lymphoma and murine plasmacytoma cells. Proc Natl Acad Sci U S A *79*, 7837-7841.

Thomas, M. J., Platas, A. A., and Hawley, D. K. (1998). Transcriptional fidelity and proofreading by RNA polymerase II. Cell *93*, 627-637.

van 't Veer, L. J., Dai, H., van de Vijver, M. J., He, Y. D., Hart, A. A., Mao, M., Peterse, H. L., van der Kooy, K., Marton, M. J., Witteveen, A. T.*, et al.* (2002). Gene expression profiling predicts clinical outcome of breast cancer. Nature *415*, 530-536.

Westbrook, T. F., Martin, E. S., Schlabach, M. R., Leng, Y., Liang, A. C., Feng, B., Zhao, J. J., Roberts, T. M., Mandel, G., Hannon, G. J.*, et al.* (2005). A genetic screen for candidate tumor suppressors identifies REST. Cell *121*, 837-848.

Wilson, B. E., Mochon, E., and Boxer, L. M. (1996). Induction of bcl-2 expression by phosphorylated CREB proteins during B-cell activation and rescue from apoptosis. Mol Cell Biol *16*, 5546-5556.

Wu, S., Cetinkaya, C., Munoz-Alonso, M. J., von der Lehr, N., Bahram, F., Beuger, V., Eilers, M., Leon, J., and Larsson, L. G. (2003). Myc represses differentiation-induced p21CIP1 expression via Miz-1-dependent interaction with the p21 core promoter. Oncogene *22*, 351-360.

Yeh, C. H., and Shatkin, A. J. (1995). A cis-acting element in Rous sarcoma virus long terminal repeat required for promoter repression by HeLa nuclear protein p21. J Biol Chem *270*, 15815-15820.

Zeng, Y. X., Somasundaram, K., and el-Deiry, W. S. (1997). AP2 inhibits cancer cell growth and activates p21WAF1/CIP1 expression. Nat Genet *15*, 78-82.

Figure legends

Figure 1. Expression of TCEAL7 in normal and cancer tissues. **A**, Northern blot analysis of TCEAL7 expression indicating a single 1.35 kb transcript in normal tissues. **B**, Northern blot analysis of ovarian cancer cell lines indicating the down-regulation of TCEAL7 in cancer. **C**, Northern blot analysis of 24 primary ovarian tumors indicating the down-regulation of TCEAL7 in majority of tumors. Lower panels are ethidium bromide stained agarose gels showing 18s and 28s RNA as loading controls. **D**, Analysis of TCEAL7 expression in 50 ovarian samples using custom cDNA microarray. BLT denotes borderline tumors. **E**, RT-PCR expression analysis of neighboring genes, pp21 homolog and Bex3/NADE, indicating robust expression in cancer cell lines. Loading order: 1, OSE; 2, OSEtsT; 3, OV167; 4, OV177; 5, OV202; 6, OV207; 7, OV266; 8, OVCAR3; 9, OVCAR5; 10, SKOV3; 11, HMEC; 12, MCF-7; 13, MCF-10A and 14, MDA-MB-157. The relative positions of Bex3/NADE, pp21 homolog, TCEAL7 and NADE homolog in band Xq22.1-22.2 along with the map of X chromosome is shown below. Lower panels with GAPDH represent loading controls.

Figure 2. Expression of TCEAL7 in various cancers. RT-PCR expression analysis of TCEAL7 in various cancers highlighting the down-regulation of TCEAL7 in various cancers. Loading order is as follow: Cervical cell lines (1, normal keratinocytes; 2, SiHa; 3, CaSki; 4, HT-3; 5, HeLa; 6, SW756; 7, MS751; 8, C-33-A; 9, C-4-A; and 10, ME-180), Hepatocellular carcinoma cell lines (1, Hep3B; 2, HepG2; 3, HUH7; 4, SNU182; 5, SNU387; 6, SNU423; 7, SNU449; 8, SNU475; 9, SKHep1; and 10, PLC5), Prostate cell lines (1, BPH: benign prostate epithelium; 2, DU145; 3, LnCAP; and 4, PC3), Brain cell lines (1, Total brain; 2, D32; 3, D37; 4, M067; 5, T989; 6, U148; 7, U251; 8, U373) and Primary brain tumor samples 1-10, and Breast cell lines (1, HMEC :Normal Human Mammary Epithelial Cells; 2, MCF-7; 3, MCF-10A; 4, MDA-MB-157; 5, MDA-MB-361; 6, MDA-MB-435; 7, MDA-MB 468; 8, UACC812; 9, UACC893; 10, BT474; 11, T47D). M: 100 bp ladder.

Figure 3. HeLa cells were transfected with GFP-tagged TCEAL7 for 24 hrs and fixed for 15 min at room temperature in 4% parformaldehyde for confocal fluorescence analysis. **A,** Fluorescence imaging of GFP-tagged TCEAL7 indicates nuclear localization (upper panels). Free GFP is localized to both nucleus and cytoplasm (lower panels). Rhodamine-conjugated Phalloidin was used to visualize F-actin and DAPI too visualize nuclei. **B**, Immunofluorescence staining of endogenous TCEAL7 with anti TCEAL7 monoclonal antibody (2pG7) in OSEtsT cells indicates nuclear localization. Nuceli were stained with DAPI. **C**, Immunofluorescence staining of myc-tagged TCEAL7 with anti myc antibody indicating cytoplasmic and nuclear staining. **D**, Sequence alignment with other proteins containing known nuclear export signal shows a putative nuclear export signal in TCEAL7. Conserved sequences are shown in boxes.

Figure 4. TCEAL7 interacts with Bin1 through Bin1's BAR-C domain. **A**, Apoptosis antibody array analysis indicates potential TCEAL7-interacting proteins. E1=Bin1, E5=FAST, and K4=DcR2. **B**, TCEAL7 co-localizes with Bin1 in the nucleus. Hela cells seeded on glass cover slips were transiently transfected with GFP-tagged TCEAL7 and full length Bin 1 construct, and detected with monoclonal antibody 99D for Bin 1 as described in the Materials and Methods. Immunofluorescence staining of TCEAL7 GFP and Bin1 indicates co-localization of both proteins to nuclei. **C**, Co-Immunoprecipitation of TCEAL7 and Bin 1. Endogenous TCEAL7 was immunopercipitated using antiTCEAL7 antibody followed by western blot analysis with anti Bin1 (left panel). Reverse co-immunoprecipitation of Bin1 followed by western blot analysis with anti-TCEAL7 antibody showed negative results (Right panel). **D**, Domains and deletion constructs of Bin1. **E.** Co-immunoprecipitation of Bin1 and c-Myc with immunoprecipitation of TCEAL7.

Various deletion constructs of Bin1 were transiently transfected into HeLa cells and immunoprecipitated with anti TCEAL7 antibody. Western blot analysis with anti HA (top panel), anti Myc (middle panel) and anti TCEAL7 (lower panel) antibodies show that both Bin1 and Myc co-immunoprecipitates with TCEAL7. **F**, Endogenous TCEAL7 was immunoprecipitated using antiTCEAL7 antibody followed by western blot analysis with anti Myc (left panel). Reverse co-immunoprecipitation of Myc followed by western blot analysis with anti-TCEAL7 indicate that endogenous TCEAL7 associates with endogenous Myc. **G.** Reverse co-immunoprecipitation of TCEAL7 with immunoprecipitation of c-Myc or Bin1. Both TCEAL7 and full length Bin1 constructs are transiently transfected into HeLa cells as indicated in the panel, followed by immunoprecipitation with either anti Myc antibody or anti HA antibody as indicated. Western blot analysis of immunoprecipitated products with anti TCEAL7 antibody indicates that TCEAL7 binds to both Myc and Bin1.

Figure 5. Suppression of c-Myc transcriptional activity by TCEAL7. **A**, TCEAL7 suppresses c-Myc transcriptional activity as determined by Ornithine decarboxylase (pODC) promoter luciferase activity. HeLa cells were seeded at 5 $x10^5$ per well in six well plates (in triplicates) one day prior to transfection. 0.5 μg Vector-GFP and 0.5 μg TCEAL7-GFP and/or various Bin 1 constructs were cotransfected with 0.5 μg pODC and 0.1 μg Renilla reporters, and luciferase activity was measured 24 hr post-transfection with Promega's Dual-Luciferase Reporter (DLR) assay system according to manufacturer's instructions. The relative light units (RLU) are expressed per μg protein after normalizing with Renilla luciferase. **B**, TCEAL7 suppresses c-Myc transcriptional activity as determined by E-box Myc Binding Site promoter luciferase activity. For c-Myc transcriptional activity luciferase assay, cells were transfected with Renilla luciferase plasmid, pEMS, and various constructs of Bin1 and TCEAL7. Twenty four hours after transfection, cells were lysed in passive lysis buffer and luciferase activity was measured with Promega's Dual-Luciferase Reporter system according to manufacturer's instructions. **C**, TCEAL7 enhances promoter activity of Bcl2 and p21. The luciferase activity was measured as above in the presence of either Bcl2 or p21 promoter reporters co-transfected with Renilla luciferase plasmid and TCEAL7 expression construct. The graphs depict luciferase activities relative to reporter (without TCEAL7) only controls. The data represents three trials performed in duplicates. All luciferase activities were normalized with Renilla luciferase activity to account for variability in transfection efficiency, and expressed as a percentage of the vector control.

Figure 6. TCEAL7 transcriptionally downregulates cyclin D1. **A**, TCEAL7 suppresses cyclin D1 promoter activity. HeLa cells were seeded at 5 $x10^5$ per well in six well plates (in triplicates) one day prior to transfection. 0.5 μg Vector-GFP and 0.5 μg TCEAL7- GFP constructs were cotransfected with 0.1 μg Renilla reporter and 0.5 μg of cyclin D1 promoter (D1-973LUC) driving luciferase reporter. Luciferase activity was measured 24 hr post-transfection with Promega's Dual-Luciferase Reporter (DLR) assay system according to manufacturer's instructions. The relative light units (RLU) are expressed per μg protein after normalizing with Renilla luciferase. **B**, TCEAL7 down-regulates cyclin D1 expression. Following 48 hrs of TCEAL7 transfection into HeLa cells, cell lysates were resolved on SDS-PAGE, and expression of cylcin D1 was determined with anti cyclin D1 antibody. Three lanes represent three independent transfections. **C**, Quantification of cyclin D1 expression by densitomeric analysis indicates down-regulation of cyclin D1 by TCEAL7. **D**, 24 hours doxycycline treatment of 293T FlpIn-TRex cells containing stable integration of TCEAL7 results in TCEAL7 expression (Lane 2). **E**, Doxycycline induced TCEAL7 expressing cells were subjected to ChIP analysis with anti TCEAL7 antibody and PCR amplified with specific cyclin D1 promoter primers as described in the Methods section. ChIP analysis indicates PCR amplification of cyclin D1 promoter containing E-box in sample pre-treated with doxycycline (with -36R and -555F primers). Lower panels show absence of cyclin

D1 promoter PCR product outside the region of E-box in ChIP samples (-781R with -997F and -784F with -571R primer sets). Positions of primers and E-box are indicated in the schematic representation of cyclin D1 promoter relative to transcriptional start site. **F**, Suppression of cyclin D1 expression by TCEAL7 in cell-cycle synchronized HeLa cells. HeLa cells grown to 60-80% confluence in 10 cm dishes were treated with 2.5 μM nocodazole for 16 hours. Mitotic cells were collected, centrifuged, washed 2 times in PBS, and replated in regular growth medium. Cells lysates were collected at different time points and immunoblotting was performed using anti-cyclin D, E and A antibodies. Please note the basal levels of cyclin D1 in vector-transfected controls and upregulation of cylcin D1 in these cells 18 hrs after the cell-cycle release. In contrast, TCEAL7-tranfected cells showed induction of cyclin D1 only after 24 hrs following cell-cycle release. **G**, TCEAL7 expression results in reduction of BrdU-positive cells. BrdU labeling was performed as described in the methods section. Incorporated BrdU was detected by TRITC-conjugated anti-BrdU antibody (Becton Dickinson, Mountain View, CA). The *red* color, indicating BrdU staining, and TCEAL7-GFP positive cells were documented using a Spot camera. The total numbers GFP positive cells as well as BrdU-labeled cells were counted in 5–10 different fields of each well. **H**, Quantification of BrdU-positive cells in vector control and TCEAL7-tranfected cell populations.

Figure 7. TCEAL7 suppress colony forming efficiency of cancer cells. Hela cells were transfected with 1 μg of full length Bin1 or BAR-C deleted Bin1 with or without TCEAL7 as indicated in the figure. The cells were plated in 35mm dishes in triplicates and allowed to grow for 12-14 days before staining with Coomassie blue. The experiments were performed twice. Ectopic expression of TCEAL7 in HeLa cells suppresses colony-forming efficiency of the cells. Ectopic expression of Bin1 also suppresses colonies. Co-expression of TCEAL7 and Bin1 does not result in further enhancement of suppression, indicating that TCEAL7 and Bin1 may be components of the same pathway. As indicated previously, expression of Bin1ΔBAR-C does not result in suppression of colony formation. It has no effect of TCEAL7 when co-expressed with TCEAL7.

Figure 8. Down-regulation of TCEAL7 promotes soft-agar growth of OSEtsT/hTERT. **A**, Stable transfection of shRNA targeted to TCEAL7 transcript results in down-regulation of TCEAL7. Agarose gel electrophoresis of RT-PCR products of TCEAL7 transcript levels in two stable pSR vector clones 1-1 and 1-3 (Lanes 2 and 3, top panel). Down-regulation of TCEAL7 expression is seen in pSR- TCEAL7 shRNA clones 2-1 and 3-6 (Lanes 4 and 5, top panel). 1 Kb ladder is shown in lane 1. Lower panel shows control GAPDH levels in the clones tested. **B**, Immunoblot analysis of TCEAL7 in these cells indicates that stable transfection of shRNA resulted in down-regulation of TCEAL7. Lower panel shows β-actin as protein loading controls. **C**, Down-regulation of TCEAL7 promotes soft-agar growth of immortalized non-transformed OSEtsT/hTERT. Control pSR and TCEAL7 shRNA down-regulated OSE(ts/hTERT*)* cells (20,000 per well; vector 1-1 and 1-3 or TCEAL7 shRNA down-regulated clones 2-1 and 3-6) were grown on soft agar for 3 weeks in triplicates. pSR- TCEAL7 shRNA clones 2-1 and 3-6 formed colonies on soft agar indicating anchorage independent growth, while the control pSR vector transduced clones did not. **D**, Representative photomicrographs of OSEtsT/hTERT cell lines grown on soft-agar. Colonies were stained with 1 ml of PBS containing 0.5 mg/ml p-iodonitrotetrazolium violet, which is converted into colored product by live cells only. Micrographs were taken at 10x using a Spot II-RT digital camera (Nikon, Millburn, NJ), and stained colonies were counted. **E,** Growth was measured with the MTS assay. Data represent the mean $\pm$ SEM for two independent experiments. **F,** Potentiation of basal c-Myc transcriptional activity following TCEAL7 down-regulation. Down-regulation of TCEAL7 augments the basal c-Myc transcriptional activity as determined by Ornithine decarboxylase

(pODC) promoter luciferase activity. pSR-vector 1-1 and pSR-TCEAL clones 2-1 and 3-6 in OSE(tsT\hTERT) ells were seeded at 5 $x10^5$ per well in six well plates (in triplicates) one day prior to transfection. 0.5 μg pODC and 0.1 μg Renilla reporters were cotransfected, and luciferase activity was measured 24 hr post-transfection with Promega's Dual-Luciferase Reporter (DLR) assay system according to manufacturer's instructions. The relative light units (RLU) are expressed per μg protein after normalizing with Renilla luciferase.

Figure 9. Proposed model for suppression of c-Myc by TCEAL7. **1**, Myc induced transcriptional activation requires dimerization of Myc with Max. **2**, Mad inhibits Myc activity by interacting with Max. **3**, Max-Mad interaction titrates Max away from Myc, thus suppressing Myc activity. **4**, Interaction of Bin1 and/or TCEAL7 with Myc may titrate Myc away from Max thus leading to inhibition of Myc activity. **5**, Interaction of Bin1(-10/-13) and TCEAL7 may titrate TCEAL7 away from Myc, thus relieving its suppression on Myc. **6**, Inhibition of Myc may result in suppression of cyclin D1 promoter activity and colony formation efficiency.

SUPPLEMENTARY FIGURE LEGENDS

Supplementary Figure 1. Northern blot analysis of multiple tissue expression array (Clontech) indicating the predominant expression of TCEAL7 in several regions of the brain. It is also expressed in ovary (Grid #G8).

Supplementary Figure 2. Meta-analysis of TCEAL7 expression in brain, breast, and prostate cancers. Oncomine.org was used for Meta-analysis of TCEAL7 expression. Number of samples analyzed in each study is indicated in brackets. *P* value from each analysis is shown in a row denoted by P. cDNA microarray analysis of 190 normal tissues and 20 brain tissues by Ramaswamy *et al* (Ramaswamy et al., 2001) indicates that TCEAL7 expression is higher in brain tissues compared to other normal tissues. This data is consistent with our northern blot analysis indicating highest expression of TCEAL7 in brain tissues. The same study also reports a statistically significant down-regulation of TCEAL7 in 10 Glioma samples compared to 20 normal brain tissues (p =0.008). cDNA microarray analysis by van't Veer *et al* (van 't Veer *et al*., 2002) indicates that TCEAL7 expression is down-regulated in 78 breast tumors with Grade 3 compared to 12 breast tumors with Grade 1 (p =0.008). In addition, TCEAL7 is down-regulated in breast tumors with lymphocytic infiltration (N=28) compared to those without infiltration (N=89) (p = 1.4E-5) (Figure 2). Analysis of metastasis phenotype by Ramaswamy *et al* (Ramaswamy et al., 2003) also indicates TCEAL7 down-regulation in metastatic prostate cancer compared to primary prostate cancer.

Supplementary Figure 3. TCEAL7 is a nuclear protein belonging to the family of transcription elongation factor A-like (TCEAL) proteins. **A**, Sequence alignment of members of TCEAL family. Conserved residues are highlighted by blue. **B**, Dendrogram clustering of the family of TCEAL proteins. Phylogenetic tree analysis indicates TCEAL6 (Q9UHQ7) to be the closest homolog of TCEAL7 (Figure 3B). TCEAL6 was originally named as pp21 homolog/WWBP1 (WW domain-binding protein 1). Its mouse ortholog is known as WWBP5. However, we also named it TCEAL6 because the name has not been previously assigned to any other gene and it is clustered close to TCEAL7. TCEAL7 and TCEAL6 share 40.59% amino acid sequence identity. All TCEAL genes map to Xq21-22. Base positions of these genes on human X chromosome and Unigene cluster IDs corresponding to the genes are listed in Figure 3B. Of four genes mapping to Xq22.1-22.2, *TCEAL8* (*bex1*), *TCEAL7* (*bex4*), *NADE* (*bex3*) and *TCEAL6* (*pp21 homolog)*, only *TCEAL7* was selectively inactivated showing complete loss of expression in >90% of the primary ovarian tumors and cell lines compared to other genes in this region (see Figure 1E).

Figure 1.

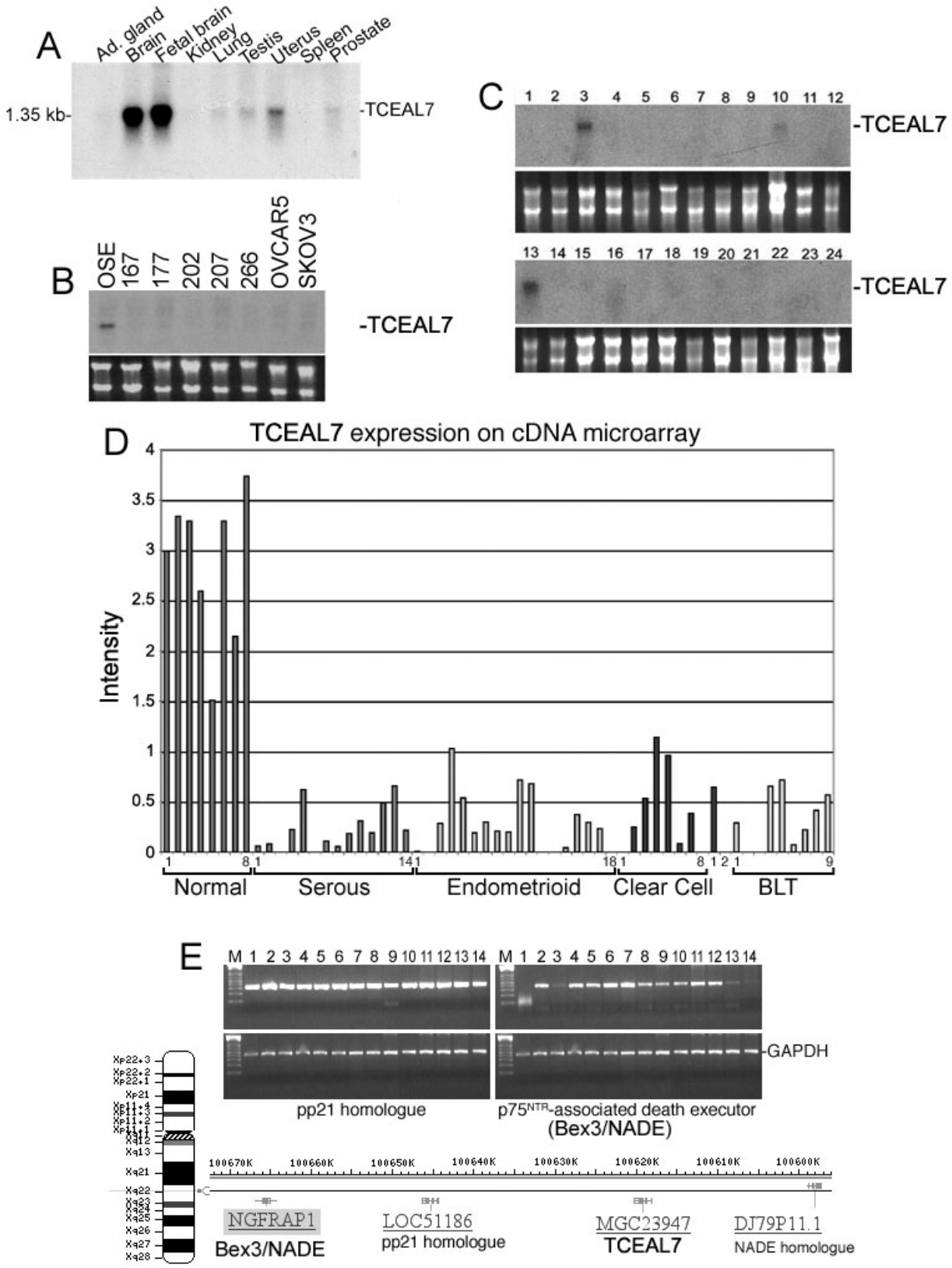
A
Ad. gland
Brain
Fetal brain
Kidney
Lung
Testis
Uterus
Spleen
Prostate
1.35 kb-
-TCEAL7
B
OSE
167
177
202
207
266
OVCAR5
SKOV3
-TCEAL7
C
1 2 3 4 5 6 7 8 9 10 11 12
-TCEAL7
13 14 15 16 17 18 19 20 21 22 23 24
-TCEAL7
D
TCEAL7 expression on cDNA microarray
Intensity
Normal
Serous
Endometrioid
Clear Cell
BLT
E
M 1 2 3 4 5 6 7 8 9 10 11 12 13 14
-GAPDH
pp21 homologue
p75NTR-associated death executor
(Bex3/NADE)
100670K
100660K
100650K
100640K
100630K
100620K
100610K
100600K
NGFRAP1
Bex3/NADE
LOC51186
pp21 homologue
MGC23947
TCEAL7
DJ79P11.1
NADE homologue

Figure 2.

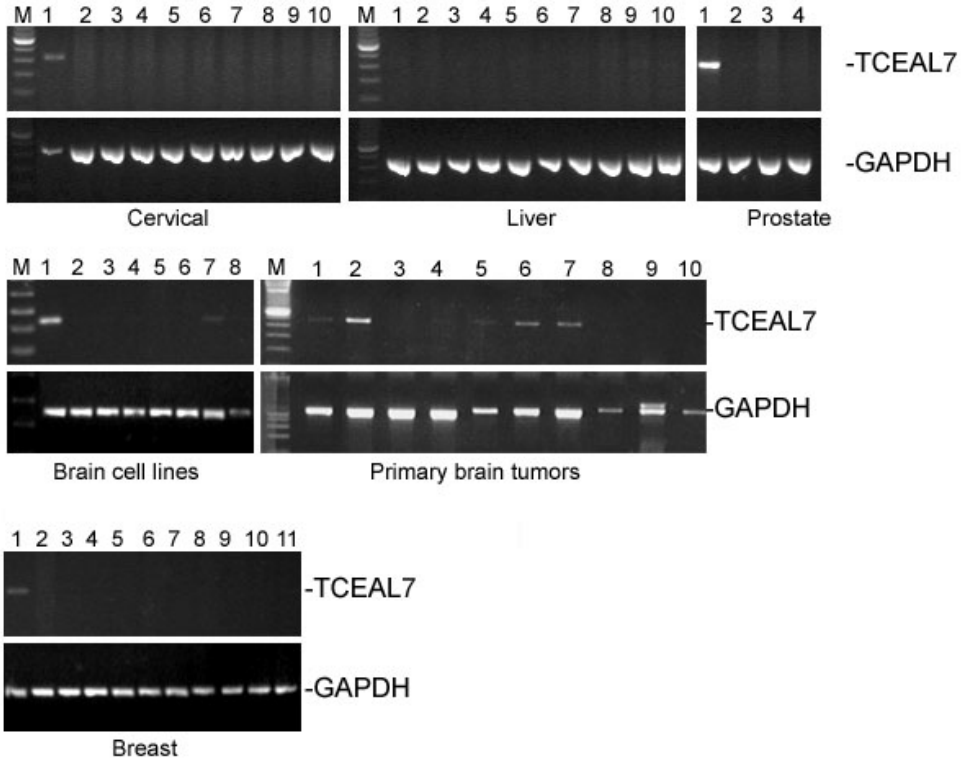

Figure 3.

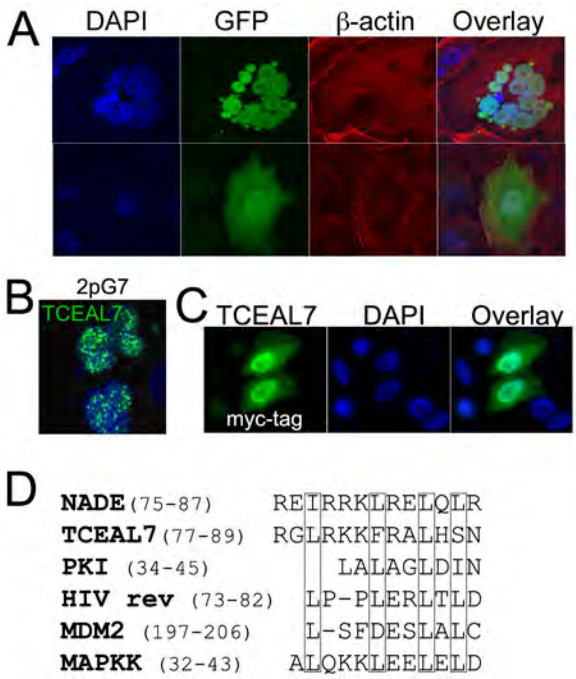

Figure 4.

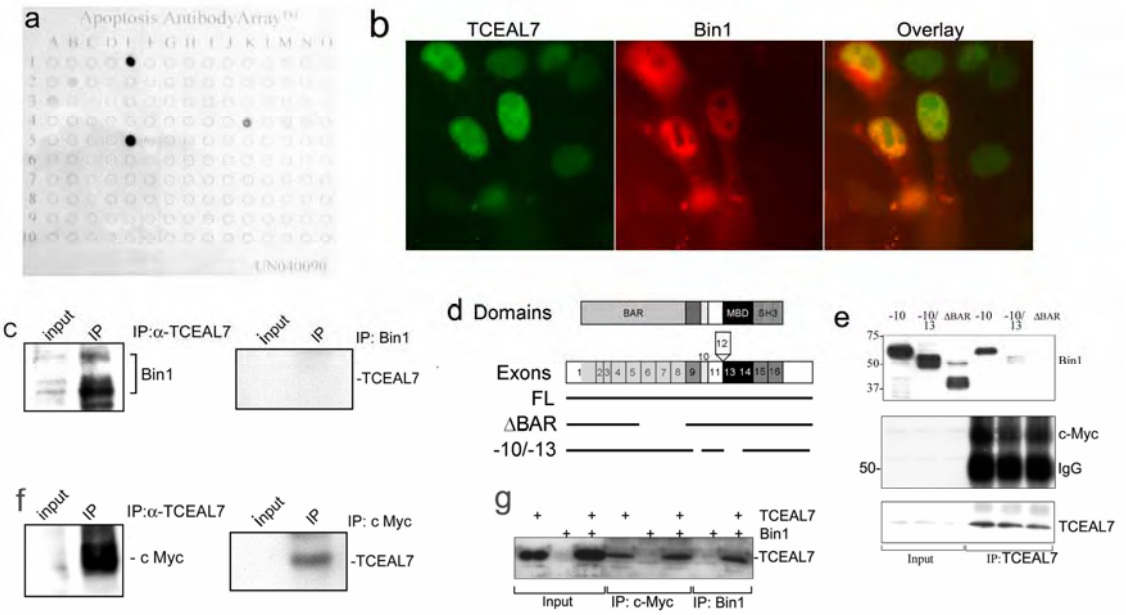
a
Apoptosis AntibodyArray™
b
TCEAL7
Bin1
Overlay
c
input
IP
IP:α-TCEAL7
Bin1
IP: Bin1
-TCEAL7
d Domains
BAR
MBD
SH3
Exons
FL
ΔBAR
-10/-13
e
-10
-10/13
ΔBAR
75
50
37
Bin1
c-Myc
IgG
50
TCEAL7
Input
IP:TCEAL7
f
IP:α-TCEAL7
- c Myc
IP: c Myc
-TCEAL7
g
TCEAL7
Bin1
-TCEAL7
Input
IP: c-Myc
IP: Bin1

Figure 5.

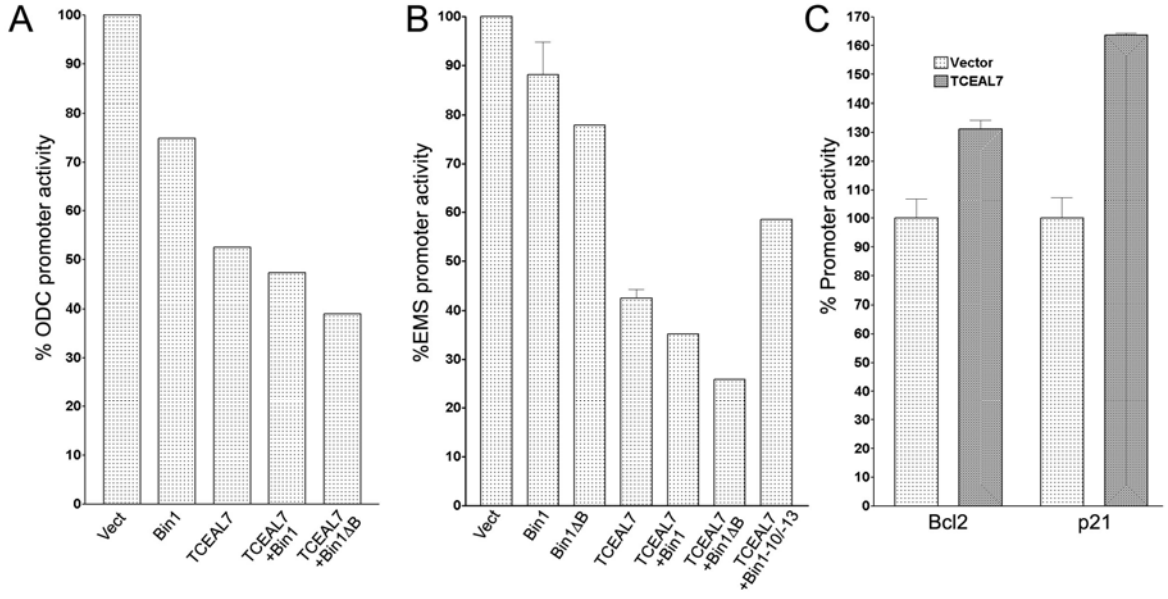

Figure 6A-E

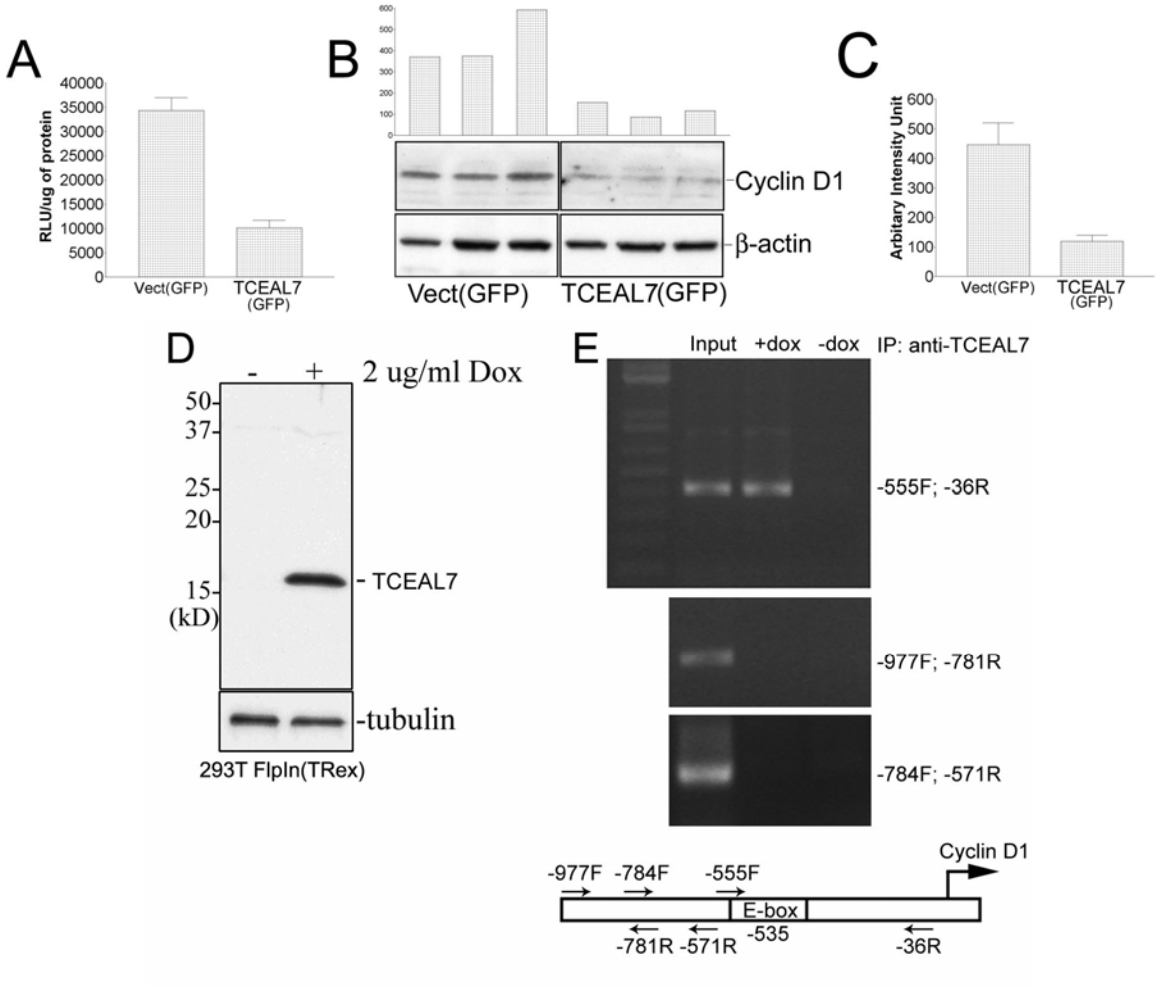

Figure 6F-H

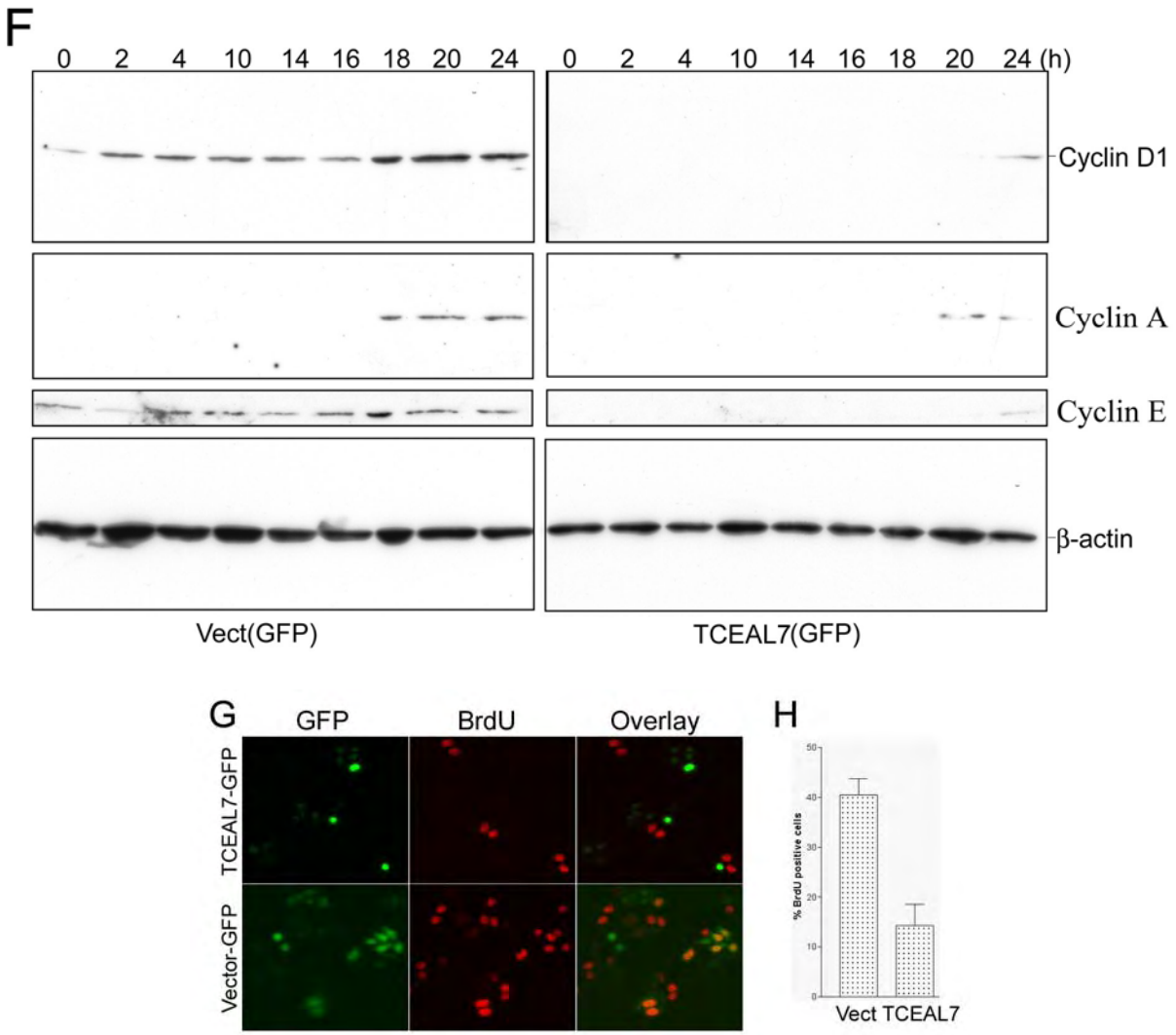
F
0 2 4 10 14 16 18 20 24 0 2 4 10 14 16 18 20 24 (h)
Cyclin D1
Cyclin A
Cyclin E
β-actin
Vect(GFP)
TCEAL7(GFP)
G
GFP
BrdU
Overlay
TCEAL7-GFP
Vector-GFP
H
% BrdU positive cells
Vect TCEAL7

Figure 7

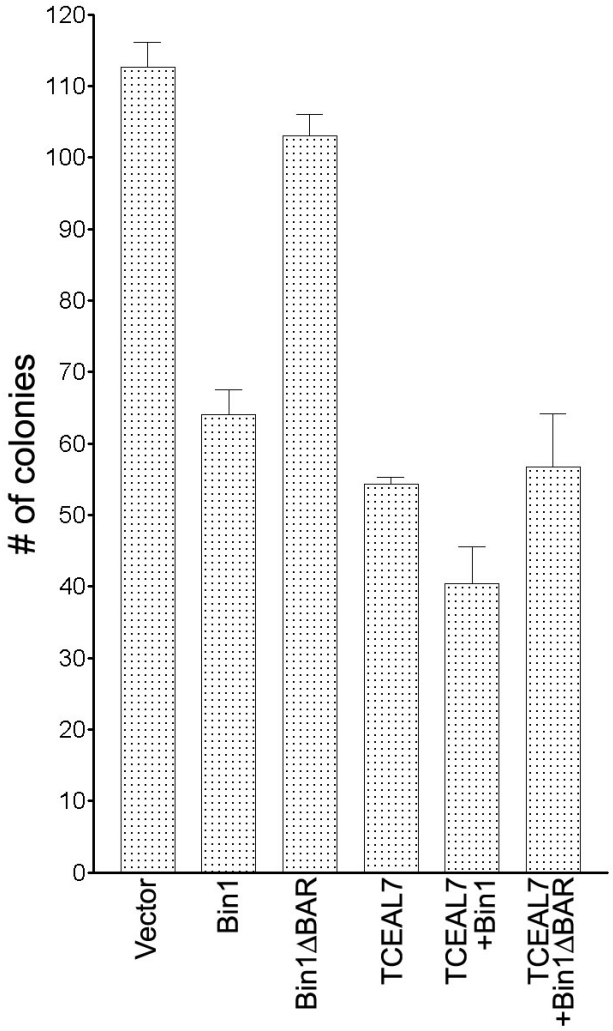
# of colonies
120
110
100
90
80
70
60
50
40
30
20
10
0
Vector
Bin1
Bin1ΔBAR
TCEAL7
TCEAL7 +Bin1
TCEAL7 +Bin1ΔBAR

Figure 8

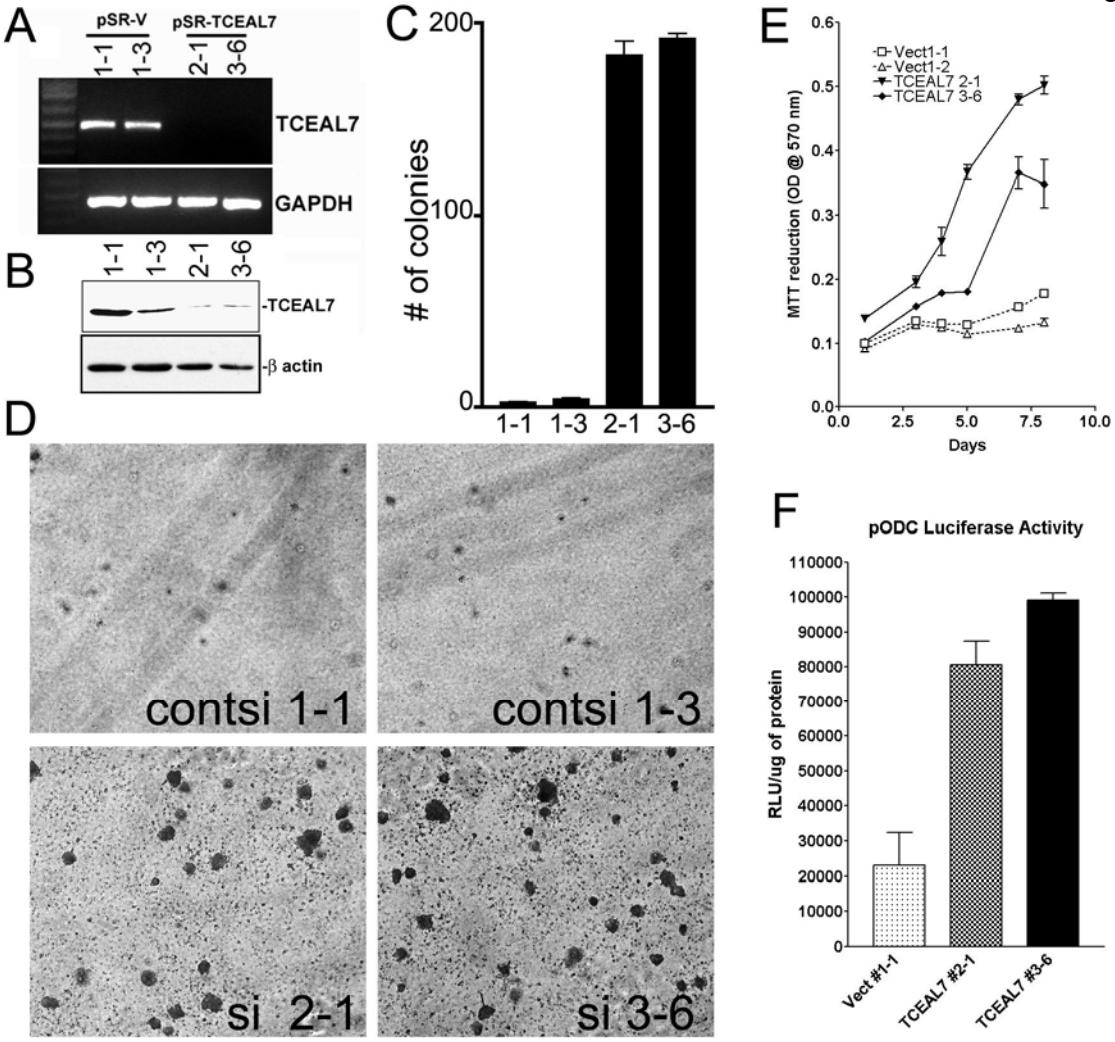

Figure 9

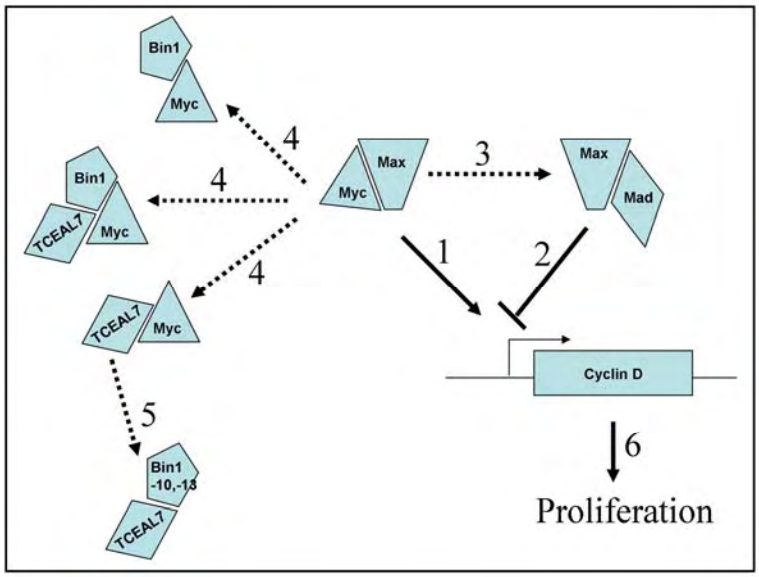

Supplementary Figure 1

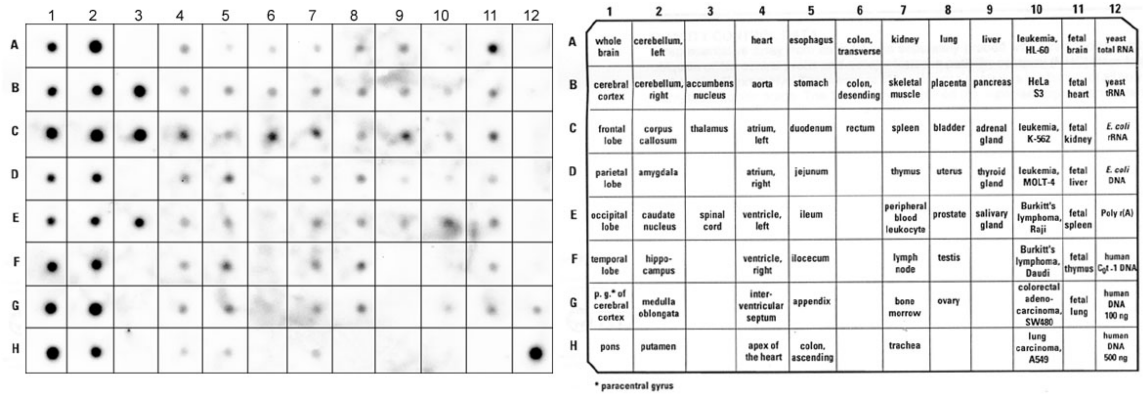

	1	2	3	4	5	6	7	8	9	10	11	12
A	whole brain	cerebellum, left		heart	esophagus	colon, transverse	kidney	lung	liver	leukemia, HL-60	fetal brain	yeast total RNA
B	cerebral cortex	cerebellum, right	accumbens nucleus	aorta	stomach	colon, desending	skeletal muscle	placenta	pancreas	HeLa S3	fetal heart	yeast tRNA
C	frontal lobe	corpus callosum	thalamus	atrium, left	duodenum	rectum	spleen	bladder	adrenal gland	leukemia, K-562	fetal kidney	*E. coli* rRNA
D	parietal lobe	amygdala		atrium, right	jejunum		thymus	utorus	thyroid gland	leukemia, MOLT-4	fetal liver	*E. coli* DNA
E	occipital lobe	caudate nucleus	spinal cord	ventricle, left	ileum		peripheral blood leukocyte	prostate	salivary gland	Burkitt's lymphoma, Raji	fetal spleen	Poly r(A)
F	temporal lobe	hippo-campus		ventricle, right	ilocecum		lymph node	testis		Burkitt's lymphoma, Daudi	fetal thymus	human Cot-1 DNA
G	p. g.* of cerebral cortex	medulla oblongata		inter-ventricular septum	appendix		bone merrow	ovary		colorectal adeno-carcinoma, SW480	fetal lung	human DNA 100 ng
H	pons	putamen		apex of the heart	colon, ascending		trachea			lung carcinoma, A549		humen DNA 500 ng

* paracentral gyrus

Suplementary Figure 2

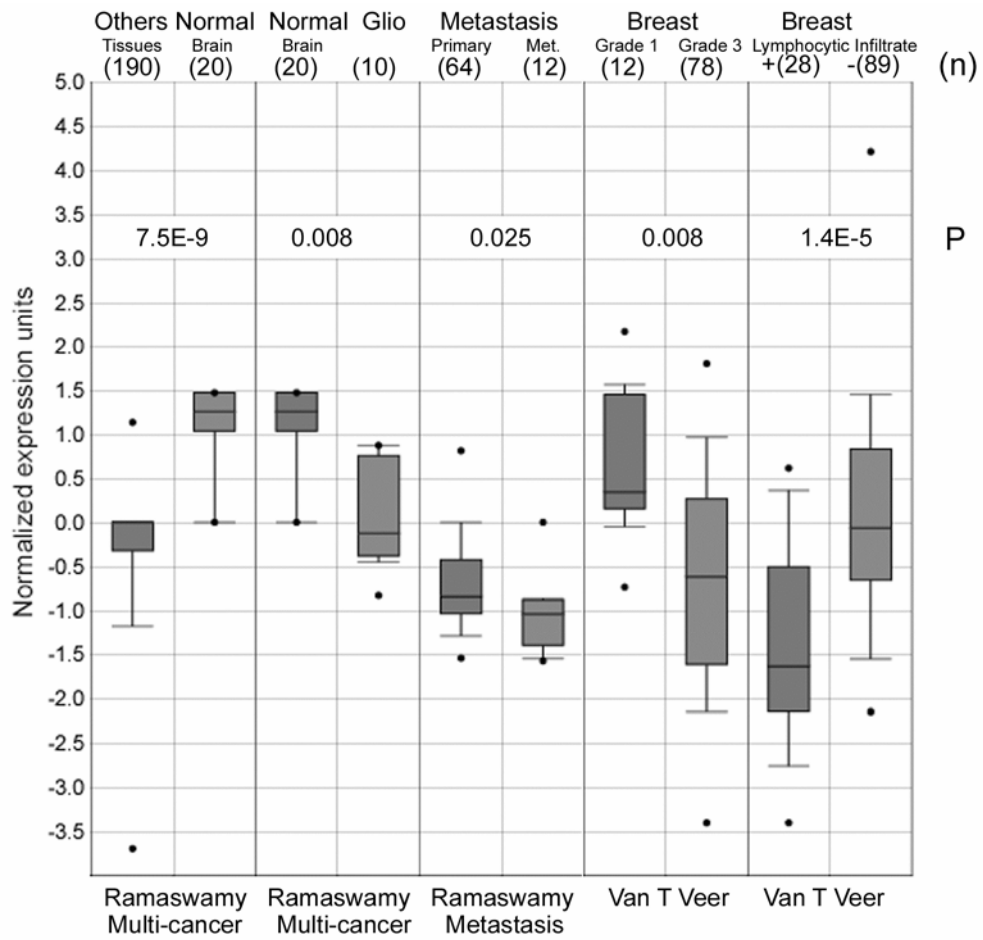

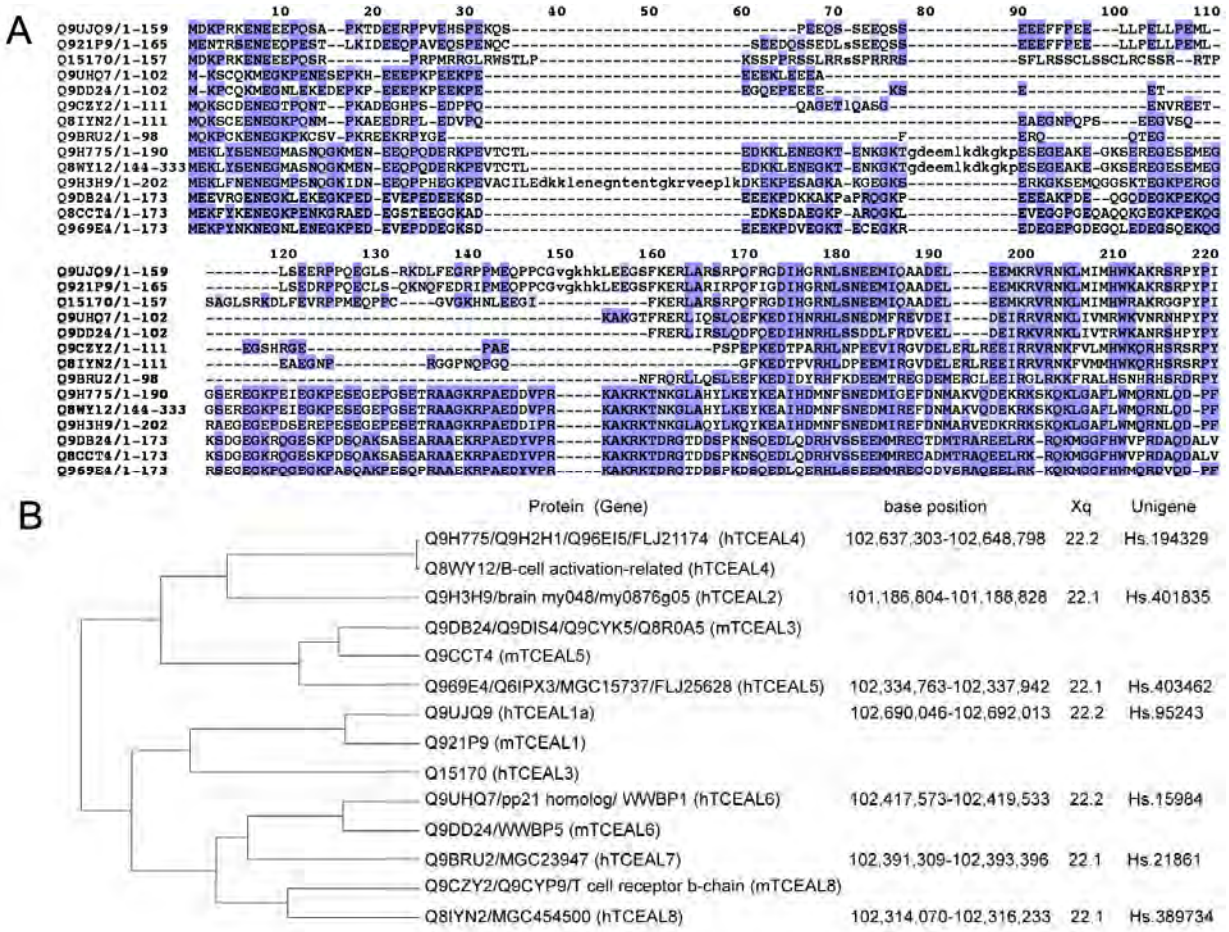
A
B
Protein (Gene)
base position
Xq
Unigene
Q9H775/Q9H2H1/Q96EI5/FLJ21174 (hTCEAL4)
102,637,303-102,648,798
22.2
Hs.194329
Q8WY12/B-cell activation-related (hTCEAL4)
Q9H3H9/brain my048/my0876g05 (hTCEAL2)
101,186,804-101,188,828
22.1
Hs.401835
Q9DB24/Q9DIS4/Q9CYK5/Q8R0A5 (mTCEAL3)
Q9CCT4 (mTCEAL5)
Q969E4/Q6IPX3/MGC15737/FLJ25628 (hTCEAL5)
102,334,763-102,337,942
22.1
Hs.403462
Q9UJQ9 (hTCEAL1a)
102,690,046-102,692,013
22.2
Hs.95243
Q921P9 (mTCEAL1)
Q15170 (hTCEAL3)
Q9UHQ7/pp21 homolog/ WWBP1 (hTCEAL6)
102,417,573-102,419,533
22.2
Hs.15984
Q9DD24/WWBP5 (mTCEAL6)
Q9BRU2/MGC23947 (hTCEAL7)
102,391,309-102,393,396
22.1
Hs.21861
Q9CZY2/Q9CYP9/T cell receptor b-chain (mTCEAL8)
Q8IYN2/MGC454500 (hTCEAL8)
102,314,070-102,316,233
22.1
Hs.389734